KTH Industrial Engineering and Management

Development of a GIS-based multiprocessing modelling approach for assessing the wind and solar potential in Mongolia

Alexander Harrucksteiner

KTH Industrial Engineering and Management

Master of Science Thesis EGI 2010:TRITA-ITM-EX 2020:55

Development of a GIS-based multiprocessing modelling approach for assessing the wind and solar potential in Mongolia

Alexander Harrucksteiner

Approved	Examiner	Supervisor
	Semida Silveira	Jagruti R. Thakur Katja Franke
	Commissioner	Contact person
		Jagruti R. Thakur

KTH Royal Institute of Technology
Unit of Energy and Climate Studies (ECS)

Brinellvägen 68
10044 Stockholm
Sweden

Supervisor: Jagruti R. Thakur Ph.D.
Examiner: Semida Silveira Ph.D.

Fraunhofer Institut für System und Innovationsforschung
Competence Center Energy Policy and Energy Markets (CCX)

Breslauer Straße 48
76139 Karlsruhe
Germany

Supervisor: Katja Franke M.Sc.

This master thesis research has been conducted in cooperation with the Competence Center of Energy Policy and Energy Markets at Fraunhofer Institute for Systems and Innovation Research ISI as part of the Sustainable Energy Engineering Master of Science Program at KTH Royal Institute of Technology.

School of Industrial Engineering and Management
Master of Science in Sustainable Energy Engineering (SEE)

November 2019

Abstract

Despite the vast wind and solar energy potential, Mongolia is still highly depended on coal-fired electricity generation. At the same time, the pressure on Governments is increased due to the urgency to fight climate change. It is therefore essential to identify the techno-economic wind and solar energy potential of Mongolia, to improve data on its renewable resources.

A GIS-based multiprocessing modelling approach for renewable energy site suitability is developed, to incorporate physical-geographical constraints such as slope and socio-geographical constraints such as buffer distances to settlements into the potential calculation. Subsequently, an energy system model named Enertile, developed by Fraunhofer ISI, is used to calculate the techno-economic potential, based on the LCOE method. Final economic interpretations are made in Excel and Python, using the NPV approach.

The results support statements by earlier studies, that Mongolia has vast domestic wind and solar resources. The total technical wind and solar potential is estimated at 7.25 TW capacity and 12.17 PWh/year of electricity. The study also reveals, that electricity from ground-mounted PV is the cheapest renewable source and can generate electricity at a very competitive LCOE starting at 48.6 $/MWh. However, due to a very low regulated electricity rate, all renewable technologies still require a Feed-in Tariff.

The detailed results showed an economic wind potential capacity of 1.15 GW (3.05 TWh/year). Least cost locations for wind farms are found in the south of the country and could generate electricity at a LCOE of 70 $/MWh (185.5 MNT/kWh).

The total economic potential of for ground-mounted PV was 5.12 TW (9.57 PWh/year). Highest solar irradiation locations can generate electricity starting at a LCOE of 48.6 $/MWh (127.9 MNT/kWh).

The analysis of rooftop PV showed a 1.11 TW (1.92 TWh/year) economic potential. Rooftop solar PV systems installed at locations with the best solar irradiation, generate electricity at a LCOE starting at 69.8 $/MWh (183.7 MNT/kWh).

The ground-mounted and rooftop PV results indicate, that the current FiT support scheme is oversized. Hence, a revision of the Feed-in Tariff support scheme for solar photovoltaic systems is proposed and an adjusted FiT rate is calculated.

In case of ground-mounted PV, a FiT adjustment between 58.4 $/MWh and 85 $/MWh should be made in order for Mongolia to reach its 2030 renewable targets. In case of a full decarbonization of the electricity system, a FiT adjustment between 58.9 $/MWh and 85.7 $/MWh is recommended. In order to promote the installation of rooftop PV systems in the capital Ulaanbaatar, a FiT in the range of 108.1 to 147.8 $/MWh is required.

In conclusion, this study recommends further promoting the renewable energy technologies, especially utility scale PV, which are available at a comparatively low LCOE, enhance environmental sustainability and increase energy security for Mongolia.

Sammanfattning

Trots den omfattande potentialen till vind- och solkraft är Mongoliet fortfarande i hög grad beroende av koleldad elproduktion. Samtidigt sätts en högre press på världens regeringar i takt med klimatförändringarnas brådskande angelägenhet. Det är därför nödvändigt att identifiera den tekno-ekonomiska potentialen för vind- och solkraft i Mongoliet, för att förbättra data över landets förnybara resurser.

En multiprocess-modelleringsmetod har utvecklats för att bedöma lämpligheten för förnybara energianläggningar. Modelleringsmetoden är GIS-baserad för att ta hänsyn till begräsningar i det fysiska landskapet, såsom lutning, och det samhälleliga landskapet, såsom säkerhetsavstånd till bebyggelser, i bedömningen. Därefter har en energisystemmodell vid namn Enertile, utvecklat av Fraunhofer ISI, använts för att beräkna den tekno-ekonomiska potentialen baserat på LCOE-metoden. De slutliga ekonomiska bedömningarna har utförts med hjälp av Excel och Python baserat på nuvärdesmetoden.

Resultaten stödjer tidigare forskning som visat på omfattande inhemska vind- och solresurser i Mongoliet. Den totala tekniska potentialen för vind- och solkraft är uppskattad till 7.25 TW kapacitet och 12.17 PWh el/år. Vidare visar detta arbete att el från markmonterade solcellssystem utgör den billigaste förnybara energikällan och att sådana system kan generera el till konkurrenskraftiga LCOE, från 48.6 $/MWh. Men på grund av en bristfällig reglering av elpriset kräver förnybara energitekniker fortfarande en inmatningstariff (FiT).

Enligt de mer ingående resultaten ligger den ekonomiska vindkraftspotentialen på 1.15 GW kapacitet (3.05 TWh/år). Kostnaderna som berör vindkraftsparkernas placering är som lägst i landets södra delar, där elen genereras till ett LCOE om 70 $/MWh (185.5 MNT/kWh).

Den totala ekonomiska potentialen för markmonterade solcellssystem var 5.12 TW (9.57 PWh/år). De områdena med högst solinstrålning kan generera el från 48.6 $/MWh LCOE (127.9 MNT/kWh).

Undersökningen av takmonterade solcellssystem visade en ekonomisk potential om 1.11 TW (1.92 TWh/år). Systemen installerade på de platserna med mest gynnsammast solinstrålning kan generera el från 69.8 $/MWh LCOE (183.7 MNT/kWh).

Resultaten för de markmonterade och takmonterade solcellssystemen indikerar att det rådande FiT-stödsystemet är överdimensionerat. Därav är en granskning av FiT-stödsystemet för solcellssystem föreslaget och en anpassad FiT beräknad.

I fallet med markmonterade solcellssystem bör FiT justeras med 58.4 $/MWh till 85 $/MWh för att Mongoliet ska nå de nationella målen om förnybar energi till 2030. För att nå ett helt fossilfritt elsystem rekommenderas att FiT justeras med 58.9 $/MWh till 85.7 $/MWh. För att främja installationen av takmonterade solcellssystem i huvudstaden Ulaanbaatar krävs en FiT mellan 108.1 till 147.8 $/MWh.

Sammanfattningsvis föreslår detta arbete att fortsätta främja förnybara energitekniker, framförallt storskaliga solcellsanläggningar, som är tillgängliga till relativt låga LCOE, öka den ekologiska hållbarheten samt öka energisäkerheten i Mongoliet.

Acknowledgements

This study would not have been possible without the great support of my two amazing supervisors Katja Franke and Jagruti Thakur. Katja Franke, a researcher at Fraunhofer ISI, always provided me with insightful feedback and supported me with setting up Enertile. I would like to thank Katja deeply for taking the time to answer my questions, but foremost for giving me this once in a lifetime opportunity to work at Fraunhofer ISI.

I would also like to thank Jagruti Thakur, a post-doc researcher at KTH and my supervisor, for giving me valuable input and for sharing your knowledge with me. Thank you, for always believing in me and also supporting me personally, by providing me with job opportunities etc.

Moreover, I want to express my gratitude towards Professor Semida Silveira for her valuable feedback during the presentation and the interesting discussion.

Endless gratitude goes to my incredible friend and Master Thesis buddy Paulina Grim, whose support was indispensable in keeping up my motivation. Without our countless 45 minutes focus sessions, this Master Thesis would not have turned out the way it did. I would not hesitate to write another thesis with you as my thesis buddy. Congratulations for finishing your master studies.

For helping me translate Mongolian Cyrillic and support me with my research, I also want to give a special thanks to Bolor Dorjderem. You are a true friend, no matter the distance.

I am also very grateful for the friendships I made at Fraunhofer. Thank you, Martina, Kathi, Fubi, Rosa, Stefan, Maria, Dinar, Felix and Tieza for the fun times we had in Karlsruhe. I will truly miss you!

Big thanks goes also to the my friends and family back in Austria, especially to my mother, my brother, my father, Gerry and Luisa for supporting me emotionally and for proof-reading my thesis. Thank you Paul, for giving me feedback on my code.

I also want to express my gratitude for Jindan, without whom there would be no Sammanfattning.

Lastly, I would like to express my gratefulness to the CCX team at Fraunhofer ISI, especially to Gerda Deac for providing expertise on evaluating my results, Eva Schönmann for supporting me in assessing the solar irradiance data and Anatolis Vasilio for his expertise input on the economic potential assessment.

Table of Contents

Abbreviations and Nomenclature

AuES	Altai-Uliastai Energy System
CES	Central Energy System
CF	Capacity Factor
CHP	Combined Heat and Power
COI	Country of interest
CPU	Central Processing Unit
DAFIF	Digital Aeronautical Flight Information File
DEM	Digital Elevation Model
DES	Dalanzadgad Energy System
DiffHI	Diffuse Horizontal Irradiance
DirHI	Direct Horizontal Irradiance
DTED	Digital Terrain Elevation Data
ECMWF	European Center for Medium-Range Weather Forecast
EES	Eastern Energy System
EEZ	Economic Exclusive Zone
ERC	Energy Regulatory Commission
ESA	European Space Agency
FiT	Feed-in Tariff
FLH	Full load hours
FLOWA	Fuzzy Logic Ordered Weight Averaging
GDP	Gross Domestic Product
GEBCO	General Bathymetry Chart of the Oceans
GHG	Greenhouse gas
GHI	Global Horizontal Irradiance
GIS	Geographic Information System
IPCC	Intergovernmental Panel on Climate Change
IPP	Independent Power Producer
IRENA	International Renewable Energy Agency
IRR	Internal Rate of Return
ISI	Institute for Systems and Innovation
LCCS	Land cover classification system
LCOE	Levelized Cost of Electricity
LULC	Land-Use and Land Cover
LULUCF	Land use change and Forestry

NGA	National Geospatial Intelligence Agency
NPV	Net Present Value
NREL	National Renewable Energy Laboratory
OM	Operation and Maintenance
PA	Referred to as Purchasing Agency
PPA	Power Purchase Agreements
RES	Renewable Energy Sources
RMSE	Root Mean Square Error
SDG	Sustainable Development Goals
SHS	Solar Home Systems
SOE	State-owned enterprises
SRTM	Shuttle Radar Topography Mission
STC	Standard test conditions
UCL	Université catholique de Louvain
UNEP	United Nations Environment Programme
USGS	United States Geological Survey
WACC	Weighted Average Cost of Capital
WDPA	World Database on Protected Areas
WES	Western Energy System
WiSo-GERI	Wind and Solar – Geospatial Energy Resource Identification

Table of Figures

Table of Tables

1 Introduction

This chapter frames the challenge of climate change. The state of research on renewable energy potential assessment using Geographical Information Systems (GIS) is provided. The contribution, the scope and the objective of this study are also elaborated.

1.1 Background

The recent release of the Special Report on climate change on the 8th of October 2018 by the Intergovernmental Panel on Climate Change (IPCC) highlighted once more, that immediate action is necessary to limit global average temperature increase to 1.5°C. Since the pre-industrial period the global carbon budget for a 1.5°C future has decreased by 2200 $GtCO_{2,eq}$, hence leaving a remaining budget of around 420 $GtCO_{2,eq}$ by the end of 2017. This carbon budget was calculated using the same method as used in the fifth assessment report by the IPCC and states that remaining within this carbon budget will limit the global warming to 1.5°C with a 66% probability. However, the report also states that many uncertainties might even lessen the global carbon budget. Given the current annual greenhouse gas (GHG) emissions worldwide of about 42 $GtCO_{2,eq}$, reveals the alarming fact, that the remaining carbon budget will be spent by the end of the 2020s given a continuation of the status quo. [1]

The combustion of fossil fuels accounts for the majority of anthropogenic GHG emissions. In 2018, energy-related CO_2 emissions reached 33.1 $GtCO_{2,eq}$. Little less than half of those GHG emissions, namely 14.6 $GtCO_{2,eq}$, can be traced back to the burning of coal, making it responsible for around 30% of total GHG emissions [2]. Looking into the future, 190 Gt GHG emissions are already committed, when taking into account the lifetime emissions of the existing coal-fired power plants by the end of 2016. An additional 150 $GtCO_{2,eq}$ are locked in, if also incorporating coal-fired power plants that are under construction or are planned to be constructed [3]. Adding those numbers up yields 310 $GtCO_{2,eq}$, which in turn accounts for around 73% of the remaining 1.5°C budget.

Coal is also the major contributor of GHG emissions in Mongolia. Despite Mongolia's small contribution to the total global GHG emissions, the per capita GHG emissions surpass those of many European countries, based on data of 2014 [4]. The high per capita GHG emissions can partly be attributed to its reliance on coal for both power generation and heat supply for the cold winters. In fact, 90% of Mongolia's total primary energy supply comes from coal. Coal in Mongolia represents an abundant resource since the reserves are estimated to be around 173 billion tons. In addition to negative impacts on the climate, Mongolia is also facing severe issues with local air pollution. Mongolia's capital Ulaanbaatar was declared one of the most polluted cities by the World Health Organization [5]

Acknowledging the challenges, Mongolia has introduced targets to reduce GHG emissions by introducing Renewable Energy Sources (RES) in its energy matrix. By 2023, the installed capacity share of renewable energy technologies should rise to 20% and increase further to 30% in 2030. Introducing more renewable energy technologies can also reduce local air pollution. [6]

Still, investors and energy utilities struggle with identifying suitable locations for both wind farms and solar farms. Grassi et al. even called the prospecting of suitable land for wind farms a "treasure hunt" and one of the biggest challenges in developing a wind energy project [7]. With a higher penetration of RES, the decentralized nature of some RES also highlights the increasing importance of the spatial dimension when it comes to policy decisions [8].

This study aims to support the decision-making process in Mongolia by developing a land suitability modelling approach based on a Geographic Information System (GIS) for wind and solar site suitability. The analysis in this study will provide information on ideal location of wind and solar power plants. In addition to that, a energy systems modelling approach is used to estimate the total techno-economic wind and solar potential in Mongolia.

1.2 Literature review and research gap

Assessing renewable energy (RE) potential with the help of a GIS such as ArcGIS is not a new practice. In fact, one of the first assessments for wind energy potential was performed by Voivontas et al. [9]. In three consecutive steps, Voivontas et al. assessed the wind energy potential on the island of Crete. First, Voivontas et al. calculated the theoretical potential using geographical and topological constraints. Furthermore, they used existing technology parameters to assess the technological potential and lastly, costs were included in determining the economic potential. Using weighted criteria based on a survey among council bodies and wind experts from the private sector, Baban and Parry developed a decision support system for locating suitable sites for wind farms in the UK [10].

A very early study in the field of solar thermal energy was again performed by Voivontas et al., who assessed solar heating systems for residential buildings in Greece in the year 1998 [11]. Since the early stages of RE potential analysis using GIS, technological progress was made in terms of data availability and advancements in GIS technology. Newer studies include Grassi et al., which assessed the technological wind power potential in the State of Iowa, USA [7]. Grassi et al. also included an economic sensitivity analysis on the Internal Rate of Return (IRR) considering different levels of Power Purchase Agreements (PPA). A study for entire India was performed by Mentis et al., looking at the techno-economic wind power potential [12]. Mentis et al. calculated the Levelized Cost of Electricity (LCOE) in order to identify profitable wind farm sites. Gass et al. analyzed the wind power potential of Austria, proposing a Feed-in Tariff adjustment based on their results [13]. Further areas, where GIS-based wind potential assessments were conducted include Sweden [14], Nigeria [15] and Colorado [16].

In terms of solar energy potential assessment, new studies include Nguyen and Pearce, which used an open-source GIS tool named GRASS in order to determine the photovoltaic energy yield potential for Ontario [17]. Another study worth mentioning was performed by Charabi and Gastli in 2010 [18]. Charabi and Gastli were first in applying Fuzzy Logic Ordered Weight Averaging (FLOWA) approach to map appropriate sites for Photovoltaic (PV) power plants in Oman.

Yuschenko et al. assessed both solar PV and concentrated solar power for West Africa. They used a combination of GIS and Multi-Criteria Decision Making (MCDM) methods. As a first step, Yuschenko et al. define restrictive criteria and then they performed the MCDM. For weighting the different criteria, they used a well-documented system called the Analytic Hierarchy Process (AHP) [19]. Areas which were also assessed for their solar potentials are Vietnam [20], India [21], a new city development project in South Korea [22] and Murcia, Spain [23].

The studies mentioned so far have been focusing on a local scale, yet other studies also selected larger regions as their area of interest. Regional studies were performed by Mentis et al., who took upon the task to map the entire African continent in terms of its techno-economic wind energy potential [24].

Balmuş also developed a decision support system using a weighted overlay approach to identify suitable land for both wind and solar installations [25]. The output from her analysis was transferred into the Enertile (formerly known as PowerACE) energy systems analysis tool developed by Fraunhofer Institute for Systems and Innovation Research (ISI). The area assessed by Balmuş was Europe, the Middle East and North Africa.

The literature review for Mongolia showed few studies on techno-economic RE potential assessment. Credits have to be given to an extensive study that was performed in 2001 by the National Renewable Energy Laboratory (NREL) [26]. It was the first study assessing the wind energy potential of Mongolia using GIS. NREL used global data that was complemented by surface and upper-air weather stations found in Mongolia to assess the prevailing wind characteristics. The meteorological data was combined with terrain data at a spatial resolution of 1 km², resulting in wind power map for each grid cell. Due to its pioneering character and its 18 years of existence, the study has become outdated as technologies in the renewable energy sector improved. This is manifested in some of the assumptions made for the analysis. An example is the average wind turbine hub height of 30 m used in the analysis, arguing that this was a compromise height between large-scale and small-scale wind turbines. According to NREL, the hub height of large-scale

wind turbines at that time was between 30-80 m. These figures are outdated, since an assessment performed by Fraunhofer IEE showed that newly installed onshore wind turbines in Germany in 2017 had an average hub height of 128 m [27]. In 2001, the predominant wind turbine capacity was 500 kW according to International Renewable Energy Agency (IRENA), whereas the average capacity of newly installed wind turbines in 2018 was around 3.34 MW. Additionally, the study performed by NREL does not consider economic data, hence only assessing the technical wind energy potential.

IRENA updated the wind energy potential for Mongolia in its Renewable Readiness Assessment report in 2016, using the NREL study as a basis [5]. The technical potential was extrapolated using more up-to-date data such as wind turbines with the average hub height of 100 m. The geospatial analysis was not updated by IRENA even though the spatial resolution of geodata improved significantly, as can be seen in the Digital Elevation Model (DEM) [26]. NREL used a DEM with a spatial resolution of 1 km², whereas the offered DEM geodata from the United States Geological Survey (USGS) in 2019 has a spatial resolution of approximately 250 x 250 m [28]. The spatially improved data will be incorporated into this study.

A more recent study conducted by Sheng et al. [29] assessed the technical wind energy potential in Mongolia. The study was an addition to a series of studies working on the evaluation of a Northeast Asian Super-grid. Four suitability criteria to assess suitable wind farm locations were used: wind resource, distance from cities, distance to roads and finally distance to the grid. Based on the Multi-Criteria Decision Analysis method, the different criteria were classified and assigned a weight. The criteria were then joined using the weighted linear combination tool in ArcGIS, resulting in a composite suitability map. Even though this study is using more updated parameters; it is still missing the economic analysis. Additionally, the study only considered areas within a 200 km distance to 220 kV substations, excluding lower voltage levels. This neglected other three out of four electricity systems in Mongolia, since 220 kV substations are only found in the Central Energy System. [29]

In case of solar energy potential in Mongolia, several researchers and institutions mapped out the solar irradiation apparent in Mongolia. Some of them are the Global Solar Atlas by the World Bank Group and ESMAP [30], as well as IRENA's Global Atlas for Renewable Energy [31]. On the country-level Bayasgalan et al. mapped out the solar irradiation in Mongolia based on both satellite data and in-situ measurements [32]. All studies so far lack technical and economic considerations, making the information only partly useful for decision-makers.

Based on data coming from NREL and the Mongolian National Renewable Energy Center (NREC), IRENA estimated the solar energy potential, but a thorough geospatial analysis is still missing in the report [5].

From the literature review, it was observed that very few studies focused on both the wind and solar energy potential in Mongolia. Also, the literature found for Mongolia do not include economic considerations when assessing renewable energy potentials. Since this study will include geographical, technical and economic considerations into the analysis, the results will pose an essential addition to the current existing body of knowledge. Additionally, this study will include up-to-date data, which is highly important considering that the wind energy potential calculation was performed in the year 2001.

Following the literature review, the additionality of this study will be provided through following considerations:

- Inclusion of economic considerations for both wind and solar
- Up-to-date geographical, technological and economic parameters
- Development of a GIS-based multiprocessing modelling approach for renewable energy site suitability in Mongolia

1.3 Research objective and question

The objective of this study is to assess the techno-economic energy potential of wind (onshore) as well as photovoltaics (ground-mounted and rooftop) of Mongolia.

The research questions that the study aims to answer are

1. Where are the possible cost-optimal locations for installing wind and solar power plants in Mongolia?
2. What is the accumulative economically feasible potential of wind energy (onshore) and solar energy (ground mounted and rooftop) for Mongolia?

Ultimately, the result of this study can act as a decision support system, to assist policy makers in deciding where and how much renewable energy sources at what cost should be installed in Mongolia.

1.4 Scope and limitations

The scope of this study includes only wind energy (onshore) as well as photovoltaic energy (both ground-mounted and rooftop systems). In terms of the geographical extent only Mongolia is considered. In this study a techno-economic potential analysis is performed, excluding the theoretical. Geographical restrictions such as protected areas are considered. Technical parameters for up-to-date technologies and economic parameters based on Enertile's database are included. Economic factors includes cost related factors on the expenditure side, as well as the Feed-in Tariff and regulated electricity rates on the income side. The regulatory framework is not considered. Social factors such as acceptance of wind turbines are accounted for in terms of buffer distances.

The study does not incorporate a power flow analysis assessing the renewable energy grid integration.

Since this is a study on the mesoscale level, applicability of this study in terms of direct wind site identification are highly limited, however, this study can act as a hot spot identification/prospecting tool for further investigation. This study shall not be mistaken with a pre-feasibility study, which requires a more complex analysis of the prevailing situation of a location of interest.

The time horizon for this study is limited to the assessment of the technical potential in 2020 and in 2050. All geospatial datasets are considered for both time horizons. Consequently, spatial transformations such as land-use changes over long periods of time are not part of this study. Geospatial data on the electrical grid is not incorporated in the spatial analysis, since the available data was outdated.

2 Theoretical Background

This chapter will introduce Mongolia, including a general country profile, an introduction into the physical electricity system and the electricity market structure. Additionally, the situation of renewable energy is described, including the current challenges. Different steps of energy potentials are defined, as well as an explanation of GIS and Enertile are provided.

2.1 Country profile: Mongolia

Mongolia is a landlocked country located in Central Asia, surrounded by the Russian Federation in the north and the People's Republic of China in the south [5]. Three million inhabitants live on a total land area of 1 566 500 km², which makes Mongolia one of the sparsest inhabited countries in the world. The entire area is further divided into 24 sub-administrations, namely 21 provinces called aimags and three municipalities. The capital of Mongolia is Ulaanbaatar, where almost 50% of the country's populations is residing. [6]

Mongolia is a resource-rich country due to its vast reserves in Copper, Gold and Coal. The mining industry is the largest sector of the economy accounting for about 35% of total Gross Domestic Product (GDP). Mining contributes to 80% of its exports [5]. Despite its vast mining activities, the GDP per capita in Mongolia is only at 3 891 $ [33].

Net GHG emissions, including Land use, Land use change and Forestry (LULUCF) were 10.03 $MtCO_{2,eq}$ in 2014 [34], hence Mongolia's contribution to the global GHG emissions is around 0.00028% (calculation based on Levin [35]. However, its per capita GHG emissions are 7.1 $tCO_{2,eq}$ in 2014 [34], which is around the same per capita GHG emissions as China [36] and even higher than some European countries such as Austria, Denmark and France [4].

2.1.1 Electricity System of Mongolia

The electricity system is divided into five independent electricity systems. Yet, about 90% of the national electricity is supplied through the Central Energy System (CES), supplying 13 aimags with electricity. The major load center Ulaanbaatar is also part of this energy system and all major generation units, mostly Combined Heat and Power (CHP) plants are located there as well. In some literature, one of the five energy systems, namely the Dalanzadgad Energy System (DES), is also considered to be part of the CES. A 220 kV transmission line is connecting the CES to the Russian power grid and the Chinese power grid. The import statistic of 2015 shows, that 1 200 GWh were imported from China and 176 GWh from Russia to the CES [37]. These numbers amount to about 15% and 5% of the total electricity consumption, respectively. The CES is considered to be highly dependent on electricity imports, which is against the Mongolian Government's long-term goal to increase energy security [6].

The Western Energy System (WES) is also connected to the Russian power grid via a 110 kV line. This Energy System is operating a 12 MW hydro power plant, however most of its electricity demand is covered by imports coming from the Russian power system [5]. According to the Mongolian Energy Economics Institute, 107 GWh were imported in 2015, which amounts to 75% of total electricity demand in WES [37], hence making it highly dependent from Russian imports. This has led to higher electricity rates for consumers and the need to subsidize consumer electricity prices with 132.25 MNT/kWh [38].

The main generating unit in the Eastern Energy System (EES) is a thermal power plant with a capacity of around 36 MW, however also this energy system relies partly on electricity imports from Russia. [5]

The Altai-Uliastai Energy System (AuES) has no interconnection between Russia and is mainly supplied by a 11 MW hydro power plant. [6]

Historically, three of the five electricity systems were created in close proximity of coal reserves. The total installed electrical power capacity of Mongolia was 1082 MW in the year 2015. 85% of the installed capacity

are coal-fired Combined Heat and Power (CHP) plants, which are essential for also providing heat during the cold winter months. [5]

According to the Mongolian Energy Regulatory Commission (ERC), a total of 6 625 GWh electricity was generated domestically in 2018, of which 92.9% originated from Coal-fired CHP plants and 7.1% from RES. 72% of the 7.1% were generated by wind power plants. 11% was generated by solar PV and the remaining 17% by Hydro power. Nevertheless, domestic electricity generation could not fully serve the electricity demand, hence an addition of 1 687 GWh had to be imported. [39]

The total installed capacity of Mongolia was 1 190 MW in 2017 [34], of which only approximately 69% was available, because of aging power plants, which is one of the reasons Mongolia has to import electricity [40].

In terms of GHG emissions, the ERC reported 8.55 $MtCO_{2,eq}$ coming from the six CHP generation units found in the CES [39]. Data on other energy systems is not published by the ERC.

When looking at the electrification rate, around 98% have access to modern electricity services, despite Mongolia's vast territory. This can partly be attributed to the efforts of the Mongolian government and the World Bank to increase electrification rates in the past decade and a half. In very remote areas electricity is supplied through Solar Home Systems (SHS) or Mini-grids. Mobile SHS play an important role, especially for the Mongolian citizens still engaged in the nomadic lifestyle. [5]

2.1.2 Electricity market and regulatory framework

The electricity market is not yet fully liberalized in Mongolia. It is considered to have a Single Buyer market structure, where there exists one large entity which is buying electricity from the generation units and distributing it to distribution companies [41]. This means that the generation side is fully liberalized, however, most stakeholders in the generation market are still commercialized state-owned enterprises (SOE). Only one entirely private enterprise is operating in the generation sector: Salkhit windfarm, hence making it the only Independent Power Producer (IPP) in the market (numbers based on 2015). [6]

The Single Buyer in the electricity system is the National Power Transmission Grid Company, henceforth referred to as Purchasing Agency (PA). The PA buys electricity from generation companies at a fixed electricity rate and further sells it to the distribution companies, which are also regulated to sell it at a fixed rate to end-consumers. [6]

The rates for electricity generation, transmission and distribution are set by the ERC, the regulatory authority of the energy sector. Interestingly, according to a report of the Government of Mongolia, the rates are too low to recover costs and hence subsidies are distributed for coal-fired power plants. Next to deciding on the electricity rates, the ERC is also responsible for authorization of new generating capacity, compliance, monitoring sector activity and wholesale market structure. [6]

Other important entities in the energy electricity sector are the Ministry of Energy, which is charge of approving the state policies, the Unfair Competition Regulating Authority [6], which addresses anti-competitive behavior and the National Dispatching Center, which is responsible for dispatch arrangements according to the network codes. [40]

2.1.3 Role of Renewable Energy

In 2007, the Mongolian Government set in place a Renewable Energy Law exploring the use of Feed-in Tariffs (FiT) for renewable energy generators. Additionally, this law organizes roles, rights and privileges for all parties involved in renewable energy power plant projects. [5]

One of the main issues of the early stages of the Renewable Energy Law was the currency selected for the FiT payments. In order to reduce currency exchange risks for foreign investors, US Dollars were chosen as payment currency. However, due to the weakening Mongolian currency, this has put high financial pressure on the Mongolian treasury. Another issue resembled the inadequately financed FiT system, which impacted the National Transmission Company's ability to fund essential investments. Both issues called for an

amendment of the Renewable Energy Law. In June 2015 the Renewable Energy Law was amended, dealing with the inadequate financing of the FiT system by changing it to a Feed-in Premium, where renewable generators are paid the difference between market price and FiT support system price. Henceforth, the Feed-in Premium will still be referred to as FiT [37].

By 2023, Mongolia aims to reach 20% renewable share of total installed capacity, which should increase to 30% in 2030 [5]. This means adding another 75 MW until 2023 and 450 MW until 2030 (based on 2015 numbers) [6]. On the other hand, Mongolia plans to add another 1 950 MW of coal-fired capacity manly in the south and around Ulaanbaatar [42].

In 2018, the ERC reported that 339 GWh electricity were generated by wind power plants, 79 GWh from Hydro power plants and 51.1 GWh from PV plants [39]. According to IRENA, 101 MW of wind, 25 MW of PV and 29 MW of hydro power was installed in 2017 [43]

Mongolia is also looking into exporting renewable electricity to its neighboring countries in particular China, since Mongolia, with its approximately three million inhabitants, has a very low domestic electricity demand compared to China. It therefore proposed the Asian Supergrid (ASG) initiative, which should promote a stronger cooperation between China and Mongolia, but also South Korea. In particular, Mongolia is trying to connect the large load centers found in the Beijing area, with the high RES potential area in the Gobi Desert. [6]

2.1.4 Challenges for the sustainable energy transition

Several barriers for promoting the sustainable energy transition are found throughout the literature [6], [34], [40], [44], [45].

One main challenge is identified to be the abundant availability of cheap coal as a resource [6], [44]. In addition to that coal is also a subsidized fuel, further decreasing costs [6]. Some of the older coal-fired power plants are already fully depreciated and amortized, making it even harder for new entrants to compete [6].

Mongolia's energy sector is also heavily relying on the CHP plants for providing heat to its citizens. This strong relationship between electricity and heat is a feature that many of the renewable energy sources cannot provide. [6]

In addition to the fierce competition coming from coal, renewable energy sources have their own intrinsic issues, such as resource rich areas are sometimes located far away from the load centers of the country and transmitting the electricity volumes would come at a high cost. Furthermore, the low domestic electricity demand also poses a challenge, since establishing a supply chain which could leverage economies of scale is difficult when demand is low. [40]

Another big challenge is the perceived risk coming from investors and lending institutions. According to the Government of Mongolia, payment issues with the FiT system were reported in the past. On top of that renewable energy systems also experienced curtailment, since there is no priority dispatch legislation in-place for renewable energy systems. Investors also face the uncertainty, that once investing into a license for the development of a renewable power plant, it is not certain that the power plant can be built, since no transparent maximum absorption capacity reports for intermittent renewable energy sources are released. [6]

Lastly, there are also issues with finding qualified labor. SE4ALL reports a lack of experienced labor for renewable energy technologies [45] and the Government of Mongolia identified a lacking Operation and Maintenance (OM) industry [6].

2.2 Levels of energy potential

The energy potential level definitions are based on the approach of the World Energy Council [46] and Hoogwijk [47].

In those publications five levels of potentials are defined: theoretical, geographical, technical, economic and implementation potential. The implementation potential is sometimes also referred to as market potential [48]. The five potentials are illustrated in Figure 1. As indicated in this figure, the energy potential is reduced with every potential step.

The theoretical potential, in the context of this study, is the energy content of the total wind and the solar irradiation found inside of Mongolia. This potential will not be evaluated in this study as already mentioned in the limitation chapter.

The geographical potential, according to Hoogwijk, is measured in km² and assesses the suitable land for installing wind and solar farms, given certain geographical constraints [47]. In some literature, the geographical potential is measured in energy unit per year. These studies calculate the energy resource available on the suitable land [49]. However, in the present study the first approach is considered.

The technical potential combines the suitable land with state-of-the-art energy conversion technology, such as photovoltaic modules and wind turbines. This means that conversion losses of the technologies from resource to usable energy is taken into account.

The economic potential expands the concept of the technical potential by adding economic considerations. Wind and solar farms are only added to the economic potential, if they are economically feasible in terms of costs.

The market potential complements the economic potential by looking at specific market entry aspects as well as the regulatory and policy framework apparent in that particular market. This study will only partly consider specific market aspects. Included in this study are subsidy schemes and electricity pricing from competing generators. Regulatory aspects are not considered.

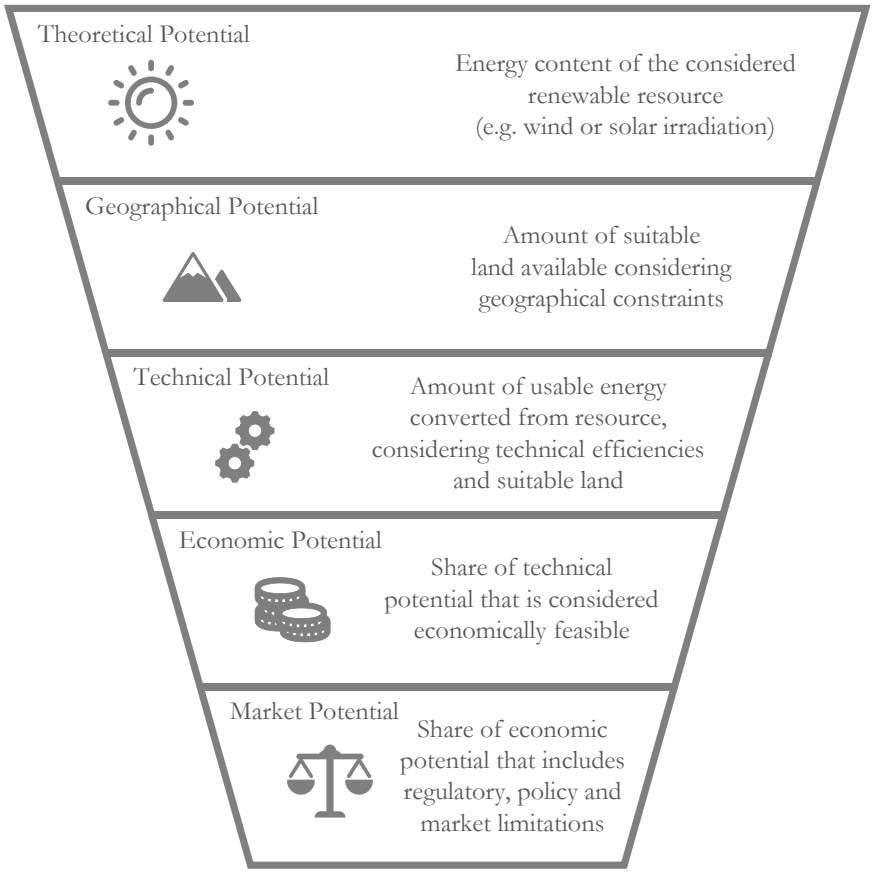

Figure 1: Potential steps for energy resources[1]

[1] icons from flaticon.com

2.3 Software and Models

The software ArcGIS created by ESRI along with Enertile RE Potential model is used for the analysis in the study.

2.3.1 ArcGIS

A geographic information system is used for gathering, managing and analyzing data. Its roots are based in geography and hence spatial locations plays an integral role in arranging and organizing the data, to also allow a deeper understanding of the data. GIS allows to perform tasks such as monitoring change, identifying problems, perform forecasting and understanding trends. Spatial analysis furthermore allows for making suitability assessments to support decision-making. A suitability assessment is also performed by the developed tool for this study. [50]

The main software used for this assessment is ArcGIS for Desktop 10.5. This software is developed by ESRI. ArcGIS is able to perform tasks such as data visualization, data management, spatial analysis and data compilation. [51]

2.3.2 Enertile RE-Potential model

Fraunhofer ISI has developed a collection of energy system models, which individually analyze a sector of the energy system, such as the electricity system or the transport system. All models interact and together they try to capture a holistic view of the energy system. The energy system models include energy demand models as well as energy supply models. These in turn are linked to a macro-economic model, which can analyze economic effects of the energy transition. All models are supplemented with an extensive database, containing relevant empirical data from academia and industry (see Figure 2).

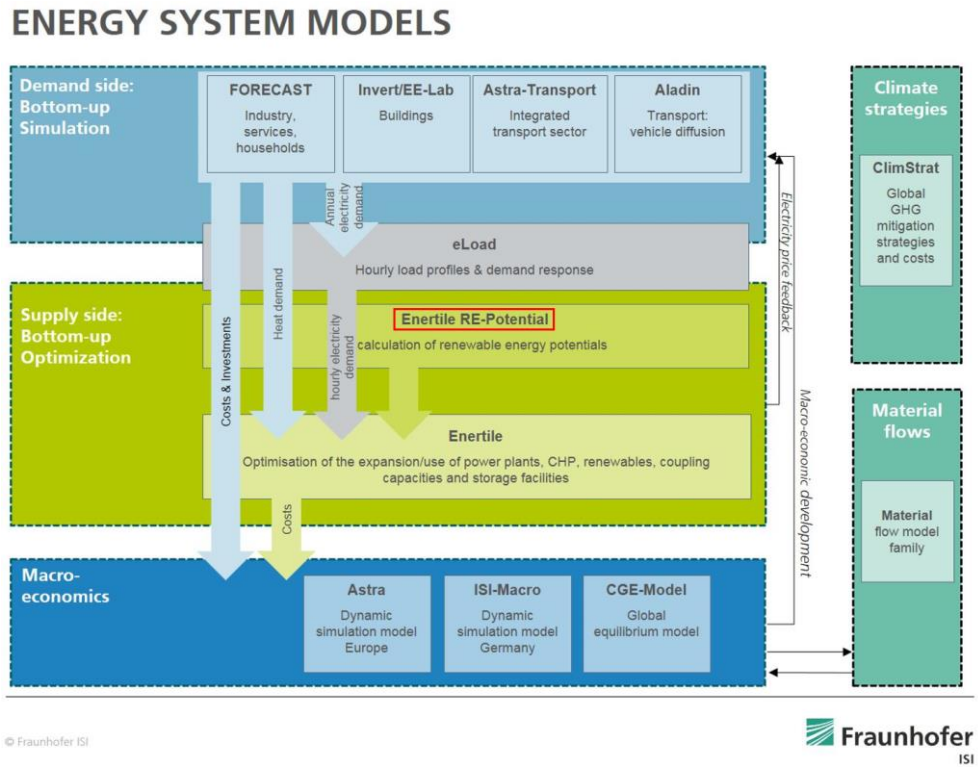

Figure 2: Energy System Models developed by Fraunhofer ISI [52]

The study is focused on the techno-economic renewable potential analysis, hence the Enertile RE-Potential model is relevant for this study. Enertile RE-Potential is a bottom-up energy supply model. Based on the data coming from the land suitability model (in this case WiSo-GERI) Enertile RE-Potential assesses the

economic potential, by calculating parameters such as feasible capacity per grid cell, full load hours (FLH) per potential class and investment costs per potential class. The results from the Enertile RE-Potential model include Levelized Cost of Electricity. [52]

A supplementary analysis by the author of this study is performed using the results coming from Enertile RE-Potential and involves the calculation of the Net-Present Value.

Henceforth the Enertile RE-Potential model will only be referred to as Enertile for simplicity reasons.

3 Methodology

In this chapter, the methodology of the techno-economic analysis of the wind and solar energy potential is described. This includes a description of the used data to ensure transparency and replicability. Furthermore, the methodological approach of the geographical potential analysis in WiSo-GERI as well as the techno-economic potential analysis in Enertile *are explained.*

Data collection is the first step in the methodology workflow (see Figure 3). Data is collected at a global scale as well as on a national scale. The national data, if existing, is meant to complement the global scale data and is only collected for the area of interest in this study: Mongolia. However, due to lack of data availability, most of the data is collected on a global scale.

Most of the spatial data collected needed to be processed to fit the requirements of the Wind and Solar-Geospatial Energy Resources Identification (WiSo-GERI) and Enertile. All spatial data for example is projected to the same projection. In addition, geographical, technical and economic parameters are researched. Geographical parameters include physical-geographical constraints such as maximum slope and socio-geographical constraints such as distance to settlements. Technical parameters concern technical specifications of the two renewable energy technologies such as the wind power curve in case of wind power. Lastly, economic parameters are included for example specific technology costs.

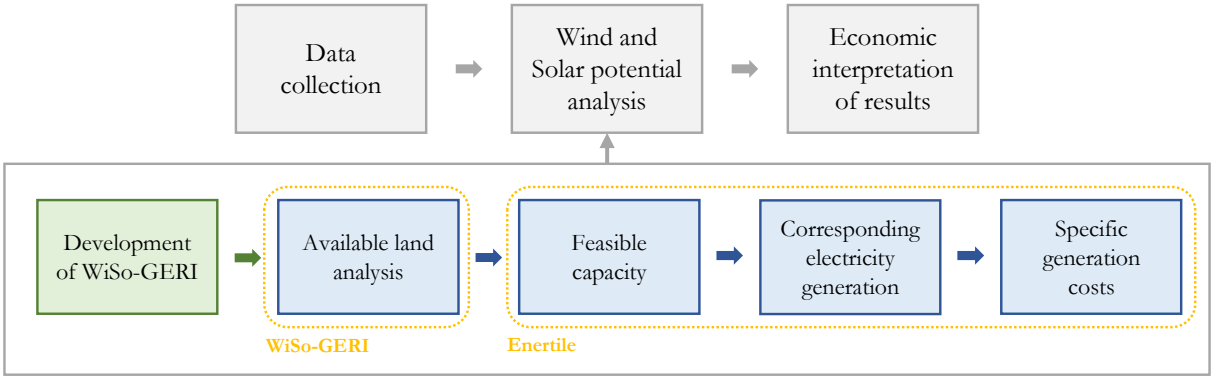

Figure 3: Techno-economic workflow chart

The next step in the methodology workflow is the analysis of the techno-economic wind and solar potential of Mongolia. This step includes several sub steps, which are performed in two different models: WiSo-GERI and Enertile. The first model, WiSo-GERI, is developed in the framework of this Master Thesis. WiSo-GERI identifies available land for developing wind and solar power plant projects considering physical-geographic and socio-geographic constraints. Therefore, the output of this model could be referred to as geographical wind and solar potential. The WiSo-GERI model is based on Python 2.7, utilizing Python modules such as tqdm, os, multiprocessing and arcpy. The arcpy module is developed by ESRI and is used for spatial analysis of both raster and vector data [53].

The output of the WiSo-GERI model is imported to Enertile, which is a tool to calculate the techno-economic potential for various renewable energy sources. It was developed by Fraunhofer Institute for Systems and Innovation Research in Karlsruhe. Initially, Enertile identifies the feasible capacity given the available land area in Mongolia. By adding wind speed and solar irradiance maps, Enertile is capable of calculating the location specific electricity generation. As a final step in Enertile, economic factors are added to calculate costs.

In the last step, the results of the analysis are interpreted outside of Enertile, since Enertile only includes cost aspects. The economic interpretation of the results is performed in Excel and Python. Finally, policy implications are derived from the quantitative analysis.

3.1 Data collection

The geospatial data used in this study is gathered from various sources. A main requirement to the collected data is its availability on a global scale. Higher resolution and more up to date data is given preference.

In Table 1 geospatial data sources are listed. Other parameters such as technical and economic ones are listed in upcoming chapters. Some geodata displayed in Table 1 were collected by Crisitina Balmuş, a scholar at Fraunhofer ISI in 2015, which developed the previous generation of the land suitability model. The data accessed by Crisitina Balmuş is kept in case there are no registered changes to the data since 2015. All other geospatial data is updated, and newer versions are selected.

Category	Dataset name	Provider	Year released	Resolution / Scale	Available from	Date accessed
Country borders	Countries 2014 - Administrative Units	EUROSTAT	2011	1:3 million	http://ec.europa.eu/eurostat/web/gisco/geodata/reference-data/administrative-units-statistical-units	26.06.2015[1]
Maritime Exclusive Economic Zones	Maritime Boundaries Geodatabase	VLIZ Flanders Marine Institute	2014	n/s	http://www.marineregions.org/about.php	25.06.2015[1]
Land Use and Land Cover	GlobCover 2009	European Space Agency	2009	300 m	http://due.esrin.esa.int/page_globcover.php	5/6/2019
Digital Elevation Model	GMTED2010	United States Geological Survey	2010	250 m	https://earthexplorer.usgs.gov/	5/6/2019
Bathymetry	GEBCO	British Ocenaographic Data Center	2019	500 m	http://www.gebco.net/data_and_products/gridded_bathymetry_data/	5/15/2019
Airports	World Airport Locations	OurAirports	2019	n/s	http://ourairports.com/world.html	8/1/2019
Protected Areas	WDPA	UNEP	2019	n/s	http://www.protectedplanet.net/	8/5/2019
Navigable waterways	Global Shipping Lane Network	Oak Ridge National Labs	2013	n/s	http://geocommons.com/datasets?id=25	25.06.2015[1]
Roads	gROADS	Socioeconomic Data and Applications Center	2013	n/s	https://sedac.ciesin.columbia.edu/data/set/groads-global-roads-open-access-v1	8/6/2019
Railways	VMap0 version R5	GIS-Lab	2000	1:1 million	http://gis-lab.info/qa/vmap0-eng.html	5/6/2019
Wind and Solar resource	ERA5	European Centre for Medium-Range Weather Forecast	2010	31 km	https://cds.climate.copernicus.eu/cdsapp#!/dataset/reanalysis-era5-land?tab=form	n/s

[1] accessed by Balmuş

Table 1: Geospatial data sources and descriptions

In the following chapters, the geodata is described including important factors such as accuracy estimates, if available.

Countries 2014 – Administrative Units

The Countries 2014 – Administrative Units geodata is a product of the Geographic Information System of the Commission. It is a unit within Eurostat and is responsible for managing geographical information needs for the European Union and its member states. The Countries 2014 dataset is a vector dataset. It is available at scale of 1:3 million, meaning that the country border lines are coarse and do not fully reflect real country borders. [54]

Maritime Boundaries

The Maritime Boundaries geodata describes the global Exclusive Economic Zones and is managed by Flanders Marine Institute. The service was created by merging the VLIMAR Gazetteer and VLIZ Maritime Boundaries Geodatabase. The Maritime Boundaries are less simplified and therefore not as coarse as the Countries 2014 dataset. [55]

Global Land Cover Map (GlobCover 2009)

GlobCover 2009 is a global Land-Use and Land Cover (LULC) raster map, which is the joint product of the European Space Agency (ESA) and the Université catholique de Louvain (UCL). The land cover classification system (LCCS), with its 22 land cover classes, is used to categorize the areas.

The data for the GlobCover 2009 raster map is taken from the EnviSat satellite. Installed on-board the EnviSat satellite is the Medium Resolution Imaging Spectrometer Instrument sensor, short MERIS, which can collect up to fifteen spectral bands at a swath width of 1150 km, meaning that a global coverage is reached every three days.

The overall accuracy of the GlobCover 2009 data is above 70% with a 95% confidence interval. [56]

Global Multi-resolution Terrain Elevation Data (GMTED2010)

The DEM provided by the USGS and the National Geospatial Intelligence Agency (NGA) is called GMTED2010 and is the successor of GTOPO30. GTOPO30 was a 30 arc-second DEM published in 1996. In 2010, GTOPO30 was then replaced by GMTED2010, mainly due to improved availability of high-quality elevation data, coming for example from the Shuttle Radar Topography Mission (SRTM). The GMTED2010 combines eleven data sources, of which the majority comes from the Digital Terrain Elevation Data (DTED) from the SRTM. The geodata is available at three different spatial resolutions, namely at 30, 15 and 7.5 arc-seconds. The 7.5 arc-second version, which is the resolution of choice for this study, has a Root Mean Square Error (RMSE)[2] of between 26 and 30 m. [58]

General Bathymetry Chart of the Oceans (GEBCO)

The GEBCO 2019 dataset was developed under the framework of the Seabed 2030 project, which is a collaboration between the Nippon Foundation of Japan and GEBCO. GEBCO is the name of the organization responsible for assembling the different data sources going into the joint dataset GEBCO 2019 and consists of an international group of experts under the patronage of the International Hydrographic Organization and the Intergovernmental Oceanographic Commission of the UNESCO. The Nippon Foundation of Japan on the other hand is a philanthropic organization providing funding to the project.

The basis of the GEBCO 2019 dataset resembles the SRTM15+ dataset which contains both measured and estimated seafloor topography. This dataset is complemented by data coming from national and regional mapping initiatives.

The GEBCO 2019 dataset is available at a 15 arc-seconds resolution. Download options include a global netCDF file with 12 GB or alternatively custom smaller tiles that can be selected on the regional scale. [59]

World Airports

The service of OurAirports was created in reaction of the shutdown of the Digital Aeronautical Flight Information File (DAFIF) run by the Australian government, which formerly provided data on airports around the world. David Megginson established the platform "ourairports.com" to fill the gap that the closing of the DAFIF left behind. The OurAirports database contains not just big commercial airports but also smaller airports which are not flown to by commercial airlines. To date, the database contains information on 55 502 airports (09.2019).

The data is provided as csv file. The csv file includes latitude and longitude coordinates and airport names. [60]

World Database on Protected Areas (WDPA)

The WDPA is a joint product of the United Nations Environment Programme (UNEP) and the International Union for Conservation of Nature. It is updated on a monthly basis and is used for tracking

[2] RMSE determines the error of a regression line and actual observed values [57]

progress of some Sustainable Development Goals (SDG). The WDPA came to life in 1981 and the online interface with the name "protectedplanet.net" was added in 2010 and updated in 2015.

The dataset includes areas that are defined as protected areas according to the International Union for Conservation of Nature standard and the Convention on Biological Diversity definition. Spatial accuracy is addressed in the documentation file accompanying the dataset, however an accuracy metric is not provided. The Protected Planet team works with data providers to continuously improve the quality. [61]

Global Shipping Lane Network

The Global Shipping Lane Network was created by the Oak Ridge National Labs CTA Transportation network Group. It was published in 2013. There was no documentation found for this dataset, hence no statement on accuracy of the data can be made. [62]

Global Roads Open Access Data Set (gROADS)

The gROADS was developed by the CODATA Global Roads Data Development Task Group. This task group is supported by the Information Technology Outreach Services team from the University of Georgia and the Center for International Earth Science Information Network from Columbia University.

The basis for the dataset is the Vector Smart Map Level 0 (VMap0). Due to its low spatial accuracy, VMap0 is complemented with country level data. An investigation of the VMap0 data has shown, that the average RMSE is 900 m, while the RMSE of the complemented country specific data had a RMSE of 30-500 m. The roads of Mongolia did not receive an update from the gROADS team, hence the RMSE values of the VMap0 data apply for Mongolia's roads. [63]

Railways

Data on global railways map is created by the NGA but provided by "gis-lab.info". The railways map is part of the larger dataset VMap0. The VMap0 also includes power transmission lines and roads. The RMSE can be assumed to be approximately 900 m. [64]

ERA5

ERA5 is a climate reanalysis dataset and is developed by the Copernicus Climate Change Service (C3S) and the European Center for Medium-Range Weather Forecast (ECMWF). The ERA5 dataset includes several parameters for the time period from 1979 up until 2-3 months before the present. Parameters include wind speed, Global Horizontal Irradiance (GHI), Direct Horizontal Irradiance (DirHI), air density and temperature data, which are also used for this study. The spatial resolution is 31 km and the temporal resolution of the five parameters mentioned before is 1 hour. [65]

For Mongolia 2429 data points containing hourly wind speed, GHI, DirHI, air density and temperature data are available. Grid cells are assigned an ERA5 data point according to spatial proximity. The five parameters are available for the year 2010.

3.2 Data preprocessing

The collected data needed to be processed to fit the requirements of WiSo-GERI and Enertile. The geographical coordinate system of all spatial datasets is adjusted to GCS_WGS_1984. Additionally, the analysis required an area preserving projection, since the geospatial data is extracted by a 6.5 x 6.5 km sized grid. Therefore, all datasets are projected to the projection World Cylindrical Equal Area (WKID: 54034 by Esri).

Furthermore, the GlobCover 2009 dataset is reclassified, hence reducing the number of LULC categories to twelve. The exclusion layers are provided with a buffer zone. This process will be elaborated on in the following chapters.

3.3 Geospatial analysis in WiSo-GERI

The land suitability analysis is performed by WiSo-GERI. In summary, WiSo-GERI divides a country's sovereign territory into two categories: excluded areas and evaluation areas. Excluded areas incorporate geographical restrictions such as protected areas, which are not available for installation of wind and solar power plants (see Figure 4). The remaining land is referred to as evaluation area. From the evaluation area, relevant characteristics such as LULC class and terrain slope are extracted for further processing in Enertile. The relevant evaluation criteria for offshore areas are sea depth and distance to shore.

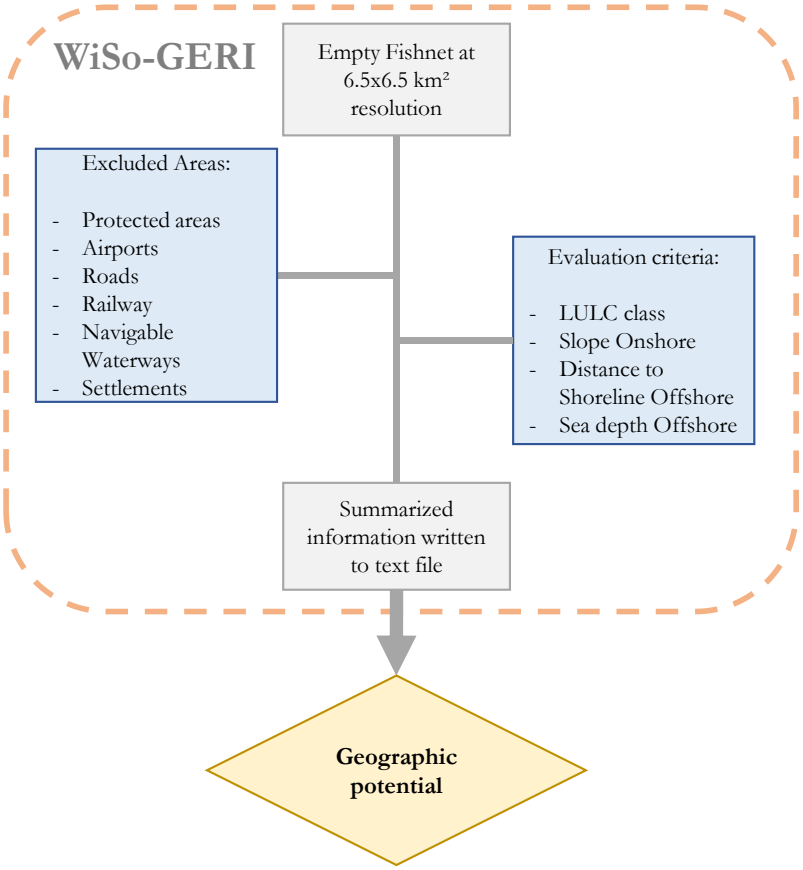

Figure 4: WiSo-GERI workflow chart

3.3.1 Excluded areas

All excluded areas are provided with a set-back distance. This is done to either address safety measures, such is the case with airports, which do not allow the construction of buildings and other obstacles in its proximity [66]. Other reasons include aesthetic reasons such as a set-back distance from protected areas and settlements [67].

Due to these social and safety factors, following buffer zones are created around the excluded features (see Table 2).

Excluded	technology relevancy	Buffer zone
Protected areas	all	1000 m
Airports	all	3000 m
Settlements	all	1000 m
Roads	all	100 m
Railways	all	100 m
Shoreline	offshore wind	5000 m
Navigable waterways	offshore wind	5000 m

Table 2: Buffer zones sizes for excluded areas

The set-back distance is defined to be 3 000 m for this study, which is in accordance to the minimum distance of Aydin et al. [66]. It is worth mentioning that others such as Siyal et al. [14] and Gass et al. [13] have selected smaller set-back distances for their analysis, nonetheless the larger set-back distance is selected in this study to ensure also safe operation in case of an expansion of the airport.

In terms of protected areas, a buffer zone with a radius of 1 000 m is defined, according to Baban et al. [10] and Blamuş [25]. This distance is chosen to protect pristine natural habitats and its biodiversity.

Settlements are supplied with a 1000 m buffer zone, due to the concerns of opposition from housing owners. The set-back distance is chosen in accordance with Gass et al. [13], Enevolsen et al. [68] and Siyal et al. [14].

Roads and railway tracks are provided with a set-back distance of 100 m, which is the value used in Baban et al. [10] and Blamuş [25]. Other studies use higher values ranging from 150 m to 240 m [7], [13], [14].

For offshore locations a buffer zone of 5 000 m is established for both the shoreline and navigable waterways according to Balmuş [25], Mekonnen and Gorsevski [69] and Beacham et al [70]. Wind farms closer than 5 000 m causes concerns of the local population based on decreasing property value. It can also affect local economies which are heavily based on recreation and tourism [69]. In terms of distance to navigable waterways a buffer distance of 5 km ensures safe navigation through the ocean [70].

All the above-mentioned areas are then defined as excluded areas by not allowing the installation of either wind or solar power plants on these premises.

3.3.2 **Evaluated areas**

Once all excluded areas are removed from the total area of a country, the remaining area is being evaluated on its suitability for wind and solar power plants, henceforth it is referred to as evaluated area. Two sets of criteria are used to evaluate onshore areas: LULC class and terrain conditions. For offshore areas other two criteria are used for the evaluation: sea depth and distance to shore. The evaluation is performed in Enertile, hence an in-depth description of Enertile's methodology will be provided in the following chapter.

3.4 Techno-economic analysis in Enertile

The results from the WiSo-GERI model are transferred into Enertile to calculate the techno-economic potential [52].

As a first step, Enertile uses the LULC data to assign utilization factors depending on LULC class and technology (see Figure 5). An area declared as 100% cropland for example is assigned a utilization factor of 20% in case of onshore wind power, meaning that Enertile builds wind farms on 20% of the area, given a certain spacing factor between the individual wind turbines. Additionally, Enertile avoids installing wind and solar farms on areas with a higher slope than a defined upper limit. This upper slope limit varies between the two technologies.

Considerations for offshore wind farms are different and include sea depth and the distance to shore to assess suitability of placing a wind farm on a particular area. Offshore wind, however, is not considered in this study.

Given the available area per grid cell, a feasible capacity is calculated. Enertile then adds wind speed and solar irradiance maps to calculate full load hours of each technology. Grid cells with similar FLH are aggregated into potential classes, for which Enertile calculates all cost related parameters. Costs include investment cost as well as OM costs. These costs are calculated for the entire operational lifecycle[3] and are then annualized with a specific discounting rate. [71]

[3] The lifetime of both technologies is assumed to be 25 years

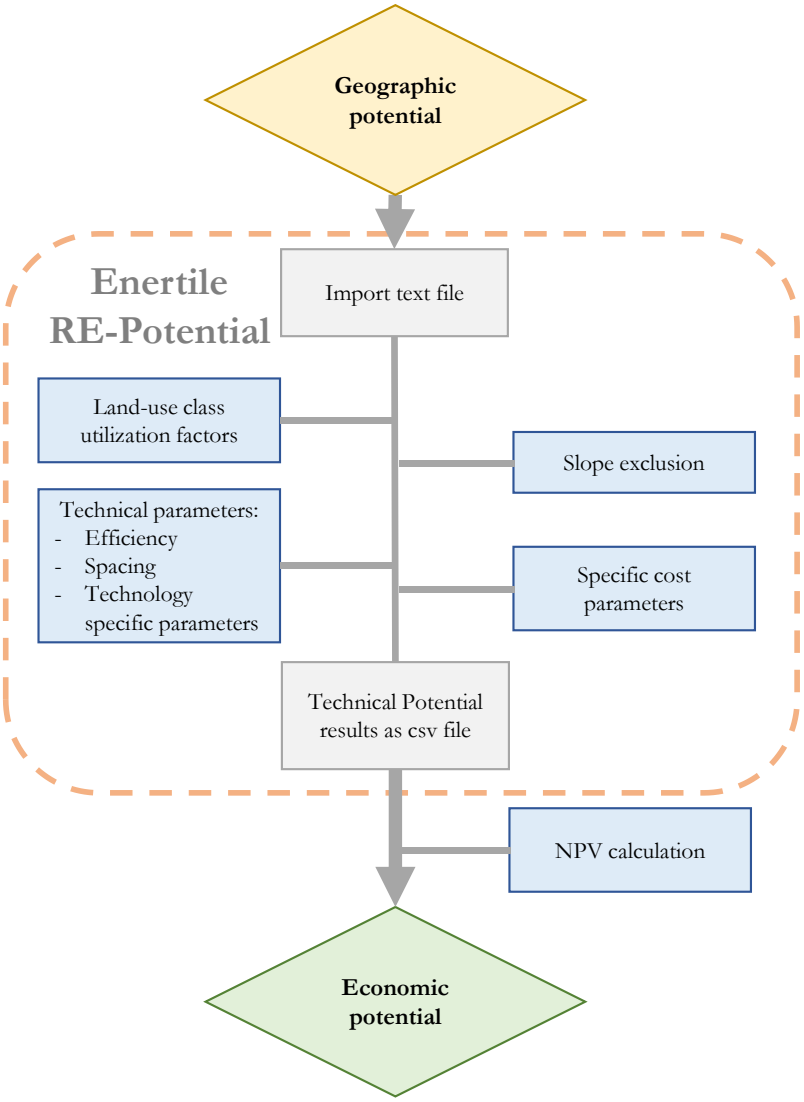

Figure 5: Workflow chart of Enertile RE-Potential model

3.4.1 LULC Utilization factors

Depending on the technology, different LULC class utilization factors are used. The utilization factors are embedded in Enertile and are taken from a scenario study which assesses possible pathways for the German energy transition. The study was conducted by Fraunhofer ISI, consentec GmbH and Institute for Energy and Environmental Research Heidelberg (IFEU) on behalf of the German Ministry for Economic Affairs and Energy (BMWi). The technology-specific utilization factors for each LULC class can be seen in Table 3.

LULC Class	Utilization factors		
	onshore Wind	ground-mounted PV	rooftop PV
Barren	25%	20%	0%
Cropland natural	20%	2%	0%
Cropland	20%	2%	0%
Forest	10%	0%	0%
Grassland	25%	3%	0%
Savanna	25%	3%	0%
Shrubland	25%	3%	0%
Snow and Ice	15%	5%	0%
Urban	0%	0%	20%
Water	0%	0%	0%
Wetland	0%	0%	0%
Excluded Areas	0%	0%	0%

Table 3: Utilization factors per LULC class and RE technology [71]

3.4.2 Terrain limitations

Slope is an important parameter when it comes to assessing site suitability for renewable energy power plants. For onshore wind farms the upper slope limit is chosen to be 13.5°. This is the truncated average of six studies (see Table 4). Areas with a too steep slope are unsuitable for operating cranes and boring machines for constructing wind turbines according to Grassi et al. [7].

A maximum slope of five degrees is chosen for the installation of ground-mounted PV farms, which is the average truncated value from nine studies (see Table 4). Flatter terrains reduce complexity of the power plant design, which directly translates into lower system costs according to NREL. Steeper sloped sites for example can require different mounting systems or additional requirements to the foundation due to increased wind loading. [72]

Technology	Upper slope limit	Sources
onshore wind	13.5°	[7], [13], [24], [26], [73], [74]
ground-mounted PV	5°	[17]–[21], [23], [25], [66], [75]

Table 4: Upper slope limits for RE technologies and sources

The available area needed for determining the feasible potential, which incorporates both LULC class and slope limits, is calculated using following equation

$$A_{av} = \sum_{LULC} A_{gc} * x_{LULC} * u_{LULC} * s_{gc} \quad (1)$$

where A_{gc} is the grid cell area of 42.25 km², x_{LULC} is the unitless proportion of a specific LULC class of the total area of the grid cell determined by WiSo-GERI, u_{LULC} is the unitless utilization factor of the LULC class and s_{gc} is a Boolean variable indicating, whether the average slope inside the grid cell exceeds the upper limit for the specific technology. In case of wind for example, s_{gc} is 0 if the average slope inside the grid cell is higher than 13.5° (see Table 4). [71]

3.4.3 Wind onshore

Enertile's internal wind model calculates electricity generation from wind power according to Hellmann [76] and software code from Enertile [77][4].

[4] The information referenced by this source is conveyed by Fraunhofer staff working on Enertile in a non-formal way, due to lack of documentation

Modelling

In terms of wind power five factors are taken into account when modelling wind turbines: wind speed, air density, hub height, wind farm layout, general wind farm losses and availability of the wind turbines. The calculations that are shown in this chapter are based on a single fishnet grid cell, meaning that these calculations are repeated for all fishnet grid cells located in the country of interest. [77]

Enertile accounts for changing air densities by calculating an air density correction factor, which is calculated with

$$c_{air} = \left(\frac{\rho_m}{\rho_{std}}\right)^{\frac{1}{3}} \tag{2}$$

where c_{air} is the unitless air density correction factor, ρ_m is the measured air density from the Enertile database in kg/m³ and ρ_{std} is the standard air density of 1.225 kg/m³. The original measured wind speed is then corrected for air density, by following equation

$$v_M = v_m * c_{air} \tag{3}$$

where v_M is the air density corrected wind speed in m/s and v_m the original measured wind speed also in m/s.

The ERA5 wind speed measurements are not available at hub height, hence the wind speed has to be extrapolated. Therefore, the power law according to Hellmann is used [76]. According to Gualtieri and Secci, the power law gives a more accurate representation of wind speed extrapolation than the logarithmic law [78]. Hence, the following equation of the power law is used to calculate wind speed at the actual hub height

$$v_H = v_M \left(\frac{h_H}{h_M}\right)^{\alpha} \tag{4}$$

with

$$\alpha = \frac{\ln\left(\frac{v_H}{v_M}\right)}{\ln\left(\frac{h_H}{h_M}\right)} \tag{5}$$

where v_H is the desired wind speed at hub height in m/s, v_M the wind speed at measurement height in m/s, h_H the hub height in meters, h_M the height in meters where the measurements are taken and α is the Hellmann exponent, also known as a unitless wind shear coefficient, which is calculated using Equation 5.

Based on the reference power curve, the resulting wind power output of the wind turbine is calculated using the following procedure

$$P_{tot} = P_{WTref}(v_H) * \mu_{WT} * c_{TL} * L_{WP} \tag{6}$$

with

$$c_{TL} = \frac{\left(\frac{A_{real}}{P_{real}}\right)}{\left(\frac{A_{ref}}{P_{ref}}\right)} \tag{7}$$

where $P_{WTref}(v_H)$ is the power output of the reference wind turbine as a function of wind speed in Megawatt (MW), μ_{WT} is 0.98 and is the unitless availability factor of the wind turbine, L_{WP} is 0.98 and summarizes the general losses of a wind farm. c_{TL} resembles a turbine layout correction factor, which adjusts the reference output to the actual wind turbine layout output. The actual wind turbine layout is cost-optimized according to three parameters, which will further be explained in the section Wind turbine design.

Equation 7 contains the variables used to calculate the correction factor A_{real} and P_{real} which are the swept area and the nameplate capacity of the actual selected wind turbine layout, A_{ref} and P_{ref} are the swept area and the nameplate capacity of the reference turbine.

Since the wind speed profile remains the same throughout one fishnet grid cell, the power of a single representative wind turbine (not the entire wind farm) is calculated at this stage of the assessment. In section Wind farm, the process of calculating the entire potential of one fishnet grid cell will be explained.

In order to obtain energy output for the representative wind turbine Equation 6 is expanded by a constant representing a time interval. Since the ERA5 wind speed data used for the calculation measures hourly values, a constant is added to represent this time interval of one hour. The total annual energy output E_{tot} is calculated using following equation

$$E_{tot} = \tau_{int} * \mu_{WT} * c_{TL} * L_{WP} * \sum_{i} P_{WTref}(v_H)_i \quad (8)$$

where τ_{int} is the time interval of the measurements (one h). The power output values are summed up for all hourly wind speed measurement points i in one year, which are 8760 h.

As a last step, full load hours FLH are calculated utilizing the equation below

$$FLH = \frac{E_{tot}}{P_{real}} \quad (9)$$

where P_{real} is the actual nameplate capacity of the wind turbine and E_{tot} is the total annual energy output. Once the FLHs for all grid cells are calculated, grid cells with similar FLHs are aggregated into potential classes. In case of wind energy, 73 potential classes are created. The potential classes are important to save computational power for the cost-related optimization.

FLH is a well-known metric in German speaking countries. Globally, however, the use of the Capacity Factor (CF) is more common, hence the capacity factor is also provided, using following equation to calculate it

$$CF = \frac{FLH}{8760} \quad (10)$$

where CF is the capacity factor and 8760 is the number of hours per year.

Wind turbine design

The configuration of the actual wind turbine is optimized using three design parameters. Depending on the location and its specific wind resource, Enertile chooses the cost-optimal configuration of a wind farm, taking into account following design parameters: Hub height, ratio between generator capacity and swept area and efficiency of the wind turbine in terms of its power curve.

In terms of hub height, Enertile chooses the configuration that has the least specific generation costs given the wind resource found inside the grid cell. Hub heights are optimized in 10 m steps between 90-140 m for the period until 2020. In 2050, the upper limit for the hub height is increased to 160 m, due to technological advancements. [71]

Two power curves from Enercon E82/2000 and Enercon E82/3000 are considered. The power curve from the Enercon E82/2000 model is used for locations with lower wind resources (IEC class 2-4)[5] defined by the International Electrotechnical Commission, whereas for locations with higher wind resources (IEC class 1) the power curve of the Enercon E82/3000 is considered. The power curves are displayed in the Figure

[5] The IEC wind classes are defined by the International Electrotechnical Commission and incorporates average wind speed, extreme wind gusts and turbulence. IEC class 1 is considered as high wind resource and IEC class 4 as very low wind resource [79]

6). The Enercon E82/2000 reaches its nameplate capacity at lower wind speeds than the E82/3000, optimal for exploiting low wind resource areas. [71]

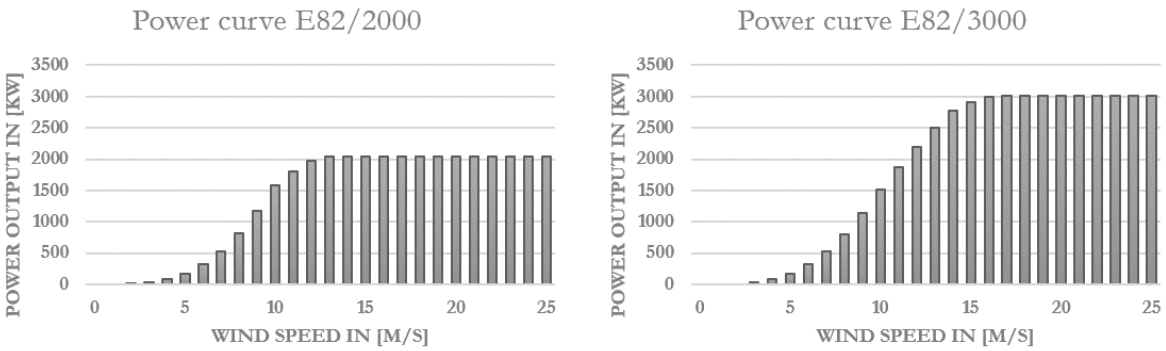

Figure 6: Reference wind turbine power curves [80]

The ratio of generator capacity to swept area is optimized using 10 W/m² steps in between the limits of 450-390 W/m² for class 1 IEC locations and 350-320 W/m² for class 2-4 IEC locations until 2020. [71]

Wind farm layout

Once the optimal wind turbine design parameters for the representative grid cell wind turbine are set, the feasible capacity per grid cell can be calculated, but first the required area of a wind farm (rate of km²/MW) has to be evaluated.

The spacing between the single wind turbines is chosen in order to lower wake effects [71]. In prevalent wind direction (indicated by the arrow in Figure 7) the spacing between the turbines is set to nine rotor diameters, whereas the spacing perpendicular to the prevalent wind direction is set to five rotor diameters (see Figure 7).

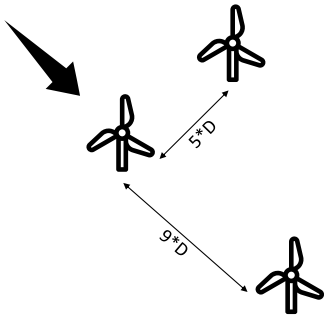

Figure 7: Wind farm layout [71]

Using the two spacing factors, expressed as ratio between rotor diameter and nameplate capacity, the required area demand can be calculated using following equation

$$A_{req} = \frac{5 * r_{sc} * 9 * r_{sc}}{0.9} \tag{11}$$

with

$$r_{sc} = \frac{D_{real}}{P_{real}} \tag{12}$$

where r_{sc} is the ratio of the rotor diameter D_{real} in meters and nameplate capacity P_{real} of the cost-optimized wind turbine layout in MW. The correction factor in the denominator of Equation 11 compensates for non-optimal geometries of the terrain which are existing in reality. [71]

The feasible capacity per grid cell pot_{wind} in MW is then calculated by using the equation displayed below,

$$pot_{wind} = \frac{A_{av}}{A_{req}} \tag{13}$$

where A_{av} is the available area per grid cell in square meters calculated using Equation 1.

Once the feasible capacity for all grid cells are calculated, the energy output of the entire grid cell is calculated using equation 13 and multiplying the result with the number of wind turbines installed inside the grid cell.

Cost related considerations

The total cost of installing a wind farm are based on the reference costs for a wind power plant from the assessment report IIe from the German Renewable Energy Sources Act with a focus on wind energy (original: EEG-Erfahrungsbericht) [81]. In 2013, which is the reference year, the average newly installed wind turbine had a hub height of 114 m and a peak capacity of 2500 kW at a rotor diameter of 90 m. The specific investment costs were 1200 €/kW. Based on these numbers, wind projects are split up into major Accounting Units (AccU) and its associated cost shares. The wind turbine itself for example is divided into three major accounting units: the tower, rotor blades and residual components. Residual components include the gearbox, generator, power converter, transformer and other smaller components. This cost structure is taken from IRENA [82]. Additionally, to the wind turbine costs, other wind project costs such as foundation, planning and approval costs are accounted for and displayed in Table 6. These additional costs are categorized according to Agora Energiewende, a German Think Tank [83].

All accounting units of a wind project have a share of the total cost of a wind project. In Enertile, all accounting units are assigned cost drivers, which are hub height, rotor diameter and nameplate capacity. Cost drivers are assigned to accounting units. The cost drivers define the increase or decrease in costs for the associated accounting unit. For further illustration an example is provided: The cost driver for the blades is the rotor diameter, meaning that if the Enertile algorithm decides to increase the rotor diameter for a more optimal energy ouput, the costs associated with the rotor blades increase. However, when Enertile decides to increase the hub height of the wind turbine tower, the cost for rotor blades will not increase, since an increasing hub height does not affect the rotor blades. The decision on whether the costs for a specific accounting unit increase or decrease, depends on whether the cost driver is higher or lower than the reference wind turbine. [71]

In addition to cost drivers, cost driver factors are introduced to account for cost drivers that affect the increase in cost more than other cost drivers. An example for clarification will be provided at the end of this section.

The total costs are then calculated using following equation

$$c_{tot} = \sum_{AccU} \left(\sum_{c_d} \left(\frac{p_{real}}{p_{ref}} - 1 \right) * c_{df} * cc_{ref} * s_{cc} \right) \tag{14}$$

where p_{real} is the parameter of concern (e.g. rotor diameter), p_{ref} is the parameter of concern from the reference wind turbine (e.g. rotor diameter of E82/2000), c_{df} is the cost driver factor, cc_{ref} cost of accounting unit (e.g. cost of the reference wind project tower), s_{cc} is the share of one cost driver on the total cost drivers (usually 1 except for the tower accounting unit). These factors are summed up over all cost drivers c_d and over all accounting units $AccU$, hence resulting in the total cost c_{tot}. [71]

The explanation of the exact parameterization is provided in the following paragraphs. As already stated, the individual wind turbine's cost structure is broken down into three main accounting units. As can be seen in Figure 8 the tower accounts for 26% of the cost of a wind turbine, followed by the rotor blades which are responsible for 22%. The remaining components account for 52% of the cost. As seen in Figure 8 the

cost driver for the rotor blades is mainly the rotor diameter, whereas for the tower three cost drivers are identified, the hub height, nameplate capacity and rotor diameter. [82]

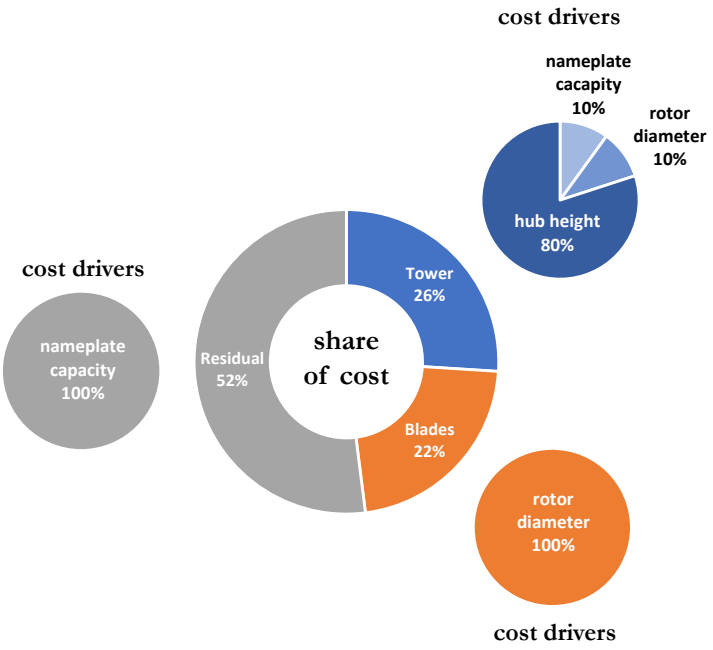

Figure 8: Cost structure and cost drivers of wind turbine [71]

The cost driver factors for the wind turbine are allocated according to Table 5. Pfluger et al. provide an example, where a 10% increase in hub height increases the tower costs by 16% because 80% of the cost driver for the tower is the hub height and the cost driver factor for the hub height is two (see equation 7). [71]

Cost driver c_d	Cost driving factor c_{df}
nameplate capacity	1
rotor diameter	2
hub height	2

Table 5: Cost driving factors for cost drivers [71]

Costs not related to the wind turbine itself are taken from the assessment report IIe from the German Renewable Energy Sources Act [81]. The entire list can be seen in Table 6. These costs are additional cost, which arise during a wind project.

Each cost parameter is assigned one of the three cost drivers (hub height, nameplate capacity and rotor diameter) already mentioned in the previous paragraph. In reality, costs can have more than one cost driver, but in this case a simplification is made. In the following paragraphs only definitions are provided for the accounting units, which are not self-explanatory. [71]

Land development costs refer to the preparational works that have to be undertaken in order to allow the installation of wind turbines. These costs have a strong variability, since wind farms located in a forest have higher land development costs than for example a wind farm located on grassland [81]. Nevertheless, the variation is not considered in Enertile, instead average values for a reference wind turbine is taken into account. The average cost is then linked with a cost driver, which is rotor diameter in case of land development costs. [71]

The cost category compensational payments is referred to payments required in case wind farms pose an interference to nature. These compensational payments are embedded in the German legislative system and is organized on a federal level. [81]

The cost category others in Table 6, includes costs such as financing costs. [81]

Pfluger et al. provides an example, where in case of a doubling of the installed wind farm capacity, by replacing 1 MW wind turbines with 2 MW turbines without increasing the number of turbines, the cost of grid connection would double from 79000 € to 158000 €. Additionally, also the internal cabling costs and other costs would double. [71]

Accounting unit AccU	Cost driver c_d	Cost driving factor c_{df}	Specific cost for reference plant
land development	rotor diameter	1	63 €/kW
grid connection	nameplate capacity	1	79 €/kW
compensational payments	rotor diameter	1	33 €/kW
planning and approval	rotor diameter	1	44 €/kW
foundation	hub height	1	58 €/kW
internal cabling	nameplate capacity	1	24 €/kW
others	nameplate capacity	1	24 €/kW

Table 6: Specific costs of the wind project divided in accounting units [71]

Operation and Maintenance costs are set at 60 €/kW in 2013. All costs are allocated an annual cost decrease of 0.5% due to a technology learning curve. [71]

3.4.4 Ground-mounted Photovoltaics

Enertile's internal PV model calculates electricity generation from solar power following the methodology of Gerda Schubert [84] and Volker Quaschning [85]. Gerda Schubert (nowadays Gerda Deac) was partly responsible for setting up the model for photovoltaic generation. The model for ground-mounted PV incorporates optimal tilt angle, south orientation, albedo and morning/evening shading.

Modelling

The PV model of Enertile takes into account two variable and several generic parameters for modelling PV output. In earlier versions of Enertile a mix three different module technologies were considered, but this has changed in the current version of Enertile, hence only c-Si modules are used for the analysis. The variable parameters are irradiance and module temperature.

The ERA5 solar irradiance dataset includes Global Horizontal Irradiance (GHI) and Direct Horizontal Irradiance (DirHI). In order to calculate the incidence irradiance onto the module surface, the ERA5 data has to be corrected for the actual tilt and azimuth angle of the module.

In Figure 9, the required angles for the upcoming calculations are displayed. $\vec{\boldsymbol{n}}$ and $\vec{\boldsymbol{s}}$ are the normal vector of the module and vector pointing towards the sun, respectively. γ_s and α_s are the elevation and azimuth angle of the sun, whereas γ_m and α_m are tilt and azimuth angle of the module surface. The angle enclosing both vectors $\vec{\boldsymbol{n}}$ and $\vec{\boldsymbol{s}}$ is called the surface incidence angle.

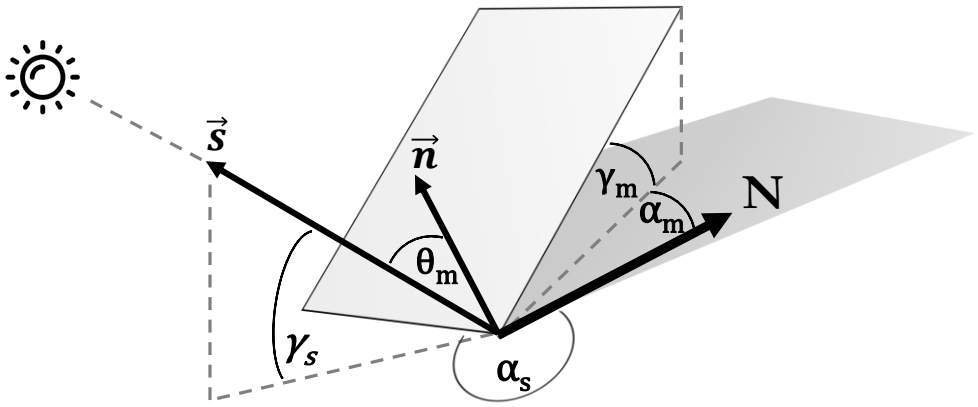

Figure 9: Solar modelling angles [85]

The basis of the solar modelling part is given by the following equation, which states that the total incidence irradiance is calculated by summing up direct I_{dir_mod}, diffuse I_{diff_mod} and reflective incidence irradiance I_{refl_mod}. The unit for the solar irradiation is W/m².

$$I_{mod} = I_{dir\_mod} + I_{diff\_mod} + I_{refl\_mod} \tag{15}$$

The direct component of the total incidence irradiance is calculated using Duffie and Beckman's approach [86]

$$I_{dir\_mod} = I_{DirHI} * \left\{ max\left(0, \frac{\cos\theta_m}{\sin\gamma_s}\right)\right\} \tag{16}$$

with

$$\theta_m = \cos^{-1}(-\cos\gamma_s * \sin\gamma_m * \cos(\alpha_s - \alpha_m) + \sin\gamma_s * \cos\gamma_m) \tag{17}$$

where I_{DirHI} is the Direct Horizontal Irradiance given by the ERA5 solar irradiance dataset, θ_m is the module surface incidence angle and γ_s is the solar elevation angle. The azimuth angle of the module α_m for ground-mounted PV is selected due south and the tilt angle of the module γ_m is optimized for energy output. θ_m is calculated using equation 17. Angles are inserted in radiant.

The diffuse part of the total irradiance is modelled using following equation

$$I_{diff\_mod} = I_{DiffHI} * 0.5 * (1 + \cos\gamma_m) \tag{18}$$

where I_{DiffHI} is the Diffuse Horizontal Irradiance (DiffHI) and γ_m is the tilt angle of the module surface. Since the DiffHI is not provided by the ERA5 dataset, it is approximated using the approach developed by Reindl et al. [87] with the following set of equations

$$I_{diffHI} = \begin{cases} I_{GHI} * (1.02 - 0.245k_T + 0.0123 * \sin\gamma_s), & k_T \leq 0.3 \\ I_{GHI} * (1.40 - 1.749k_T + 0.177 * \sin\gamma_s) , & 0.3 < k_T < 0.78 \\ I_{GHI} * (0.486 - 0.182 * \sin\gamma_s) , & k_T \geq 0.78 \end{cases} \tag{19}$$

with

$$k_T = \frac{I_{GHI}}{I_{GHI\_0}} \tag{20}$$

where I_{GHI} is the GHI given in the ERA5 dataset and k_T is the ratio between the GHI and the solar constant I_{GHI_0}. The solar constant I_{GHI_0} is the measured irradiance on a surface perpendicular to the irradiance outside of the atmosphere [85]. This constant varies in reality, however, in Enertile it is approximated with 1 367 W/m² [77].

The reflective part of the total irradiance is modelled using the method from Perez and Stewart [88] with following equation

$$I_{refl\_mod} = I_{GHI} * \varepsilon * 0.5 * (1 - \cos\gamma_m) \tag{21}$$

where ε is the unitless albedo of the ground surrounding the module. Since the albedo value is not measured, Quaschning [85] recommends the usage of an albedo of 0.2, which is used in Enertile [77].

Once the total irradiance is calculated, the PV model follows the methodology of Huld et al. to calculate PV module output by incorporating module temperature and irradiance into following equations [89]

$$P_{DC}(I_{mod}, T_{mod}) = P_{STC} * \frac{I_{mod}}{I_{STC}} * \eta_{pv}(I', T') \tag{22}$$

with

$$\eta_{pv}(I', T') = 1 + c_1 \ln I' + c_2 (\ln I')^2 + T' (c_3 + c_4 \ln I' + c_5 (\ln I')^2) + c_6 T'^2 \tag{23}$$

and

$$I' = \frac{I_{mod}}{I_{STC}} \tag{24}$$

and

$$T' = T_{mod} - T_{STC} \tag{25}$$

where P_{STC} is the power output at standard test conditions (STC), I_{STC} is the standard test condition incidence irradiance of 1000 W/m², η_{pv} is the instantaneous relative efficiency, c_{1-6} are empirical coefficients found in Table 7, T_{STC} is the STC module temperature of 25°C and T_{mod} is the actual module temperature, which is calculated using the formula explained in the next paragraph.

module coefficients	PV module technology		
	c-Si	CdTe	CIS
c_1	-0.017162	-0.103251	-0.005521
c_2	-0.040289	-0.040446	-0.038492
c_3	-0.004681	-0.001667	-0.003701
c_4	-0.000148	-0.002075	-0.000899
c_5	-0.000169	-0.001445	-0.001248
c_6	0.000005	-0.000023	0.000001

Table 7: Empirical coefficients for PV module technology [89]

T_{mod} under steady-state conditions can be estimated according to

$$T_{mod} = T_{amb} + \frac{c_T * I_{mod}}{1000} \tag{26}$$

where T_{amb} is the ambient temperature in °C and c_T are the temperature coefficients displayed for each module mounting setup in Table 8, which describes how much a PV module is heated by the incoming solar radiation. [77]

PV Module mounting setup	temperature coefficient c_T
on roof < 10cm	36
on roof > 10 cm	27
free standing	20
roof integrated	58

Table 8: Temperature coefficients for PV module technologies [77]

In terms of inverter conversion efficiency from direct current to alternating current, Schubert used the approach from Maĉedo and Zilles [90]. The modelling equation for relative inverter efficiency η_{inv} ,includes losses from self-consumption, losses proportional to current and ohmic losses which have a quadratic relationship to current

$$\eta_{inv} = \frac{P' - \left(k_0 + k_1 P' + k_2 P'^2\right)}{P'} \tag{27}$$

with

$$P' = \frac{P_{DC}}{P_{Inc}} \tag{28}$$

where k_{0-2} are empirical coefficients found in Table 9, P_{DC} is the actual output of the PV modules and P_{Inc} is the nameplate capacity of the inverter.

inverter coefficients	
k_0	-0.017162
k_1	-0.000169
k_2	0.000005

Table 9: Empirical inverter coefficients [90]

The final output P_{AC} of the solar power plant is calculated by including the inverter efficiency into following equation [77]

$$P_{AC} = P_{DC} * \eta_{inv} \tag{29}$$

PV farm layout

The feasible capacity per grid cell is calculated using following equation [71]

$$pot_{Solar} = A_{av} * c_{PV} \tag{30}$$

where pot_{Solar} is the feasible capacity per grid cell, A_{av} is the available area for installing ground-mounted PV farms in km² and c_{PV} is a generic factor of 40 MW/km². The generic factor was empirically determined according to data based on Germany. [71]

Cost related considerations

Similar to the modelling of wind power plants, PV system costs are also separated into accounting units according to the assessment report IIc from the German Renewable Energy Sources Act with a focus on photovoltaics [91]. This study was performed by the Center for Solar Energy and Hydrogen Research (original: Zentrum für Solarenergie- und Wasserstoff-Forschung ZSW) in cooperation with Fraunhofer IWES, Bosch and GfK.

All accounting units have associated costs, which are determined by interviewing solar installers all around Germany. Summing up all accounting unit costs for a reference plant of 5 MW, results in total system cost of 1000 €/kW in 2013 [91]. A 7% annual cost reduction rate between 2014-2020 is set for the PV module accounting unit. This technology learning curve is gradually decreased until it reaches 2% cost reduction between 2041 and 2050 [71]. A lower cost reduction rate of 0.5% is decided for the remaining accounting units, which include inverter, cabling, grid connection, mounting structure and others. The learning curve of these accounting units remain the same until 2050 [71].

OM costs are set to 1.5% of total investment costs and are gradually increased to 2% in 2050. Yet, the absolute OM costs decrease due to decreasing investment costs. The OM costs are set for the entire lifetime,

meaning that a PV plant constructed in 2020 will have annual OM costs of 15 €/kW, whereas a PV plant constructed in 2050 will have annual OM costs of 11 €/kW during the entire lifetime [71].

In Table 10 the predicted future costs of newly installed PV systems are shown. The future costs account for cost reduction rates mentioned above. The cost values shown in Table 10 are average values from the associated timespan. [71]

Timespan	specific investment cost	annual O&M cost
2014 - 2020	875 €/kW	15 €/kW a
2021 - 2030	715 €/kW	14 €/kW a
2031 - 2040	601 €/kW	13 €/kW a
2041 - 2050	541 €/kW	11 €/kW a

Table 10: Specific investment and OM costs of ground-mounted PV [71]

3.4.5 **Rooftop Photovoltaics**

Rooftop Photovoltaic power plants are also based on Schubert [84] and Quaschning [85] and modelled the same way as ground-mounted PV plants, with the exception of a few minor deviations, which are described in the following chapters.

Modelling

The underlying mathematical equations for modelling rooftop photovoltaic plants are the same as the ones used for modelling ground-mounted PV, with the only difference being the temperature development in the PV module. The module temperature increases at a faster rate, since ventilation is less effective for rooftop PV, compared to the ground-mounted PV.

PV farm layout

Since rooftop PV plants are only found on roofs, only areas declared as LULC class urban are used for installing rooftop PV. A utilization factor of 20% is set for urban areas. The utilization factor is based on a statistical assessment using spatial analysis of the German state of North Rhine Westphalia [71].

In order to account for dwellings facing in many different directions and different rooftop mounting types, the following mixture of rooftop PV power plants is considered (see Table 11). According to Table 11, most rooftop PV plants face exactly south and have a tilt of 37°.

Rooftop mounting setup	azimuth α_m	tilt angle Y_m	share
Type 1 - on roof with >10cm gap	140	37	3.29%
	180	32	3.94%
	180	37	9.87%
	180	42	3.94%
	220	37	3.29%
Type 2 - on roof with <10cm gap	140	32	3.36%
	140	37	8.41%
	140	42	3.36%
	180	32	10.09%
	180	37	25.23%
	180	42	10.09%
	220	32	3.36%
	220	37	8.41%
	220	42	3.36%

Table 11: Rooftop PV system layout mixture [77]

Cost related considerations

In case of rooftop solar a reference plant of 30 kW is chosen. This is due to a compromise between 5 kW systems installed on private dwellings and 500 kW systems installed on commercial or industrial buildings. The system costs associated with this reference plant are 1300 €/kW in 2013. Technology learning curves and OM costs are considered the same as ground-mounted PV, hence resulting in the costs found in Table 12.

Timespan	specific investment cost	annual O&M cost
2014 - 2020	1173 €/kW	19 €/kW a
2021 - 2030	1004 €/kW	18 €/kW a
2031 - 2040	879 €/kW	17 €/kW a
2041 - 2050	806 €/kW	16 €/kW a

Table 12: Specific investment and OM costs of ground-mounted PV [71]

3.5 Economic analysis

The economic analysis is based on two metrics: the LCOE and the Net Present Value (NPV). The LCOE per potential class is calculated using the results from Enertile. The LCOE is calculated for each potential class according to the following steps

$$ANC = \frac{(I_0 * ANF) + OM}{P_{inst}} \tag{31}$$

with

$$ANF_{t,i} = \frac{i * (1+i)^t}{(1+i)^t - 1} \tag{32}$$

concluding in

$$LCOE = \frac{ANC}{FLH} \tag{33}$$

where ANC are the annualized total cost, I_0 are the investment cost, ANF is the annuity factor, OM are the operation and maintenance costs, P_{inst} is the feasible capacity, i is the discount rate, t is a year during the lifetime of the considered technology and FLH are the full load hours. This method is a reduced version of the original LCOE calculation, since the assumption that OM costs remain the same throughout the lifespan is made. This simplified method comes with the advantage of lower computational requirements for large datasets. The discount rate is 7% and the economic lifetime for both wind and solar technologies is assumed to be 25 years[71].

The LCOE is a metric to compare costs throughout different electricity generation technologies. Nonetheless, it is not suitable to assess the viability of an investment, with the exception of the method used by Gass et al. [13]. Gass et al. assessed the economic wind power potential in Austria by calculating the LCOE and comparing it with the FiT. Therefore, they used a wind turbine lifetime of 13 years in order to be able to compare them with the Austrian support scheme period of 13 years. This approach is not applicable in this study, hence the NPV method is chosen as a metric to assess economic viability.

The NPV is calculated using a modified approach of the method used by McElroy et al. [92]

$$NPV = \sum_t nCF_t * (1 + IRR)^{-t} \tag{34}$$

with

$$nCF = R - OM \quad (35)$$

where nCF is the net cash flow, IRR is the internal rate of return, t is a year during the lifetime of the investment, R is the revenue and OM are the operation and maintenance costs. The IRR is assumed to be equal to the Weighted Average Cost of Capital (WACC). The WACC is calculated using the average of two reports from the Asian Development Bank [93] and IRENA [94]. The Asian Development Bank states a WACC of 8% for projects where risk is mostly on the private side and IRENA stipulates a WACC of 10% for non-OECD countries, hence resulting in an average WACC of 9%. Some project reports in this region support this assumption of choosing a feasibility IRR of 9% [95]–[97].

Since Mongolia has a FiT support scheme in place, the rates of that FiT are used for calculating revenue stream for the NPV during the FiT period, which is 10 years [98]. The detailed Feed-in Tariffs are displayed in Table 13. Wind and solar technologies receive different levels of FiT, with wind technologies receiving less that solar technologies. Furthermore, off-grid solutions receive a higher FiT than grid connected solutions, however, the off-grid solutions are not considered in this study, due to lacking information on demand.

Technology	Feed-in Tariff
Wind grid connected	0.08 - 0.095 $/kWh
Wind off-grid	0.10 - 0.15 $/kWh
Solar grid conected	0.15 - 0.18 $/kWh
Solar off-grid	0.2 - 0.3 $/kWh

Table 13: Feed-in Tariffs in Mongolia [98]

After the FiT period, it is assumed that the renewable energy technologies will participate in the electricity market of Mongolia, where a fixed electricity generation rate is set by the ERC and paid to the state-owned enterprises and independent power producers. The rates are different depending on electricity system. Since the CES is the electricity system with the highest demand by far, the rates in this region are considered. The detailed electricity rate structure of the CES area is displayed in Table 14. The payment from the ERC to the SOEs and IPPs amounts to 0.034 $/kWh generated electricity [99].

Expenses category	Price in MN Tugrik [MNT/kWh]	Price in US Dollars [$/kWh]
Generation	89.58	0.034
Import	10.70	0.004
Transmission	2.67	0.001
Transmission losses	8.47	0.003
Distribution	12.73	0.005
Distribution losses	31.70	0.012

Table 14: Electricity price structure of CES [99]

Since monetary values come from different sources using three different currencies (Euro, U.S. Dollar and Mongolian Tugrik) the exchange rates found in Table 15 are used for currency conversions. The exchange rate from Mongolian Tugrik to both Dollars and Euros is based on a 90 days average, whereas the exchange rate from Euros to Dollars is based on a 5-year average.

Currencies	Exchange rate	Source
Euro to U.S. Dollar	0.8834 €/$	[100]
Mongolian Tugrik to Euro	0.00034 MNT/€	[101]
Mongolian Tugrik to U.S.Dollars	0.00038 MNT/$	[102]

Table 15: Exchange rates of study currencies and source

According to the Energy Policy review report of the Asian Development Bank [44], import dependency from Russia and China has increased since 2007. The cost of imported electricity should be act as a price signal for investments in new capacity. Hence, the cost of imported electricity is assumed to be the general generation electricity rate.

As a next step, a zone with a diameter of 50 km and 100 km is established around the load center. Inside this zone viable wind and solar power plant locations are looked for, which could generate at lower cost than the imported equivalent. Only the WES and the DES are analyzed, since these are the energy systems that have a high dependency on electricity imports from the neighboring countries. The import electricity rates are assumed to be 77 $/MWh for the WES [5] and 80 $/MWh for the DES [39].

GHG emission avoidance by RES is calculated using the average carbon intensity of Mongolia coal power plants based on the data from the ERC. The average carbon intensity is calculated to be 1 390 tCO_2/MWh.

4 Wind and Solar - Geospatial Energy Resource Identification

The WiSo-GERI model is developed by the author of this thesis for Frauhofer ISI, hence in this chapter a detailed description of the WiSo-GERI is provided. This includes a description of the necessary preprocessing steps, the python code itself and additional implemented feature such as multiprocessing and progress monitoring.

The Wind and Solar - Geospatial Energy Resource Identification model, short WiSo-GERI, is a model for identifying suitable land for wind and solar power plants, considering geographical and anthropological restrictions. WiSo-GERI complements Enertile by adding a spatial level to the techno-economic analysis.

WiSo-GERI is developed in the framework of this Master Thesis for the Fraunhofer ISI with the aim to replace the already existing land suitability model used for previous studies by Fraunhofer ISI. Due to its multiprocessing capability, WiSo-GERI allows the usage of higher resolution data, while at the same time decreasing runtime of the model, compared to single process models. The code is structured in a way to allow the utilization of all cores of the Central Processing Unit (CPU).

To allow the model to run properly, some of the data must be preprocessed. These steps are elaborated in the section 4.1.

WiSo-GERI is divided into four major parts. The first part of the code allows a user to enter a country of interest (COI). The model then selects all relevant information accordingly. The second part of the code performs a LULC analysis on each fishnet grid cell located inside the COI. Therefore, the model accounts also for all restricted areas by adding another LULC named excluded. The third part of WiSo-GERI includes an analysis on slope inside each fishnet grid cell. The last part of WiSo-GERI performs an analysis on water depth and distance to shore, if the COI has access to an Exclusive Economic Zone (see Figure 10). A more elaborate description of the model is found in sections 4.2 to 4.8.

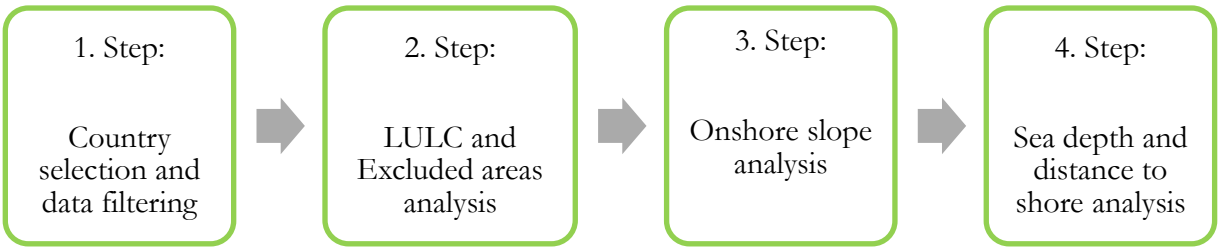

Figure 10: WiSo-GERI main steps

The foundation of WiSo-GERI resembles a global fishnet, which is a gridded net with spatial dimensions of 6.5 times 6.5 km. Each fishnet grid cell is assigned a unique *Area_ID,* allowing each grid cell to be addressed individually. Along with the *Area_ID*, the fishnet contains also information in which country or Economic Exclusive Zone (EEZ) it is located. This information is found in the attribute table in columns *FIRST_NAME* and *Territory1*. Another column in the attribute table is named Pol_type and defines whether the Maritime Exclusive Economic Zone solely belongs to one country or is a joined EEZ or even a disputed area. Disputed areas are not used for installing offshore wind farms.

All information extracted from relevant layers such as LULC, slope or bathymetry are extracted on a single fishnet grid cell scale. The extracted spatial information is then summarized and written to a text file for further processing in Enertile RE Potential.

4.1 Data preprocessing

4.1.1 Preprocessing of the LULC data

For the analysis of the land-use classes, the GlobCover 2009 raster data was selected, due to its global coverage and its high spatial resolution. This land-use and land cover data is available for the year 2009 at a spatial resolution of approximately 300 x 300 m. [103]

Originally, the GlobCover data includes 22 LULC classes, however, in preparation for the WiSo-GERI and Enertile model, these were reduced to twelve by reclassification. The reason for the reclassification is, that Enertile uses only twelve classes for its renewable energy potential calculation. The recategorized classes can be found in Figure 11. The GlobCover raster data is then stored in the WiSo-GERI geodatabase.

GlobCover2009 Classification		ENERTILE Classification	
Value	Label	Value	Label
11	Post-flooding or irrigated croplands (or aquatic)	03	Cropland
14	Rainfed croplands	03	Cropland
20	Mosaic cropland (50-70%) / vegetation (grassland/shrubland/forest) (20-50%)	02	Cropland natural
30	Mosaic vegetation (grassland/shrubland/forest) (50-70%) / cropland (20-50%)	05	Grassland
40	Closed to open (>15%) broadleaved evergreen or semi-deciduous forest (>5m)	04	Forest
50	Closed (>40%) broadleaved deciduous forest (>5m)	04	Forest
60	Open (15-40%) broadleaved deciduous forest/woodland (>5m)	04	Forest
70	Closed (>40%) needleleaved evergreen forest (>5m)	04	Forest
90	Open (15-40%) needleleaved deciduous or evergreen forest (>5m)	04	Forest
100	Closed to open (>15%) mixed broadleaved and needleleaved forest (>5m)	04	Forest
110	Mosaic forest or shrubland (50-70%) / grassland (20-50%)	07	Shrubland
120	Mosaic grassland (50-70%) / forest or shrubland (20-50%)	05	Grassland
130	Closed to open (>15%) (broadleaved or needleleaved, evergreen or deciduous) shrubland (<5m)	07	Shrubland
140	Closed to open (>15%) herbaceous vegetation (grassland, savannas or lichens/mosses)	06	Savanna
150	Sparse (<15%) vegetation	06	Savanna
160	Closed to open (>15%) broadleaved forest regularly flooded (semi-permanently or temporarily) - Fresh or brackish water	11	Wetland
170	Closed (>40%) broadleaved forest or shrubland permanently flooded - Saline or brackish water	11	Wetland
180	Closed to open (>15%) grassland or woody vegetation on regularly flooded or waterlogged soil - Fresh, brackish or saline water	11	Wetland
190	Artificial surfaces and associated areas (Urban areas >50%)	09	Urban
200	Bare areas	01	Barren
210	Water bodies	10	Water
220	Permanent snow and ice	08	Snow and Ice
230	No data (burnt areas, clouds,…)	12	No data, Excluded

Figure 11: Reclassification of LULC classes for Enertile

4.1.2 Preprocessing of the excluded areas

Some facilities or landmarks such as airports do not allow to have wind or solar power plants in close proximity, hence some of the restrictive landmarks are given a buffer zone, which resembles an exclusion area for the construction of wind and solar farms. The same procedure is applied to protected areas, settlements, roads, railway tracks, the shoreline and navigable waterways.

The sizes of the buffer zones for the different restrictive areas are found in section 3.3.1. The exclusion zones are then stored as separate maps inside the WiSo-GERI geodatabase.

A special case is the settlements map. The settlements map is derived from the LULC map by extracting all raster cells classified as Urban. A buffer ring with a width of 1000 m around the urban zones is created, according to sources specified in section 3.3.1. Since it is a ring, the raster cells classified as urban are not added to the exclusion zones, because the urban LULC must remain available for installing urban rooftop solar.

4.1.3 Preprocessing of the slope data

Information on terrain slope is highly relevant for both wind and solar energy technologies. Wind farms for example are limited in terms of slope, since it is difficult to operate cranes and transport large machinery on land with high slopes [7].

In order to obtain information on slope, the DEM named GMTED 2010 is obtained from the USGS. The slope is derived from GMTED 2010 using an arcpy function to derive slope from a digital elevation map

called *Slope*. The slope is calculated in degree and the z-factor is set to be 1, since the units of the x, y and z values are all measured in the same unit: meter. The newly created map is stored in the WiSo-GERI geodatabase.

4.1.4 Preprocessing of the Bathymetry data

The bathymetry data needed to be transformed to an accessible data format for ArcGIS, before being projected. The global geodata of GEBCO is only provided as a netCDF file. Therefore, the netCDF is first transformed into a raster layer, using function *Make netCDF Raster Layer*. Following, the raster layer is stored in a geodatabase, where it is assigned the correct geographic coordinate system and projected into the correct projection.

4.2 Input data screening

Initially, three inputs must be entered by a user of WiSo-GERI. The user chooses the country on which the analysis should be based upon, by entering the name of that country. Additionally, the user has to enter whether or not the COI has access to a Maritime Exclusive Economic Zone, by setting a Boolean variable either to True or False. If the COI has access to an EEZ, the user will also have to enter the country name into another variable, defining the name of the EEZ. In case the user sets the variable defining the existence of an EEZ to False, parts of the code such as the analysis on sea depth and distance to shore will be skipped.

A function defined as *cntry_check*, verifies whether the name entered by the user is found in the attribute table of the administrative country borders map. Another function defined as *eez_check*, verifies if the name of the EEZ entered by the user exists in the attribute table of the Maritime Exclusive Economic Zone map.

After the user input is defined, all paths to the different geodata sources are predefined and stored in variables. A user may change the input geodata by replacing the hyperlink leading to a source. All geodata is checked if it has the correct projection by a function called *prj_check*.

4.3 Country selection process

After defining all variables in the step above, the code selects the entered country by an arcpy function named *SelectByAttribute*. This function selects all fishnet grid cells that have the country name attribute of the selected country that is entered and isolates it by copying the features. If an EEZ exists, it also isolates all grid cells, which are located solely in the EEZ. Furthermore, a combination of both grid cells found on the mainland and the EEZ are isolated. In case of an existing EEZ, three temporary layers are created, whereas if no EEZ is identified, only one temporary layer is created.

4.4 LULC analysis

The result of the LULC analysis is a text file containing 13 columns separated by a semi-colon. Area_IDs are found in the first column. Written into the following twelve columns are percentage shares of each LULC class. Excluded areas are collectively included as LULC class number twelve. The percentage shares are calculated for each single fishnet grid cell and linked to the corresponding Area_ID. An exemplary result table can be found in Table 16. The result table is transferred to Enertile, where it is further processed to obtain the techno-economic wind and solar potential. More details on the following procedures in Enertile can be found in section 3.4.

AREA_ID	LULC1	LULC2	LULC3	LULC4	LULC5	LULC6	LULC7	LULC8	LULC9	LULC10	LULC11	LULC12
10532113	0	2.4	0	0	93.28	0.48	0	0	0	0	0	3.84
10532111	21.28	0	0	0	14.4	61.12	0	0	0	3.2	0	0
10532112	0	0	0	0	55.52	44.48	0	0	0	0	0	
10538281	0.48	11.36	0	0	57.76	27.52	0	0	0	0	0	2.88
10538279	3.52	9.28	0	0	32	53.6	0	0	0	1.6	0	0
10532115	4.64	0.96	0	0	36.8	47.68	0	0	0	2.72	0	7.2
10538278	0	10.24	0	0	70.4	19.36	0	0	0	0	0	0
10525948	15.36	0.48	0.32	0	6.72	32.64	0	0	0	0	0	44.48
10525944	21.92	0.32	0	0	4.96	63.68	0	0	0	7.2	0	1.92
10525947	14.24	0	0	0	6.72	51.2	0	0	0	0.48	0	27.36
10525946	20.16	0	0	0	11.68	59.84	0	0	0	0	0	8.32
10538282	0	0	0	0	56.48	43.52	0	0	0	0	0	0
10532114	0.32	7.36	0	0	76.64	14.56	0	0	0	0	0	1.12
10538280	1.92	21.44	0	0	36.32	34.4	0	0	0	4.64	0	1.28
10525945	8.16	0	0	0	5.28	76.8	0	0	0	0	0	9.76

Table 16: Exemplary result table of – LULC analysis

In short, the code overlays the Fishnet, the excluded layers and the LULC raster file and analyses the overlapping features inside each individual fishnet grid cell. The excluded areas are added as a new LULC class and then an occurrence statistic is created on a grid cell basis. This process is graphically depicted in Figure 12.

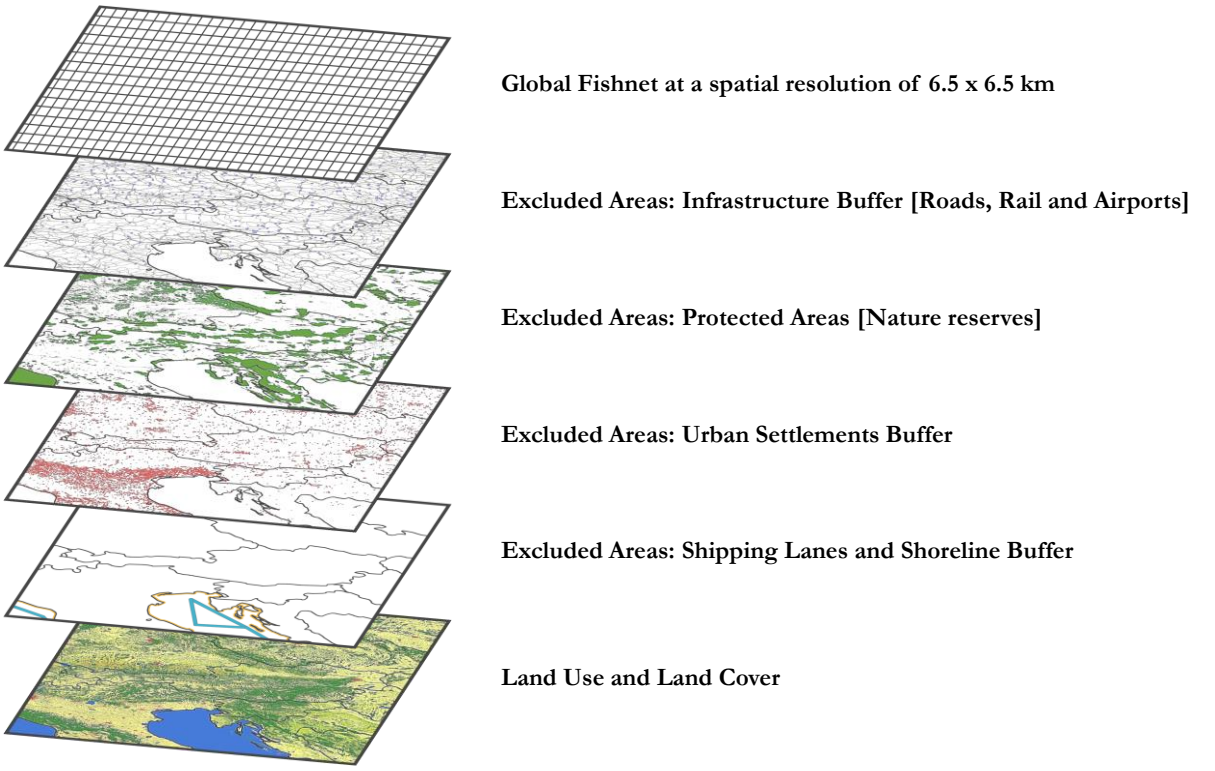

Figure 12: Layer visualization – LULC analysis

In the following paragraphs a workflow description of LULC analysis in WiSo-GERI is given, describing how to obtain the result table shown in Table 16.

The LULC block of the code starts with making a date stamp, meaning that it will store the current date in a variable. As a next step WiSo-GERI creates a text file including the date stamp and the three-letter short name of the COI in the file name. A header is written into the text file, which is indicated by the first row in Table 16. A *SearchCursor* scans all single grid cells of the isolated fishnet for two attributes: The Area_IDs and the geographical extents stored as four latitude/longitude coordinates resembling the corners of each grid cell. All five attributes are then stored in a dictionary, named *extDict*, with a corresponding counter ID, which is increased after every successful scan of a single fishnet grid cell.

As a next step WiSo-GERI loads all relevant layers, which include the global LULC layer and all excluded areas layers and stores them into a list. Depending on whether the COI is a landlocked country or not, different excluded areas are loaded. If the COI has access to an EEZ, two additional layers relevant for the offshore analysis are loaded.

After loading all layers, the multiprocessing stage begins, by first identifying all available cores of the CPU. A pool is initiated, which distributes the tasks among the CPU cores. In this case, the number of distributed tasks equal the number of CPU cores. In order to avoid overwriting mistakes, which could occur when multiple cores start writing the results into a text file at the same time, a file lock with the help of a manager function is initiated and stored as input variable.

A self-developed worker function named *execute_LULCanalysis*, which is responsible for the LULC analysis, will be called by the pool. Since, the multiprocessing module only allows one input into a worker function, the instance named *partial* is called to allow multiple inputs. The inputs to the worker function include: a file lock, a short name of the COI, the date stamp, the Boolean asking for an existing EEZ, the global LULC map and a list containing all excluded area data paths. The most important input is the *extDict* which defines that *execute_LULCanalysis* is executed on a single grid cell level. Concretely, this means that for example if eight CPU cores are available the LULC analysis is performed by parallelly computing eight grid cells per batch. This procedure is continued until all isolated fishnet grid cells are evaluated.

In the following paragraphs, the workflow of *execute_LULCanalysis,* which is the actual spatial analysis, is described. The worker functions responsible for the LULC, slope and sea depth analysis are found in a separate script (WiSoGERI_Worker.py) to ensure readability of the code. Once executed, *execute_LULCanalysis* starts with unpacking all input variables and storing them in new variables. The five variables contained in the *extDict* are also stored in new variables and the extent variables are directly used to define the extent of the current working environment, meaning that henceforth all operations will be performed on the extent of one specific fishnet grid cell.

An example area has been picked in order to display the procedure followed by *execute_LULCanalysis* (see Figure 13). This figure includes the GlobCover base layer depicting the different LULC classes, 15 fishnet grid cells and three exclusion area layers. A feature of the first exclusion layer is found in the lower right corner of the map in the shape of a lilac circle, depicting an airport (including buffer zone). Additionally, two road and one railway track features are also contained in Figure 13. They represent the other two exclusion layers. Due to the limited extent of the example area, not all exclusion layers are included.

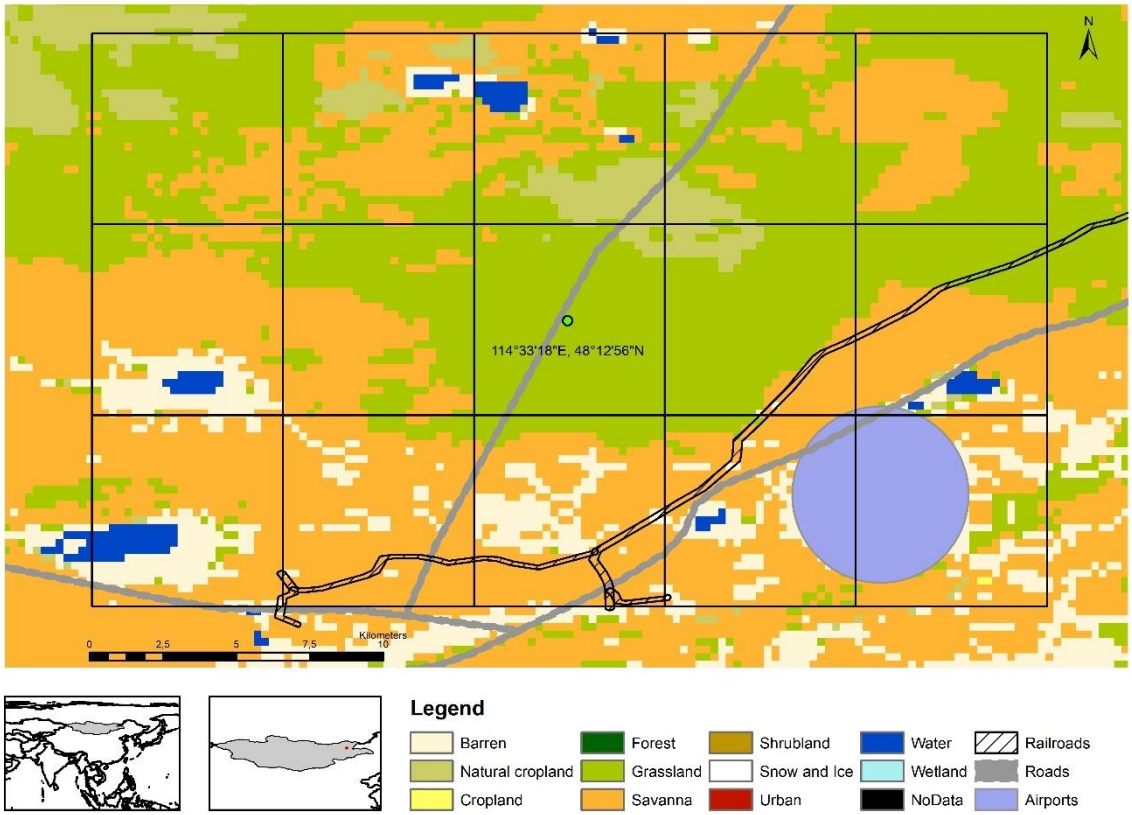

Figure 13: Layering of relevant maps

After the working extent is limited to one fishnet grid cell, a *RasterToPoint* operation is performed. This operation turns a raster file into a vector file, by turning all individual raster tiles into points and also transferring the underlying LULC value contained in the individual raster tile to the point. This conversion from raster to point file is necessary to access the individual LULC values of the raster tiles.

The newly created point file and all exclusion area layers are then converted into feature layers, using *MakeFeatureLayer*. Converting a vector file into a feature layer will allow the usage of the *SelectByLocation*. *SelectByLocation* will select all points in the point file, which intersect with one of the exclusion areas. The selection process is continued until all relevant exclusion area layers are accounted for.

Then the values contained in the selected points are overwritten and given the value 12, which is the 12th LULC class named excluded. This value replacement is performed by the *UpdateCursor*. The procedure is repeated until all excluded areas are incorporated into the point file. In Figure 14, one of the 15 fishnet grid cells from Figure 13 is picked to showcase the *RasterToPoint* operation and the exclusion procedure. In Figure 14 all points intersecting with the excluded areas appear in red and contain the LULC value 12. All other points maintain their original LULC value and appear in dark-grey. The non-excluded area is also called evaluation area.

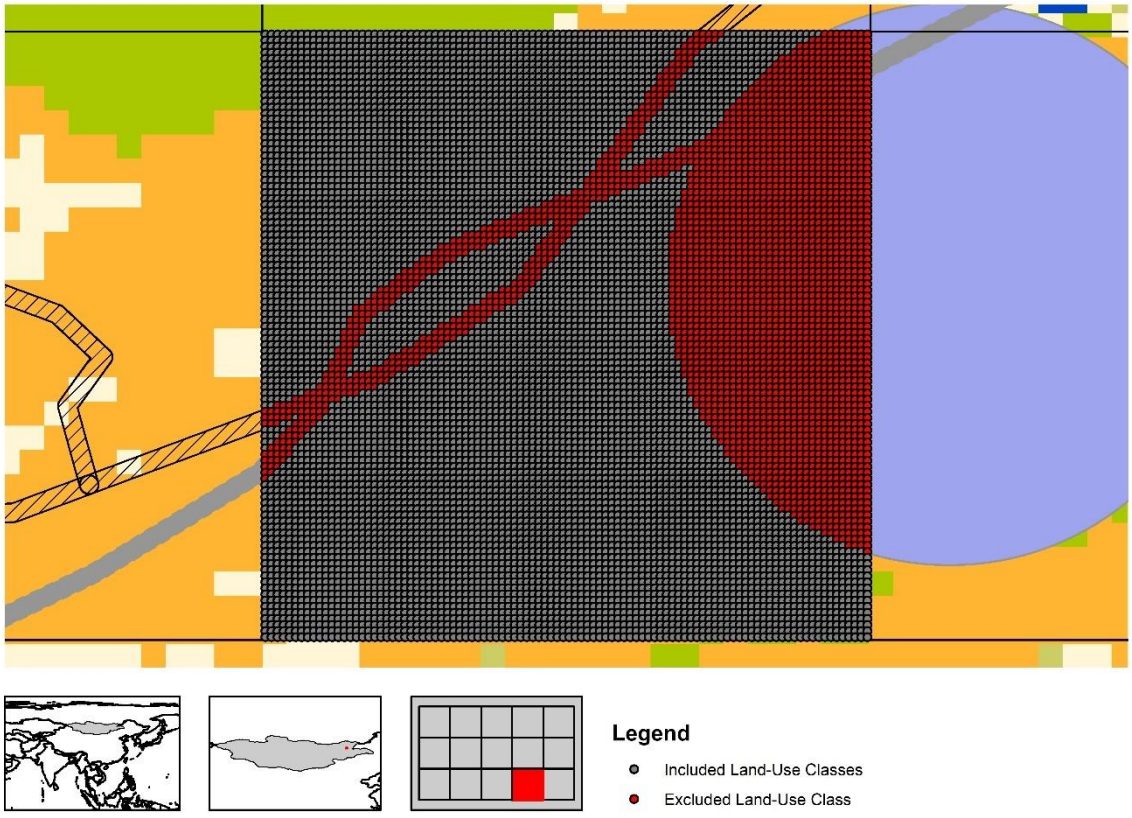

Figure 14: Raster to Point and exclusion operation

Two *SearchCursors* make up the next step of the workflow. The first one is used to count all points in the point file, giving the total number of points, which is equivalent to the number of raster tiles. The second *SearchCursor* scans all points of the point file for their LULC class value and creates an occurrence statistic of each LULC class. All twelve occurrence numbers are divided by the total amount of points and multiplied by 100 to get the occurrence percentage shares of each LULC class (see Table 16). Together with the Area_ID of the fishnet grid cell, all 12 values are stored in a list and are then written to a text file. Before the text file is opened, a file lock is acquired, in order to avoid simultaneous writing inside the text file by different parallel processes run on different CPU cores. Then the result list is written into the text file, after which the file lock is released, granting writing access for other processes.

4.5 Slope analysis

The result of the slope analysis is another text file containing two columns. The first column again contains the Area_ID and the second column contains the average slope in degrees found inside the fishnet grid cell with the corresponding Area_ID. An exemplary result table is displayed in Table 17. The same example area as in section 4.4 is used for the slope analysis, due to consistency reasons.

AREA_ID	AVERAGE_SLOPE
10532111	2.03
10532113	1.57
10538281	1.34
10532112	1.45
10525948	2.11
10532115	1.09
10538279	0.97
10538278	0.88
10525944	1.01
10525947	0.97
10525946	1.12
10538282	1.32
10525945	2.35
10532114	1.40
10538280	2.16

Table 17: Exemplary result table – SLOPE analysis

In summary, the code overlays the Fishnet and the slope raster file (see Figure 15) and calculates the average slope found inside each grid cell. In the following paragraphs a workflow description of Slope analysis in WiSo-GERI is given, describing how to obtain the results shown in Table 17.

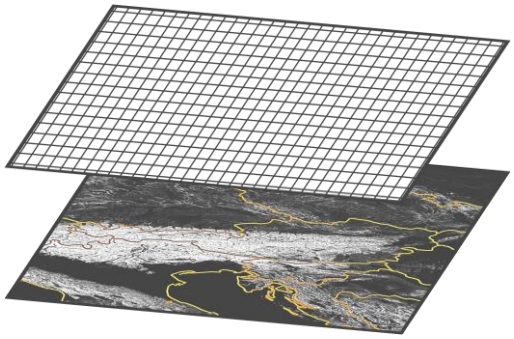

Figure 15: Layering visualization – Slope analysis

Similar to the LULC analysis, the program starts by creating a new text file and writing a header. The *SearchCursor* scans a different isolated fishnet, depending on whether it is a landlocked country or not. In case of a country with access to an EEZ, the *SearchCursor* scans the isolated fishnet, which only includes grid cells located onshore. The *SearchCursor* scans again for geographical extent and Area_ID, which are then stored in a dictionary.

The following tasks are the same as the ones described in the LULC analysis, with the only difference being that the average slope and not an occurrence statistic is made.

4.6 Bathymetry and distance to shoreline analysis

The analysis on sea depth and shoreline distance is a conditional part of the code, since this analysis is only relevant for countries connected to an EEZ. The results yielded by this analysis are displayed in Table 18. In case of the sea depth assessment, the average depth of all raster tiles found inside a fishnet grid cells is sufficient information for Enertile. The distance from the shoreline to the fishnet grid cell is analyzed by measuring the distance from a separate vector shapefile of the COI's coastline and the center of the fishnet grid cell, hence just resembling a good enough approximation. The distance to shoreline parameter is measured in kilometers and the average depth in meters. Since the example area in Mongolia used for showcasing the results in the previous two sections is located onshore, a new example area several kilometers of the coast of South Korea is selected to create an illustrative Table 18.

AREA_ID	DISTANCE_SHORELINE	AVERAGE_DEPTH
9909509	86.72	-2700.75
9915676	81.70	-2656.86
9915677	85.87	-2729.09
9909510	90.67	-2669.10
9903343	95.96	-2688.29
9903344	99.80	-2563.34
9915678	88.77	-2751.96
9903342	92.24	-2742.75
9909508	82.88	-2690.99
9909511	94.72	-2379.13
9909512	98.39	-2580.75
9903341	88.63	-2587.38
9903345	103.74	-2577.00
9915679	90.42	-2763.46
9915675	77.62	-2707.61

Table 18: exemplary result table – DEPTH analysis

The sea depth and distance to shoreline part of the WiSo-GERI, henceforth referred to as depth analysis, commences with a conditional statement asking, whether the variable asking for an existing EEZ is set to true or to false. In the absence of an EEZ the main script will skip this part.

As a first step, a text file is created, and a header is written into it. Then a map with a global extent is scanned for its global XY coordinates and stored in a list. This is necessary to allow a functioning distance analysis. More details are described later in this chapter.

Similar to previous analysis steps, the extent variables of all offshore fishnet grid cells and the Area_IDs are scanned and stored in a dictionary. Input variables to the multiprocessing instance are the bathymetry layer, a shapefile representing the country's coastline, the global extent list, the fishnet extent dictionary, and the offshore fishnet itself. Once these inputs are defined, the multiprocessing module is activated and initiates the *execute_DEPTHanalysis* function.

The *execute_DEPTHanalysis* function first extracts the global extent XY coordinates and expands the working environment's extent to global. Then all other variables are unpacked and stored in new variables. Afterwards the file containing the actual fishnet (*FishnetG_EEZ*) is converted into a feature layer and the grid cell of interest is selected by *SelectByAttribute*. A *FeatureToPoint* instance is executed upon the selected grid cell, which locates the center of the square of the fishnet grid cell and creates a center point feature. This point feature is then used for another function named *Near* to measure the shortest geodesic distance between the point feature and the shoreline of the COI. After that the distance value is stored in a variable.

The program then continues by limiting the working environment's extent to the same fishnet grid cell used for the distance analysis. Now the bathymetry map is added and converted to a vector file by *RasterToPoint*. Two *SearchCursors* then calculate the total amount of points and the sum of all point values, which in this case resemble the sea depth in a single raster tile. Those two values are then used to calculate the average sea depth in this fishnet grid cell, by dividing the sum of the sea depths by the total number of points. The average sea depth is stored in a variable. Together with the Area_ID and the shoreline distance, the average sea depth is initially written into a result list and then into the text file. The file lock is also used here, to avoid overwriting issues due to the multiprocessing module.

4.7 Progress monitoring

The tqdm module is integrated into the code to improve usability of WiSo-GERI. This module allows to monitor the progress of the code by showing the number of fishnet grid cells that have already been evaluated and the remaining fishnet grid cells. A separate module such as tqdm is necessary, since multiprocessing makes it harder to track progress, due to simultaneous task processing.

Included in the progress monitoring is a progress bar and an evaluation rate indicator with the unit seconds per Grid Cell needed. (see Figure 16)

Figure 16: Progress Bar implemented in WiSo-GERI

4.8 Runtime optimization

Initial code runtime tests have shown, that it would take several days for larger countries to process amounts of data, when not implementing the multiprocessing module. To allow for the code to process the data in a reasonable amount of time, the *multiprocessing* module is included, hence unlocking the utilization of all existing cores found in the CPU, instead of just one. This required to divide the procedures into smaller tasks, henceforth addressed as microtasks. This is achieved by performing the procedures described in sections 4.4 to 4.6 on an individual fishnet grid cell basis, instead of the entire fishnet. The microtasks are then distributed by the *multiprocessing* module to all CPU cores. With the help of the *multiprocessing* module, the microtasks can be processed parallelly instead of consecutively. Processing parallelly reduces runtime.

5 Results

This chapter presents the results of the analysis, which is based on the methodology described in the previous chapters. The results for all three investigated technologies are separated into a geographical, technical and economic potential. A sensitivity analysis and the impacts on energy security and environmental sustainability are described. The results are discussed in the end.

5.1 Onshore wind power

Onshore wind power is calculated according to the methodology described in chapter 3. The results are further divided into three potentials: the geographical, the technical and the economic potential using the definition of Hoogwijk [47].

Additionally, a sensitivity analysis on the economic potential is provided. For visibility reason, the following maps are changed to a distance preserving projection.

5.1.1 Geographical potential

The geographical potential is defined as the available area for installing wind power plants, according to Hoogwijk [47], which is also the definition used in this analysis.

Initially, WiSo-GERI excludes areas, that are unsuitable for installing wind farms, followed by the exclusion of slopes exceeding 13.5° by Enertile. The grid cells containing average slopes above the threshold, are added to the LULC class excluded. The remaining areas are evaluated and suitable area proportions per LULC class are calculated, according to the utilization factors defined in Table 19.

Around 271 024 km² are excluded by WiSo-GERI, which is the equivalent size of New Zealand [104]. An additional 54 407 km² are excluded, due to the upper slope threshold for wind turbines. In sum, 325 431 km² of Mongolia's territory is not suited for installing wind farms. The total excluded area is equivalent to the size of Norway, to put this into perspective [105].

In relative terms, 19.26% of the total land area of Mongolia are made available for installing wind farms, which are 300 727 km² in absolute numbers. This is about the size of Italy [106].

LULC class	Utilization factor	Available area	Utilized area
	[-]	[km²]	[km²]
Barren	25%	682 937	170 734
Cropland natural	20%	52 142	10 428
Cropland	20%	41 366	8 273
Forest	10%	17 967	1 797
Grassland	25%	119 371	29 843
Savanna	25%	315 336	78 834
Shrubland	25%	3 262	815
Snow and Ice	15%	24	4
Urban	0%	135	0
Water	0%	3 588	0
Wetland	0%	2	0
Excluded Areas	0%	325 431	0

Table 19: Utilized area - wind

5.1.2 Technical potential

The technical wind potential of the entire suitable area found in Mongolia using the definition of Hoogwijk [47] is 2.126 TW of installed capacity. 2.126 TW of installed wind capacity would yield 2.597 PWh/year. This amount of electricity could have supplied approximately half of the Chinese economy with electricity in 2016 [107].

In comparison, the study performed by NREL in 2001 estimated a total technical wind power potential capacity of 1.1 TW that could deliver around 2.5 PWh/year. Another study performed by Sheng et al. [29] estimated a total of 0.963 TW, however they only included a 200 km area around the Central Energy System, hence only analyzing 192 607 km².

IRENA extrapolated the numbers of the NREL study, stating that the technical wind power potential capacity could be four times as high as stated in the NREL study, considering technological advancements. This updated potential could generate three times as much electricity as stated in the NREL study. [5]

In order to grasp the spatial distribution of the technical potential, several figures are provided in the following paragraphs. Figure 17 shows the installed potential per grid cell, where one grid cell has an area of 42.25 km².

Most of the country is suitable for installing between 70 and 75 MW/42.25 km². This is mainly due to the favorable LULC classes found in Mongolia, which allow high utilization factors. Except for some protected nature reserves, almost the entire southern part of the country allows for an installation of 70 to 75 MW/grid cell. This is due to the fact, that the Gobi Desert is located in that area. The Gobi Desert stretches from the south to the south-east of the country [108]. The remaining area of the country mainly consists of barren land, savannas and grassland, also allowing for installing high capacities. Only in the north, forests start to appear, which lessen the utilization rate per grid cell.

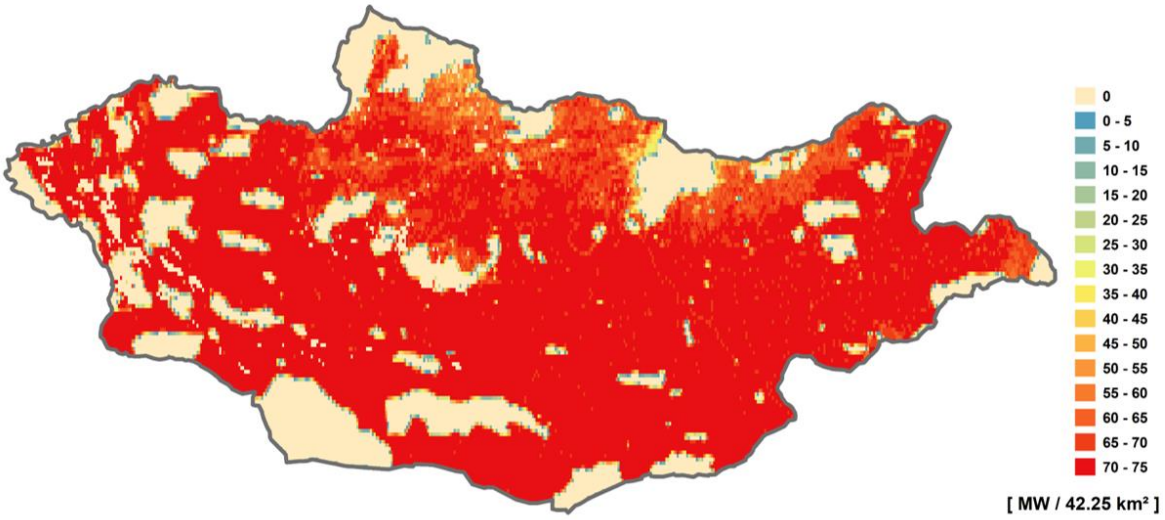

Figure 17: Technical potential capacity map - wind

When combining the potential capacity map with annual wind speed data, the annual energy output per grid cell can be calculated. The energy output map yields a more differentiated picture than the potential capacity map. The energy output intervals for Figure 18 in terms of coloring this map are set to 15 GWh/grid cell year, with an exception of the last energy output interval.

As can be seen in Figure 18, the grid cells with the highest productivity are limited to the south and south-east of the country. The maximum energy output per grid cell is 198 GWh. The black dot indicates the location of the capital Ulaanbaatar, where approximately 50% of the Mongolian population is residing [6]. Grid cells with an annual energy output between 120 – 150 GWh are located in close proximity to the capital, which also resembles a major load center.

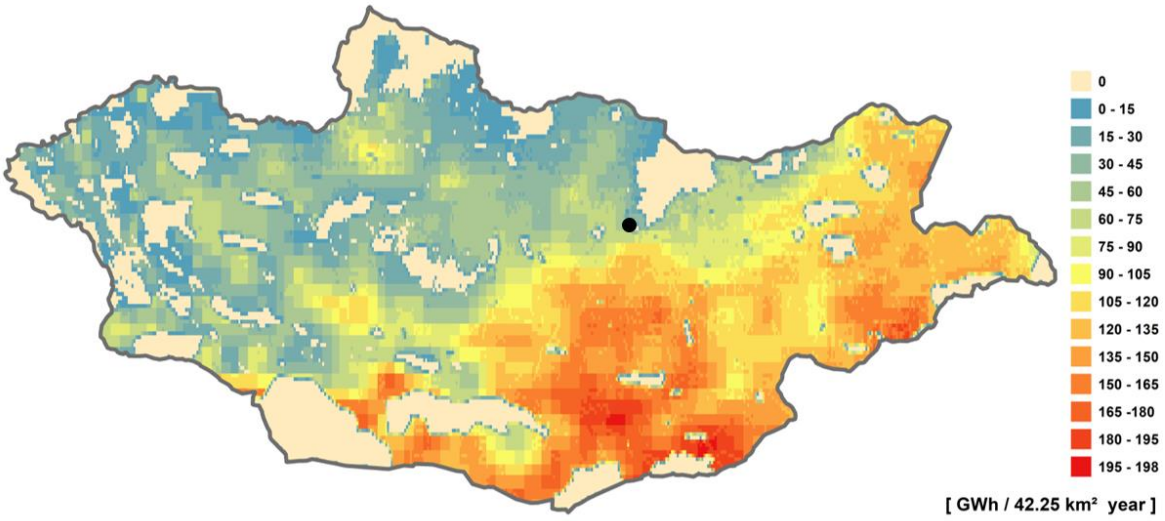

Figure 18: Technical potential energy map - wind

In terms of capacity factor distribution, following picture (see Figure 19) is revealed. The figure shows a similar distribution as Figure 18, however it appears to have a much coarser resolution. This is due to the fact that, there are limited wind data points, 2 429 to be exact, in Mongolia and all surrounding grid cells are allocated the same wind speed data if there is no other wind data point closer. The locations with the highest capacity factors are also located in the south and south-east of the country, where capacity factors between 31.6% and 17.5% are found. The highest capacity factor for wind turbines in Mongolia is 31.6%.

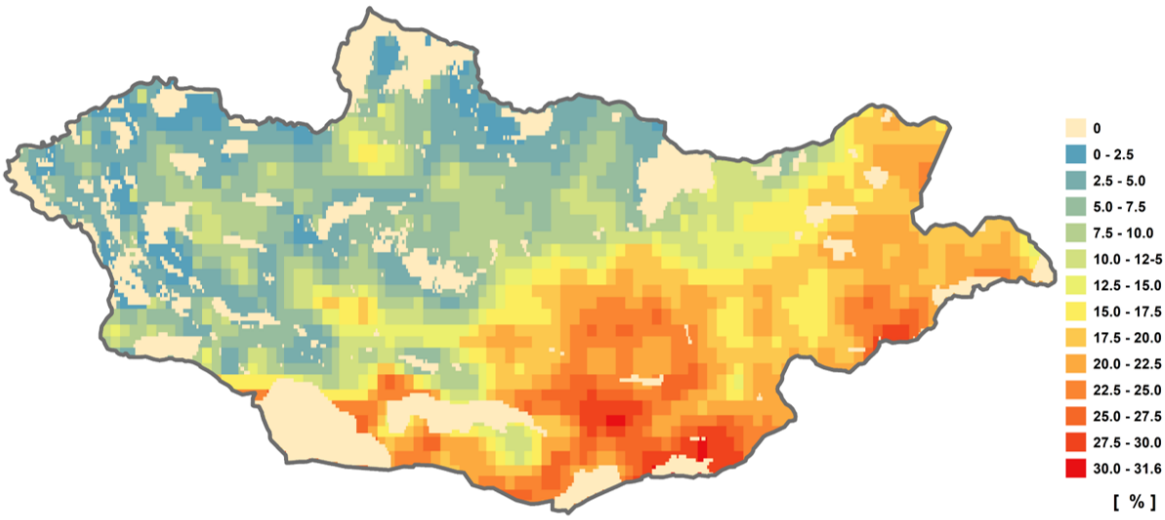

Figure 19: Capacity Factor map - wind

5.1.3 Economic potential

According to the NPV calculation, where input parameters are the FiT rate (95 $/MWh) for the first ten years and the fixed electricity rate of the ERC for the remaining 15 years, it is economically feasible to construct wind farms with a total capacity of 1.15 GW. The associated full load hours range from 2 656 to 2 764 h, which compares to a CF of 31.56% and 20.32%. Given the wind resources at those locations, 1.15 GW of wind capacity could generate 3.05 TWh of electricity. To put this into perspective: this is about half the domestic electricity generation of Mongolia in 2018 [39]. The economically feasible wind locations

are mostly found in the south of the country. A small share of the economic potential is also found in the south-east of Mongolia close to the border to China.

In terms of electricity cost, the economically feasible wind power plants could generate electricity at an average LCOE of 73.14 $/MWh or 64.62 €/MWh. This equals to 190.05 MNT/kWh. When comparing the 190.05 MNT/kWh to the 89.58 MNT/kWh electricity rate paid by the ERC to the SOEs and IPPs in 2019, it can be seen, that wind energy would be economically unfeasible in Mongolia without the FiT support scheme [99].

Figure 20 shows the LCOE across the country. Locations in the southern and south-eastern regions can generate electricity at LCOE between 70 and 120 $/MWh. In the north and the north-west, locations with LCOE higher than 130 $/MWh can be found (see Figure 20). Locations with an LCOE higher than 130 $/MWh are colored in the same color as excluded areas in this figure.

The shortest distance from the load center Ulaanbaatar to a location with a LCOE of 80-85 $/MWh is approximately 220 km. In order to reach the wind resource richest locations with a LCOE of 70-75 $/MWh a distance of 670 km has to be crossed. However, the 50 MW Salkhit wind farm operating since 2013 is located even closer to Ulaanbataar, with a distance of around 70 km [40].

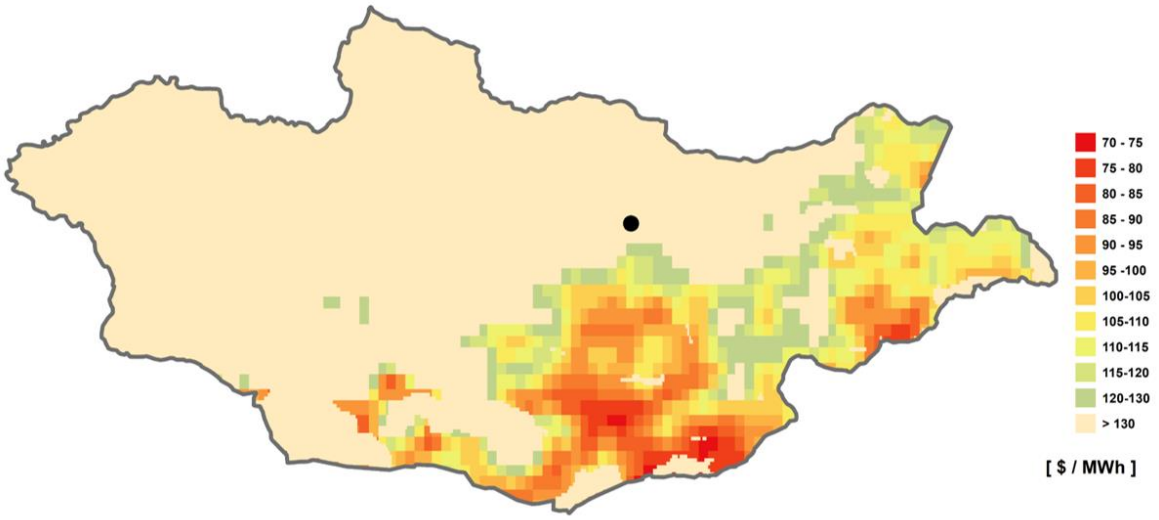

Figure 20: LCOE map - wind

2050

So far, all results have been based on the year 2020, yet, due to technological advancements costs are reduced over time, according to the learning rates found in section 3.4.3. Costs for the highest potential class can be reduced by around 8 $/MWh to 62.4 $/MWh. In 2050, many more locations generate at costs lower than 70 $/MWh.

In 2050, the total economically feasible potential, given the same FiT and electricity rate of 2019, would be 156.35 GW. If the entire economically feasible potential would be constructed it could provide around 437.84 TWh of electricity per year, which is a little bit less than the electricity consumption of France in 2016 [109]. The author is aware that these statements are very theoretical, since the FiT system will not stay in-place until 2050 and furthermore the wind regime and other parameters might change in the upcoming 30 years.

5.1.4 Hot spot analysis

The economically feasible locations are located in the south part of the country and amount to 1.15 GW capacity. The actual geographical positions of the economically feasible wind farms in decimal degrees are:

- 43.698°N and 106.651°E
- 42.616°N and 107.599°E

In spite of that, there are also other locations, which could generate electricity at a cost between 70 and 75 $/MWh but are located inside excluded areas. For example, the location with number two extents into protected territory, indicated by the green color in Figure 21, hence this potential remains unexplored.

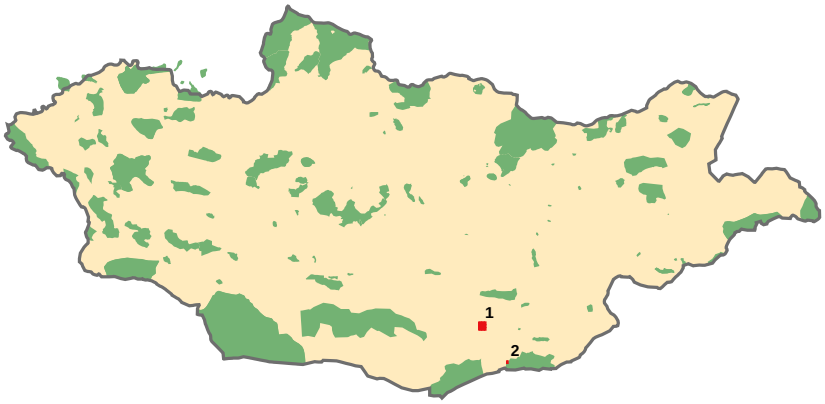

Figure 21: Hot spot map 2020 - wind

In 2050, the situation will be a bit different, with additional locations becoming economically feasible. As seen in Figure 22, economically feasible areas are increased significantly, with three major blocks establishing themselves. Location one is expanding northwards, coming closer to the capital Ulaanbaatar. Location three mostly expands inside protected areas, hence adding less to the actual economic potential considering the land-use constraints. Location two also grows northwards and location four is newly added.

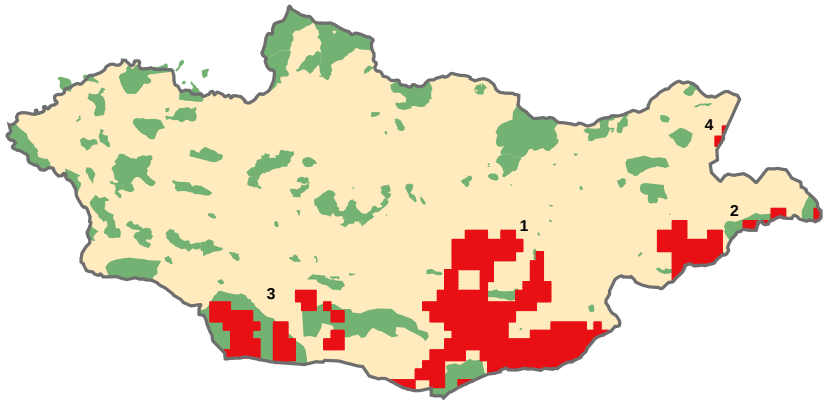

Figure 22: Hot spot map 2050 - wind

5.1.5 **Energy security and environmental sustainability**

In terms of energy security, which is one of the key targets when it comes to energy policy in Mongolia [6], two energy systems are focused on: the Central Energy System and its interconnected neighboring Dalanzadgad Energy System, since about 20% of its electricity had to be imported in 2015 [37]. The Western Energy System is also highly dependent on imports from Russia, however, since no significant wind resources are found in the most western parts of the country, the WES is assessed in the ground-mounted PV chapter.

The imported electricity to the CES amounts to around 1 376 GWh or 1.38 TWh. Theoretically, this amount of electricity could be supplied by an additional 525 MW[6] of wind farms located on the most economic areas in Mongolia. The additional wind capacity could also supply the electricity at a lower cost than the imports. According to the Energy Regulatory Commission the average price of electricity imports to the CES is at 80 $/MWh [39], whereas the wind farms on the most economical locations could provide the electricity at prices between 70 to 75 $/MWh. This calculation does not consider the fact of intermittency of wind, meaning that energy storage would be required in times where peak load and zero wind occur simultaneously.

A closer look is also taken at the DES, which includes two major electricity loads: the Oyu Tolgoi mine and the Tavan Tolgoi mine. A 600 MW coal power plant is considered for providing electricity for those two mines [42]. However, taking a closer look at the wind power potential surrounding the Oyu Tolgoi mine (see Figure 23), shows that within a 100 km radius, wind farms could generate electricity at a highly competitive price between 70 and 75 $/MWh. In a 50 km radius, wind farms could generate electricity at a price of 75 $/MWh. Exploiting this resource would both increase energy security and enhance environmental sustainability.

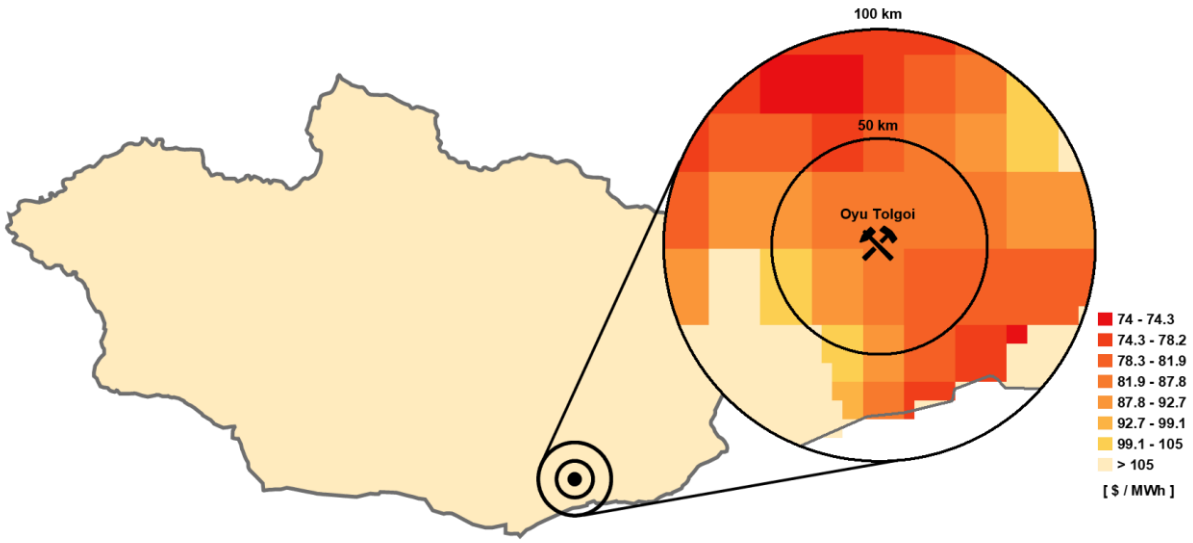

Figure 23: LCOE wind with focus on Oyu Tolgoi mine

The economic potential capacity of 1.15 GW, generating 3.05 TWh of electricity, could replace around 50% of today's electricity generation. Theoretically, this could reduce the GHG emissions by 4.24 $MtCO_{2,eq}$. This theoretical approach neglects the highly important role of the coal-fired power plants to also provide heat during the winter times.

5.1.6 Sensitivity analysis

A sensitivity analysis is provided in order to assess which parameters has the highest influence on the economic potential. Six parameters are chosen for the sensitivity assessment and all of which are increased and decreased by 30%, based on the reference parameters.

The result of the sensitivity analysis is shown in Figure 24, where the legend is found on the right side of the figure. The individual parameters listed in the legend are ranked according to their influence, starting from the highest influence on the economic potential at the top, to the lowest influential at the bottom. The initial point on the y-axis represents the 1.15 GW presented in the previous chapter.

[6] Using FLH of 2 623 h

It goes without saying that the biggest changes in feasible capacity occur, when the capacity factor is changed. A 30% increase of capacity factor results in a total feasible capacity of 271 GW. Whereas a reduction of 30% in investment cost yields a 214 GW economic potential. The FiT is the third influential parameter, if increased by 30% results in 182 GW. The OM costs are fourth in line followed by the chosen discount rate/IRR for the NPV. The least influential parameter affecting the economic potential is the electricity rate, which in this case can be explained by its very low initial value of only 34 $/MWh.

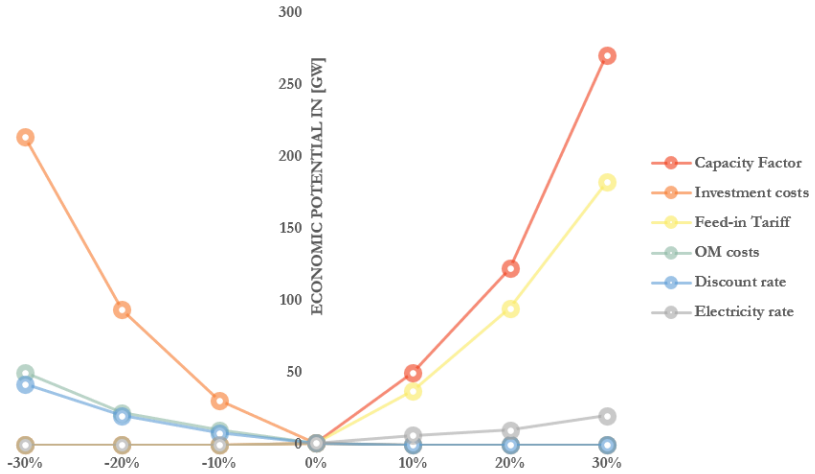

Figure 24: Sensitivity analysis economic potential - wind

5.1.7 **Critical review of the wind results**

In addition to the sensitivity analysis, a critical review of the wind results is provided by the author, acknowledging that the calculated economic potential might be over- or underestimated, due to several factors, which were difficult to estimate or due to inaccuracies in the dataset.

During the assessment of the capacity factor a comparison was made with the Global Wind Atlas provided by the World Bank and partners [110]. In this atlas, the maximum capacity factor of IEC I class wind turbines is around 56%, whereas the maximum capacity factor identified by this study is 31.6%. The difference between the two sources does not make any statement on which of the two are more accurate in terms of reflecting reality.

A factor that might have influenced the comparatively lower capacity factors, is that for this study only ERA5 wind data from the year 2010 was available. Hence, it might have been the case, that 2010 was not as windy as a typical year. Furthermore, the wind speed data for the Global Wind Atlas is a combination of the data coming from a model developed by Vortex and the ERA5 reanalysis dataset. The Global Wind Atlas data is downscaled to a spatial resolution of 3 x 3 km [111], whereas the original ERA5 data is available only at a 31 x 31 km resolution [65], which might have also influenced the results. Nevertheless, due to the different spatial resolutions and origins, it is hard to compare the two sources, but it is mentioned still to provide a complete picture.

Since financial data on wind project costs are hard to come by, because these types of data are mostly confidential, it was difficult to assess the accuracy of the costs used in this study. A report on of the wind farm projects in Mongolia suggest a 10% higher investment costs than assumed in this study [112]. However, this study is looking investment costs in the year 2020, whereas the report has data from 2017. The source, however, was not deemed credible enough to be included in this analysis.

Lastly, a report by the Government of Mongolia has shown that first experience in operating the Salkhit Wind farm has shown a 8.8% annual curtailment rate in 2013 [6]. Curtailing wind power leads to financial losses. These financial losses are also not considered in this study, since there are not enough experiences yet, on which a solid analysis could be based upon. All in all, the results emerging from this study must only be used in context with the provided methodology and assumptions.

5.2 Ground-mounted photovoltaics

The ground-mounted photovoltaic potential is calculated according to the methodology described in chapter 3. The results are further divided into three potentials: the geographical, the technical and the economic potential using the definition of Hoogwijk [47].

Additionally, an adjusted FiT is calculated to lower total cost of subsidy for the Government of Mongolia, since the current FiT rate is identified to be oversized.

5.2.1 Geographical potential

Using the definition of Hoogwijk [47] for the geographical potential, the suitable area for ground-mounted PV is calculated. WiSo-GERI excludes the same 271 024 km² as for wind, since the same restrictions apply for solar PV. However, the upper slope limit of 5° adds an additional 362 757 km² to the excluded LULC class, resulting in a total of 633 781 km², which is approximately two times the size of Poland [113].

The majority of the land that is utilized, is classified as LULC class "barren". The "barren" LULC class alone makes up 118 484 km² of the utilized area. In total, 128 011 km² are utilized for the installation of ground-mounted PV farms (see Table 20), which is about twice the size of Togo [114].

LULC class	Utilization factor	Available area	Utilized area
	[-]	[km²]	[km²]
Barren	20%	592 421	118 484
Cropland natural	2%	28 366	567
Cropland	2%	13 069	261
Forest	0%	653	0
Grassland	3%	76 772	2 303
Savanna	3%	212 992	6 390
Shrubland	3%	156	5
Snow and Ice	5%	11	1
Urban	0%	99	0
Water	0%	3 238	0
Wetland	0%	1	0
Excluded Areas	0%	633 781	0

Table 20: Utilized area – ground-mounted PV

5.2.2 Technical potential

The total technical potential capacity in Mongolia amounts to about 5.12 TW. Given the solar irradiation, 5.12 TW could generate 9.568 PWh electricity per year. According to an estimation by the Government of Mongolia, which were based on the resource maps from NREL, about 1.5 TW could be installed on 23 462 km². The estimation of the Mongolian Government included only land with high solar irradiation. The 1.5 TW estimated by the Mongolian Government could generate around 4.774 PWh of electricity per year [6]. No other studies, except the ones based on the NREL values have been performed so far.

Figure 25 shows the feasible capacity distribution throughout Mongolia. The highest feasible capacities per grid cell are located in the south and stretching to the south-west of the country and highlighted in red. The red areas correspond to the location of the LULC class "barren", since it has a utilization factor of 20% and hence allows for high capacity installation. Penetrating the red area like rivers are the orange zones. These indicate, that roads or railways are leading through the grid cells, reducing the total suitable area per grid cell. In the north-east mostly grid cells with a feasible capacity of 60 – 90 MW are found.

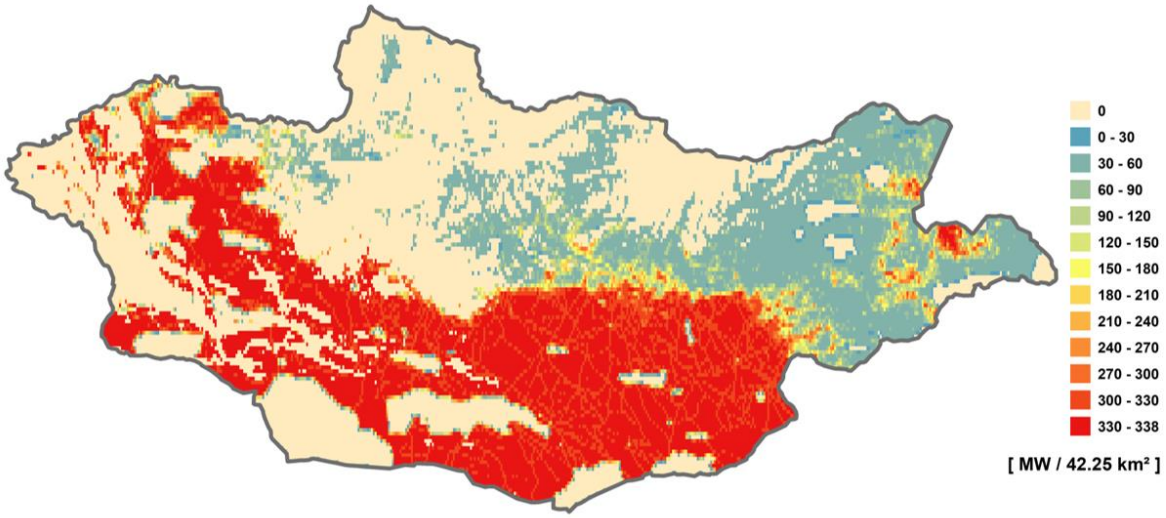

Figure 25: Technical potential capacity map – ground-mounted PV

In terms of electricity generation, the most productive location is found south-west of the country, indicated by the color red in Figure 26. In that area, grid cells with a productivity of 650 – 696 GWh per grid cell and year are located. The south and the west of the country generate between 600 – 650 GWh per grid cell and year. In the east of the country grid cells have a productivity of around 50 – 150 GWh per grid cell. Figure 26 does not make any suggestion on where to place a solar farm, this is assessed later in the economic potential chapter. The productivity of a grid cell highly reflects the LULC classification of Mongolia, meaning that "barren" land allows for high installable capacity, which in turn coupled with high solar irradiation values results in high electricity yields. The red zone reflects a combination of both a high installable capacity and high solar irradiation values.

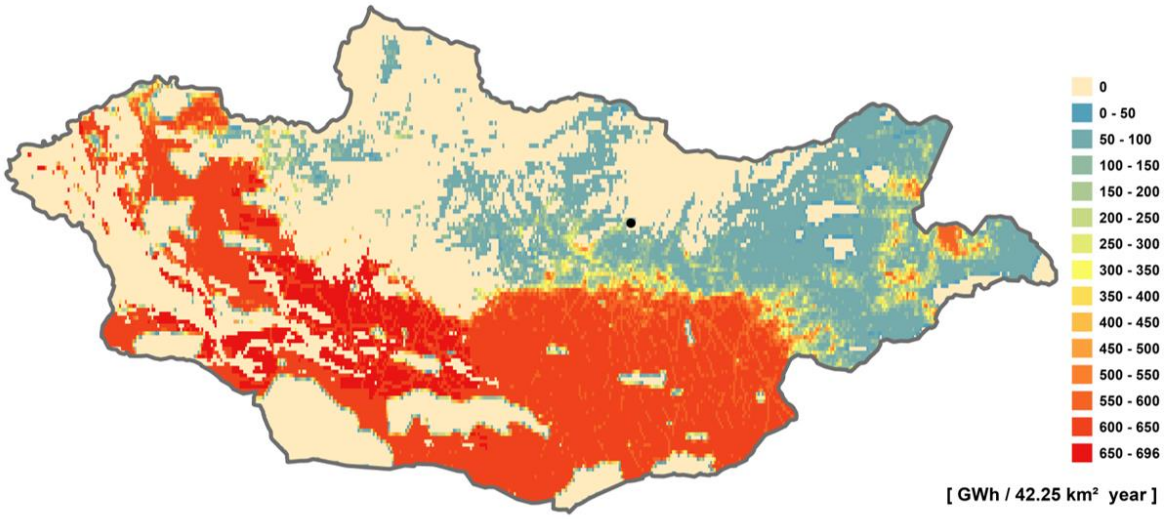

Figure 26: Technical potential energy map – ground-mounted PV

The capacity factor distribution map is shown in Figure 27. The maximum capacity factor found inside Mongolia is 23.7%, which is relatively high compared to European countries such as Germany where locations with high solar irradiation have a capacity factor of around 13% [30]. However, these two countries are not comparable, since Mongolia is reported to have high solar irradiation values and little cloudy days [6]. Additionally, low ambient temperatures increase productivity of PV modules, due to cooling effects.

Most of the PV farms installed in the country would generate at a capacity factor between 20% - 23%, only a minor share of the area has a capacity factor of 23% and above.

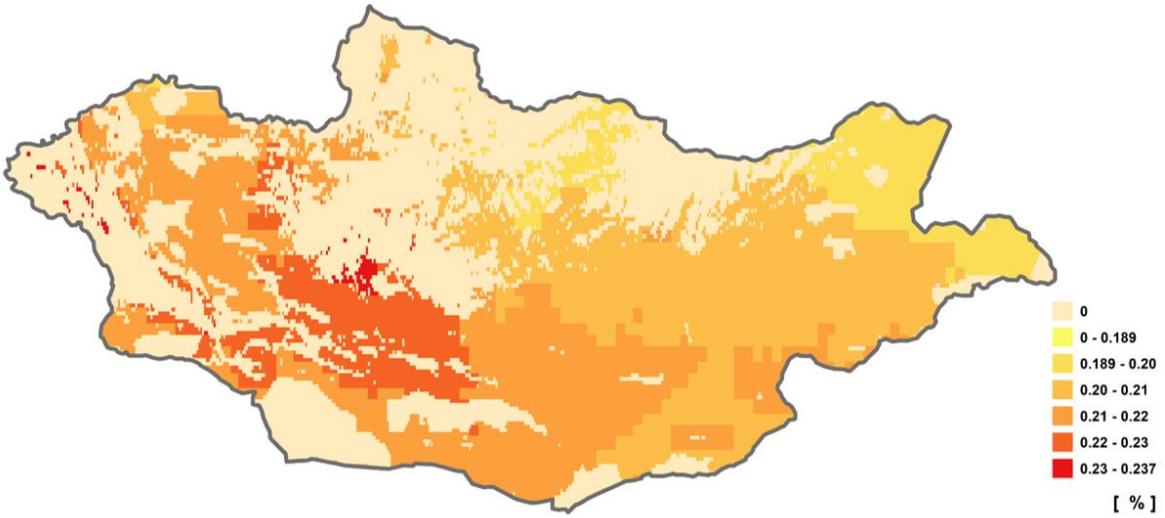

Figure 27: Capacity Factor map - ground-mounted PV

5.2.3 Economic potential

The NPV calculation per grid cell, coupled with the FiT rate of 180 $/MWh for the first ten years and the electricity rate of 34 $/MWh for the remaining lifetime as input parameters, shows that the entire technical potential of 5.12 TW is economically feasible under assumed conditions. 5.12 TW could provide 9.568 PWh electricity per year, which is almost double the electricity demand of China in 2016 [107] and is 1444 times the domestic Mongolian electricity generation in 2018 [39].

The full load hours associated with the economic potential range from 1656 to 2076 h, which equals to a 18.9 to 23.7% capacity factor.

When considering the LCOE, PV farms could generate electricity at a cost between 48.6 to 61 $/MWh or 42.96 – 53.80 €/MWh. Putting the LCOE of 48.6 $/MWh into a global perspective reveals, that the solar resource in Mongolia can be exploited at a very low cost. According to the renewable power generation costs report of 2018, average prices of auctions issued for 2020 are at 48 $/MWh [115]. A report by Carbon Tracker, a London based Think Tank even reported, that coal power plants in China have a long-run operating cost of between 46 – 48 $/MWh, hence theoretically solar PV installed in Mongolia, are already competitive with Chinese coal power plants [116].

Converting the above mentioned LCOE for PV farms in Mongolia from US Dollars to Mongolian currency and kWh yields 127.89 – 160.53 MNT/kWh, which compared to the electricity rate of 89.58 MNT/kWh is still high [99], however, far closer than the LCOE of onshore wind. Taking into account the reports made by the Carbon Tracker suggests, that the electricity rate does not reflect the true cost of electricity generation in Mongolia [116]. This will further be reflected on in the discussion chapter. Nevertheless, ground-mounted PV would not be able to compete on the free market with the current electricity rate.

About 50 km to the south-east of Ulaanbaatar, locations for solar PV plants with a LCOE of between 52 – 54 $/MWh can be found (see Figure 28).

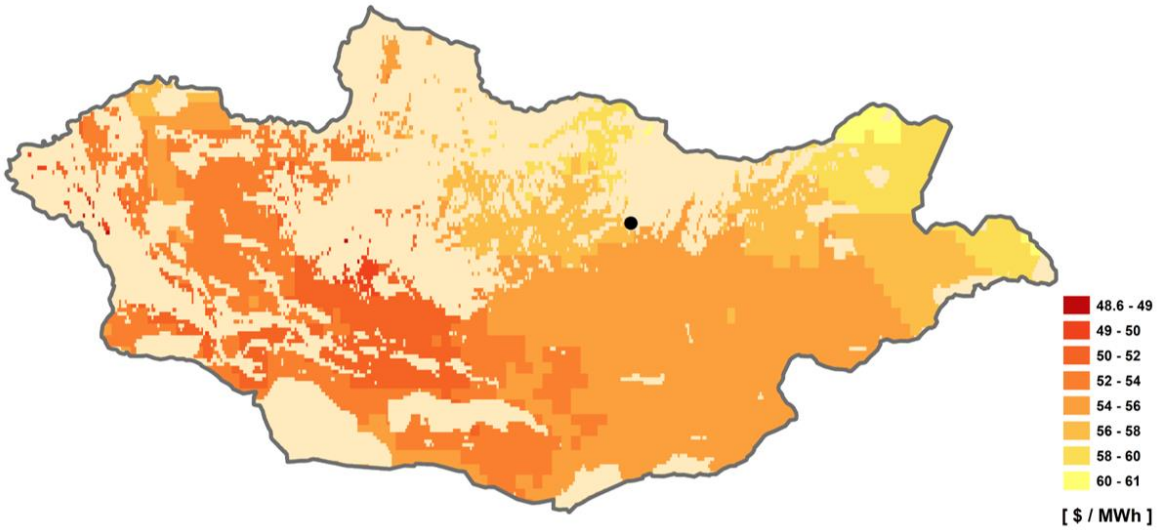

Figure 28: LCOE map - ground-mounted PV

2050

By 2050, when applying the learning rates described in the methodology chapter, the LCOE of ground-mounted PV will decrease by 21.7 $ for the lower LCOE and 26 $ for the higher LCOE, resulting in LCOEs of 26.96 $/MWh and 34.90 $/MWh, respectively. In Mongolian Tugrik and kWh this amounts to 70.94 MNT/kWh and 91.83 MNT/kWh. This in turn means, that solar PV is becoming cheaper than the electricity paid to SOEs and IPPs in 2019. Therefore, around 880 GW of capacity would become economically competitive on the free market, without requiring any FiT support scheme. This amount of capacity could generate 1 735 TWh per year.

Under the current FiT support scheme all areas not excluded by the geospatial analysis are economically feasible, hence a hot spot analysis is not required.

5.2.4 Energy security and environmental sustainability

Analyzing the energy security aspect of exploiting domestic solar PV yields interesting results. On the one hand, when analyzing the CES and the DES, it can be seen that solar PV farms with a LCOE ranging from 53.9 $/MWh to 56 $/MWh could be installed in a 100 km radius of Mongolia's largest mine [6]: Oyu Tolgoi (see Figure 29). Considering, that electricity imports to the CES are priced at an average of 80 $/MWh [39], PV power plants would provide a viable option to avoid expensive imports, while at the same time generating local added value and reducing energy dependency.

Replacing the 1 376 GWh/year of electricity imports with solar PV, would require a total installed capacity of 743 MW[7]. Currently, the construction of a 600 MW coal power plant named Tavan Tolgoi is considered to power the nearby mines [42]. One of the mines is the already mentioned Oyu Tolgoi and another one is called Tavan Tolgoi, which will be the coal mine of choice providing fuel for the coal power plant. This capacity could easily be replaced by a solar power plant in terms of the available resource. A statement on the economics of investing either in coal or solar cannot be made in this case since no data on expected LCOE of the coal power plant could be retrieved.

[7] At average FLH of 1 853 h

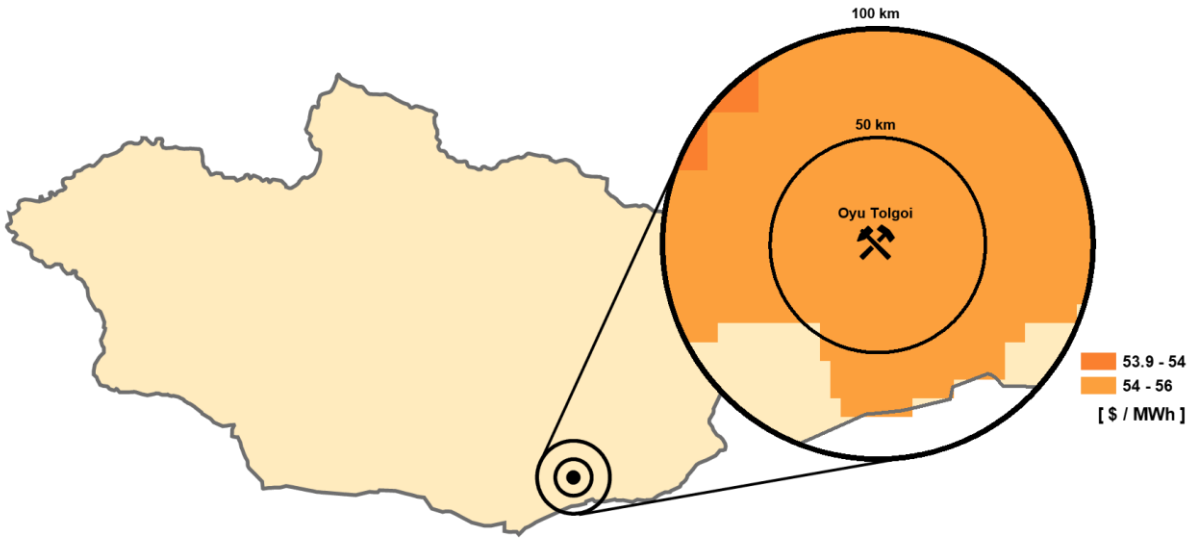

Figure 29: LCOE ground-mounted PV with a focus on Oyu Tolgoi mine

In addition to looking at CES/DES, also the WES is analyzed, since this energy system according to IRENA imports about 70% of its electricity demand [5]. In 2015, this amounted to around 107 GWh in total. Included in the analysis are the three major cities interconnected through the WES, which are Khvod, Ölgii and Ulaangom. These three cities are located in the center of each of the three circles in Figure 30, where Ulaangom is located in the center of the upper circle, followed by Ölgii in the middle circle and Khvod in the lower circle. As can be seen in Figure 30, all three cities have access to feasible locations for installing solar PV farms. Around Ulaangom, the cheapest locations could provide electricity at a LCOE of 52 – 54 $/MWh in the inner circle and between 50 – 52 $/MWh in the outer circle. In case of Ölgii, the lowest LCOE in the inner circle range from 49 – 50 $/MWh and in the outer circle even one grid cell with an LCOE of 48.94 $/MWh is found to the south of the city. The city Khvod has the cheapest resources located right at its doorstep, with LCOEs between 50 – 52 $/MWh. Comparing the availability of cheap solar energy to the average price of 77 $/MWh [5] at which imports have to be purchased, it can be inferred that PV has a price advantage. Costs for storage are not considered in this comparison.

Theoretically, a solar PV farm with a capacity of 55 MW[8] would be enough to generate the amount of imported electricity. Again, this is more a thought experiment, since energy storage capacity would be required to also provide electricity during times of no sunshine.

In both cases of the CES and the WES, solar PV could provide the necessary capacity to make electricity imports both from Russia and China redundant, boosting energy security.

[8] The capacity is calculated by dividing the electricity imports in MWh with an average FLH of 1 941 h

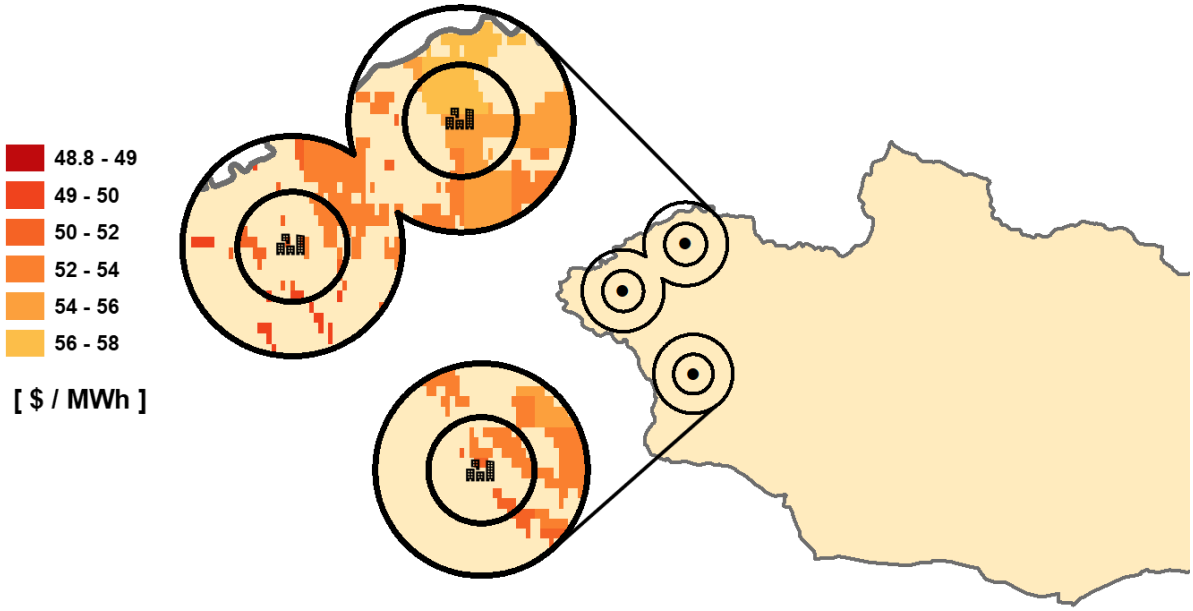

Figure 30: LCOE ground-mounted PV with a focus on western cities

When looking at the environmental impact of utilizing solar PV, it can be stated, that theoretically 8.55 $MtCO_{2,eq}$ could be mitigated, reducing the entire GHG emission coming from the electricity sector. However, this assessment again neglects the fact that the CHP plants are required for district heating, especially in the CES zone.

5.2.5 Sensitivity analysis and FiT remuneration adjustment

The result of the sensitivity analysis provides a very clear message of an oversized FiT rate, which does not reflect the drastic cost reductions that solar PV underwent the last decade. The sensitivity analysis showed that even with an 150% increase in investment costs per MW peak capacity, the economic potential would only reduce to 2.03 TW, which is about half of the entire potential. A 150% increase would mean an increase of investment costs from 990 $/kW to 2 475 $/kW for a utility scale PV system, which is highly unlikely, since global average investment costs are reported to be at 1 120 $/kW in 2018 [115] and a solar power plant project in Mongolia was announced at investment costs of 1 240 $/kW in 2017 [112]. The assumed investment costs of 990 $/kW are therefore justified.

Furthermore, a 50% reduction of the capacity factor from an average of 20.8% to 10.4% showed no effect on economic feasibility, meaning that the economic potential remained at 5.12 TW. To put this into perspective: The least economic locations for solar PV in Germany have an even higher capacity factor at around 11% [30]. Only a 75% reduction in capacity factor resulted in a 0 TW economic potential. These parameter variation examples clearly show that the current FiT rate for solar PV is oversized.

Yet another proof for the oversized FiT is the Internal Rate of Return (IRR), which is calculated using the parameters of this study. The IRR for a solar project on the most economic location is calculated to be 57% and for the least economic locations it is 39%. The average IRR is at 46.7%, which is much higher than the IRR feasibility threshold of 9% used in this study and also higher than other studies such as Grassi et al. [7], which defined a 15% feasibility threshold for the IRR. In fact, according to an article, the Government of Mongolia is looking into alternative models to the FiT for supporting renewable energy investment, due to the acknowledgement of a too generous FiT [112].

A generous FiT rate results in windfall profits for early solar PV project developers, while at the same time straining national budgets. Due to financial pressure from FiT expenditures, sudden FiT rate revisions were reported in the past, which in turn increases risk perception in the market. Such a case was observed in Spain, where a too high FiT rate led the Spanish government to reduce the FiT in 2008 by 30%, reducing

the trust of investors in the Spanish market [117]. Furthermore, too generous subsidies can decrease social welfare by increasing the deadweight loss.

Hence, an attempt is made in this study to estimate the right level of FiT for reducing the deadweight loss and decreasing the financial burden for the Government of Mongolia and ultimately the Mongolian taxpayers.

This is done using a similar approach as Gass et al. [13], where the relation between different FiT levels and the corresponding capacity investment was investigated. This relation of FiT rate and the willingness of investing in solar capacity[9] is referred to as supply curve in microeconomics. The supply curve shows what level of FiT (price) is required to trigger an investment into a certain amount of capacity/electricity produced (quantity) [118].

In order to account for data inaccuracies, a FiT range for grid-connected solar PV is recommended, using the assumptions used throughout this study as a lower limit and more pessimistic parameters for the upper limit of the FiT. The more pessimistic approach includes a 12% IRR for the NPV analysis as well as a 20% increase in investment costs. An NPV above zero will trigger an investment.

The first analysis using the parameters from this study yielded the following results displayed in Figure 31. A FiT of 58.3 $/MWh unlocks a potential of 320 MW or 660 GWh. Increasing the FiT by 0.1 $ increases the potential to 1.23 GW corresponding to 2.54 TWh. 58.6 $/MWh allows for 1.76 GW capacity and 58.8 $/MWh for 2.16 GW. In order to replace all electricity from coal-power plants and the electricity imports in 2018, a FiT of 58.89 $/MWh is required.

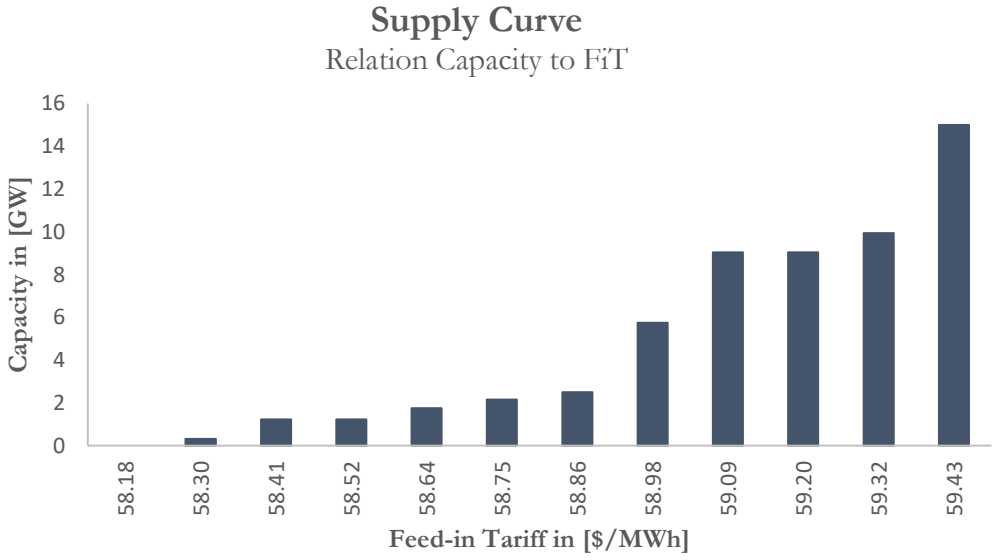

Figure 31: Supply curve energy and capacity optimistic scenario - ground-mounted PV

In a more conservative scenario, with a 20% increased investment cost and an IRR of 12%, following results are calculated (see Figure 32). A FiT of 85 $/MWh yields an economic potential of 1.23 GW. 1.76 GW are unlocked as soon as the FiT hits 85.4 $/MWh and 2.16 GW at 85.5 $/MWh. Decarbonizing the electricity system and getting rid of electricity imports would require a FiT of 85.7 $/MWh.

[9] And ultimately generate/supply electricity at a certain quantity

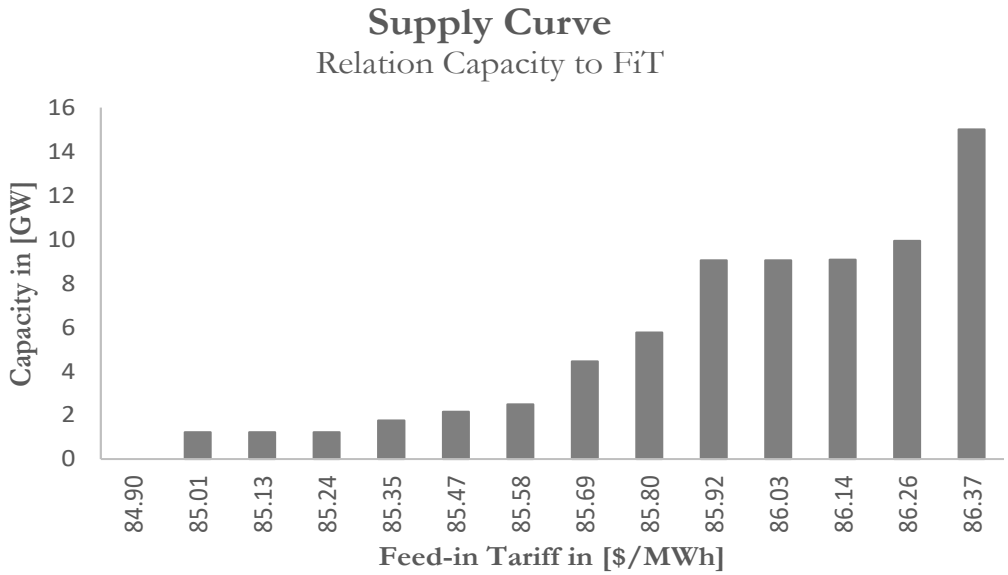

Figure 32: Supply curve energy and capacity pessimistic scenario - ground-mounted PV

In conclusion, the entire electricity sector could be decarbonized with a FiT for ground-mounted PV at 58.9 $/MWh or in case of more pessimistic assumptions at 85.7 $/MWh, which would decrease the current FiT rate by 67% and 48%, respectively.

An indication on how this measure also decreases the Deadweight Loss is provided with Figure 33. A Deadweight Loss is created, when subsidies or taxes are introduced and the sum of the consumer and producer surplus is lower with the tax in place than at market equilibrium [119].

Lowering the subsidy also lowers the financial burden of the Mongolian national budget, because a lower FiT reduces the total annual cost of subsidy, as can be seen in Figure 33. The supply and demand curves in Figure 33 are only illustrative.

At the current FiT rate of 180 $/MWh, reaching the national 2030 target of 30% renewable electricity would introduce 135.9 million dollars of annual costs for the Government of Mongolia[10]. Using the adjusted FiT of 58.4 $/MWh would reduce the total costs by 83.5% to around 22.5 million dollars. In the more conservative scenario, the annual cost would still be lowered by 65.2% to around 47.3 million dollars. In these two instances, a FiT rate adjustment could save the Mongolian Government annually either 113.5 or 88.6 million dollars, respectively.

All in all, the same decarbonization goals can be achieved with less money than under the current FiT support scheme, hence the Government of Mongolia should consider adjusting the current FiT rates for ground-mounted PV to reduce economic inefficiencies.

[10] Required annual electricity output of 0.933 TWh times the difference of the FiT rate and the regulated electricity rate (34.32 $/MWh)

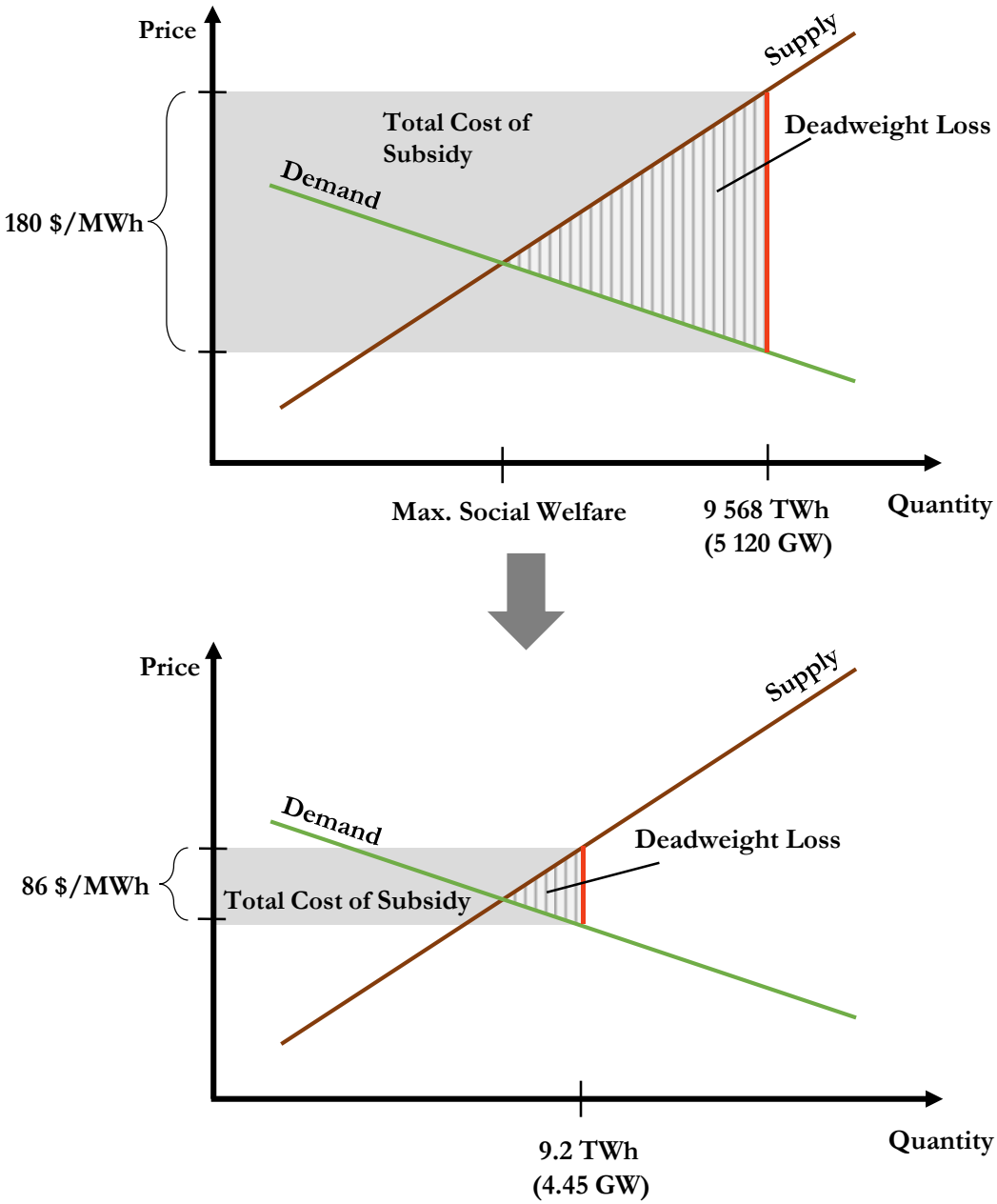

Figure 33: Illustrative supply – demand curve

5.2.6 Critical review of the ground-mounted PV results

The PV output (kWh/kWp) of the Global Solar Atlas from the World Bank were compared with the FLH of this study. Here it is observed, that the maximum PV output of the Global Solar Atlas is around 1925 h, whereas the maximum value from this study is at 2076 h. So, it could be the case, that the solar irradiation values lead to a slight overestimation of the FLH and CF in this study. This could influence the technical potential, not the economic potential, since under the current FiT scheme even a 50% reduction of the FLH or capacity factor would not result in a lesser economic potential.

Additionally, the cost of large-scale PV systems might be underestimated by around 10%, since an article on solar projects has been found, which claim specific costs of 1 240 $/MW [112]. Yet, it is important to state, that this study is looking at cost for 2020, whereas the project in the article was approved in 2017, meaning that by 2020 costs will further fall also in Mongolia. Due to missing details on the exact cost structure, the article was deemed unusable for this study.

5.3 Rooftop photovoltaics

The rooftop photovoltaic potential is calculated according to the methodology described in chapter 3. The results are further divided into three potentials: the geographical, the technical and the economic potential using the definition of Hoogwijk [47].

5.3.1 Geographical potential

For the geographical potential only the LULC class "urban" is assessed. According to the GlobCover dataset around 135 km² in Mongolia are classified as "urban". The utilization factor of 20% reduces the area to approximately 27 km² (see Table 21), available for installing rooftop PV systems. In relative terms, 27 km² translates to 0.002% of the total land area.

LULC class	Utilization factor	Available area	Utilized area
	[-]	[km²]	[km²]
Urban	20%	135	27

Table 21: Utilized area – rooftop PV

5.3.2 Technical potential

The technical potential of rooftop PV is 1.11 GW which could generate about 1 919 GWh, which is about 240 GWh more than the total electricity imports into Mongolia in 2018. This amount of electricity could replace four coal-power plants (referred to as CHPP-3, EFCHPP, DCHPP, DorCHPP by ERC [39]), which are the second, third, fourth and fifth largest coal power plants in the country.

No other studies assessed the rooftop PV potential of Mongolia so far, hence this is a benchmarking for the rooftop potential assessment of Mongolia.

In Figure 34 a map, for further understanding of the spatial distribution of the feasible capacity and its locations, is provided. The majority of the capacity is found in Ulaanbaatar (see circle 1 in Figure 34), which accounts for 65% or 724 MW of the total technical potential. The remainder is spread throughout the country. However, most of remaining potential hot spots only allow for installation of a few MW.

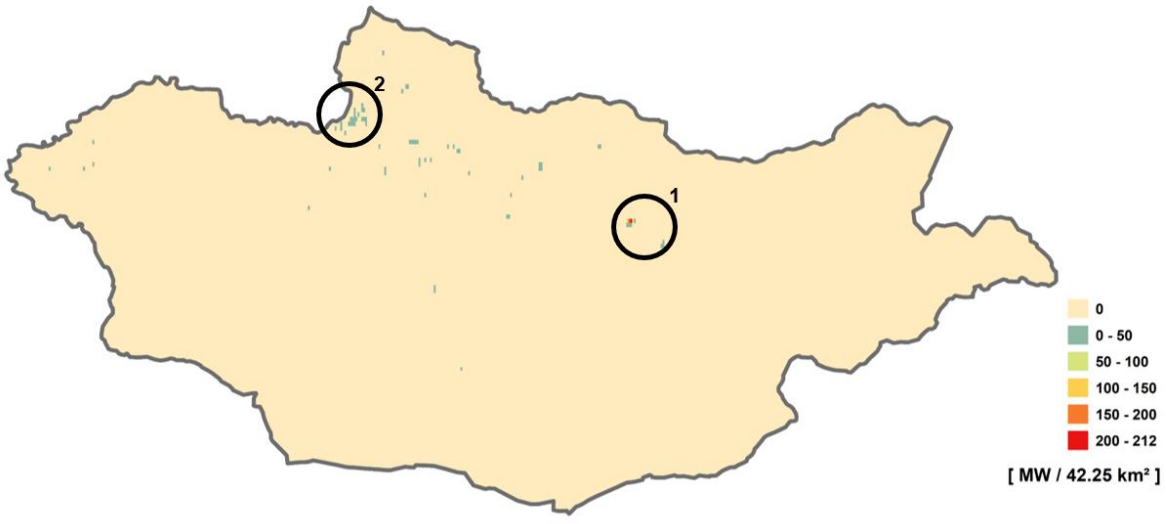

Figure 34: Technical potential capacity map - rooftop PV

The installed capacity in Ulaanbataar alone could provide 1 240 GWh (see Figure 35). Two major cities nearby Ulaanbataar, Erdenet and Darkhan, which are also connected to the CES, could provide an

additional 59.5 and 24.1 GWh, respectively. Erdenet has a potential of installing 35 MW and Darkhan 14 MW of rooftop PV.

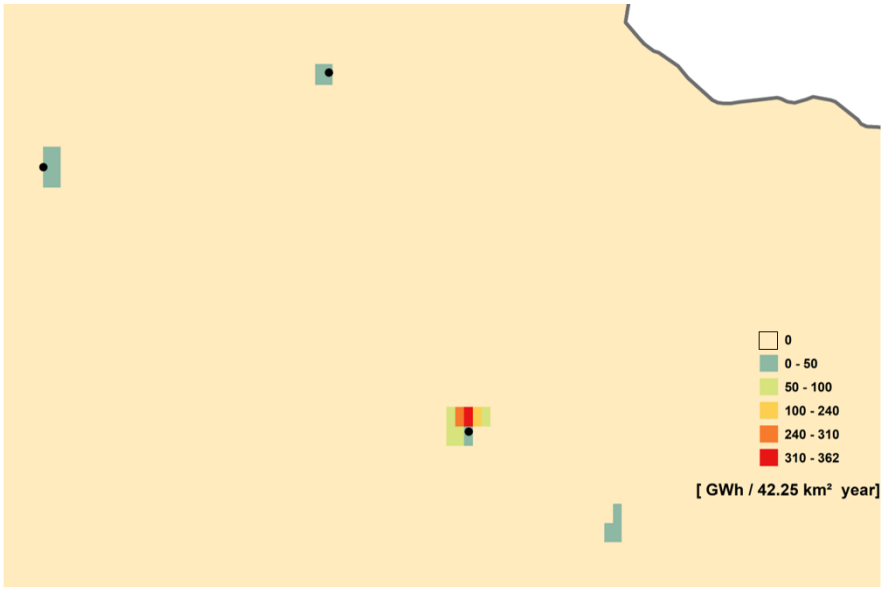

Figure 35: Technical potential energy map with focus on Ulaanbaatar - rooftop PV

5.3.3 Economic potential

The economic analysis yields similar results as the economic analysis for ground-mounted PV, although investment costs of rooftop PV are higher than utility scale PV. However, due to the generous FiT, the entire technical potential is economically feasible. 1.11 GW generating 1 919 GWh are the economic potential of Mongolia for rooftop PV.

In terms of LCOE, the best locations have an LCOE between 69.8 and 72 $/MWh, which converts to Monglian Tugrik and kilowatt hours of 183.7 MNT/kWh and 189.5 MNT/kWh (see Figure 36). The least economic sites are found in Erdenet and Darkhan where a LCOE of 80 – 82.2 $/MWh or 210.5 – 216.3 MNT/kWh. Therefore, rooftop PV is not economically feasible without the FiT support scheme.

The lowest LCOE locations are found in the WES in the city of Ölgii and in the more central and mountainous regions of Mongolia. Ulaanbataar has a LCOE of 78 – 80 $/MWh which translates to 205.3 MNT/kWh and 210.5 MNT/kWh, respectively.

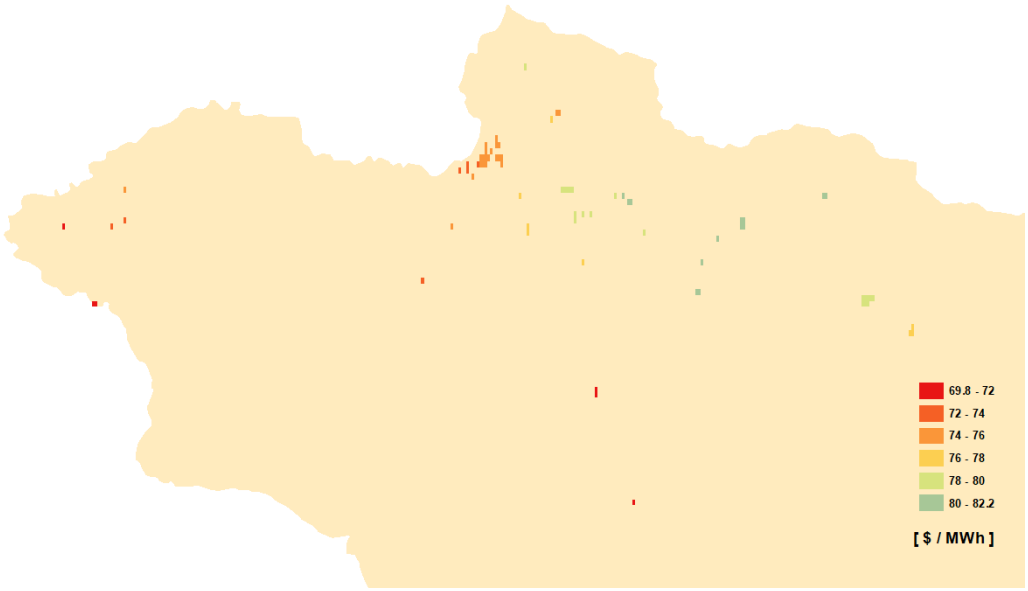

Figure 36: LCOE map - rooftop PV

2050

The economic potential, considering the current FiT and learning curves of PV technology, will remain the same in 2050, since the full potential is already economically feasible in 2020. The cost reductions for rooftop PV results in lower LCOE starting at 49.7 $/MWh, which means an absolute decrease in LCOE of 20 $/MWh from 2020 to 2050. The least economic locations will generate at a LCOE of 58.5 $/MWh. This analysis does not include an increase in available roof area due to population increase, nor the increase in PV module efficiency.

5.3.4 Energy Security and Environmental Sustainability

If the entire rooftop PV capacity is utilized, the total electricity imports in 2018 could become redundant. In addition, long-distance transmission losses could be avoided since the rooftop PV systems are be placed directly in load centers such as Ulaanbaatar.

The economic potential capacity could replace 1.919 TWh/a of electricity from coal power plants, which could reduce the total emission coming from the electricity sector by 2.67 $MtCO_{2,eq}$[11]. This reduction accounts for around 31% of the total emissions from the electricity sector.

5.3.5 Sensitivity Analysis and FiT remuneration adjustment

In this chapter a similar approach as in section 5.2.5 is considered. A sensitivity analysis is based on the same FiT considerations as ground-mounted PV, since there is no distinction between rooftop and ground-mounted PV in the Mongolian FiT support scheme.

Although the investment costs and the OM costs are higher compared to ground-mounted PV, the entire technical potential is also considered to be economically feasible, leading to the conclusion that also for rooftop PV the current FiT is too generous.

The sensitivity analysis supports the point, that the FiT is too high, since only drastic reductions in capacitiy factor and FiT renumeration lead to a 100% reduced economic potential (see Table 22)

[11] The avoided emissions are calculated by multiplying the amount of electricity replaced by RES with the average carbon intensity of Mongolian coal power plants defined in section 3.5

Parameter	Economic Potential				
	-50%	-25%	0%	25%	50%
Capacity Factor	0	1.11	1.11	1.11	1.11
Investment costs	1.11	1.11	1.11	1.11	1.11
Feed-in Tariff	0	1.11	1.11	1.11	1.11
OM costs	1.11	1.11	1.11	1.11	1.11
Discount rate	1.11	1.11	1.11	1.11	1.11
Electricity rate	1.11	1.11	1.11	1.11	1.11

Table 22: Sensitivity Analysis table - rooftop PV

Hence, an attempt is made to estimate an adequate FiT renumeration, using the same two scenarios of section 5.2.5. It is also recommended to divide the FiT for solar PV into two categories: ground-mounted grid-connected photovoltaics and rooftop grid-connected photovoltaics.

Using the rooftop PV data two supply curves are calculated. The results of the supply curve using an IRR of 9% and the cost assumptions of this study are displayed in Figure 37. The first 100 MW of capacity investment is unlocked as soon as the FiT reaches 101 $/MWh. A FiT of 107.8 $/MWh initiates a capacity investment of 300 MW. In it can also be observed that after a threshold of 108.1 $/MWh a big leap in capacity increase is made (see Figure 37). This is due to the fact that most of the capacity is found in Ulaanbaatar, which has FLH or CF in the lower Quantile at around 1 700 h or 19.4%, respectively. Surpassing the 108.1 $/MWh threshold, triggers investment in rooftop PV also in Ulaanbaatar with an additional 687 MW capacity.

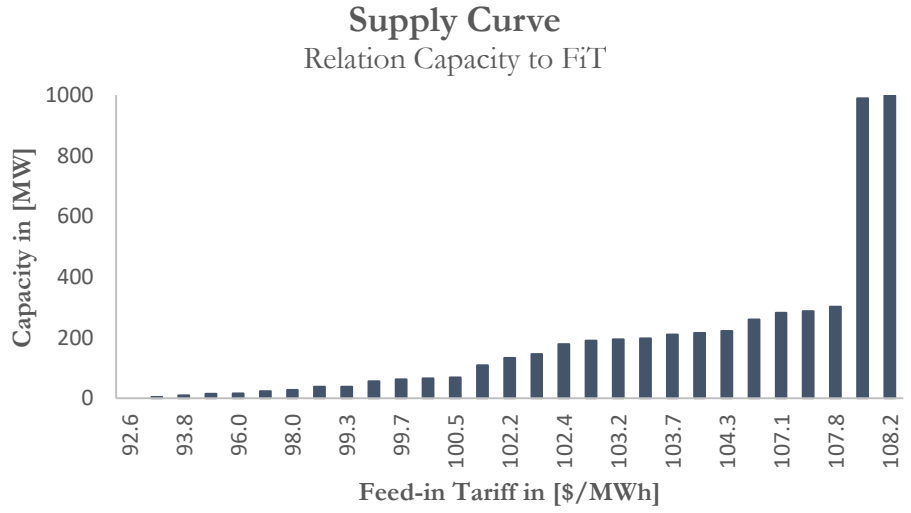

Figure 37: Supply Curve for energy and capacity optimistic scenario - rooftop PV

The results of the more pessimistic scenario, assuming 20% increased investment costs and an IRR of 12%, are displayed in Figure 38. The increased cost and IRR increase the necessary FiT renumeration to 138.9 $/MWh for reaching the 100 MW installed capacity. A capacity of 300 MW requires a FiT of 147.4 $/MWh. In order to trigger investments in rooftop PV in the capital Ulaanbaatar a FiT of 147.8 $/MWh is necessary. A FiT at this level is already close to the current lower bound of the FiT at 150 $/MWh [98] and would allow for an additional capacity of 687 MW, reaching 989 MW in total.

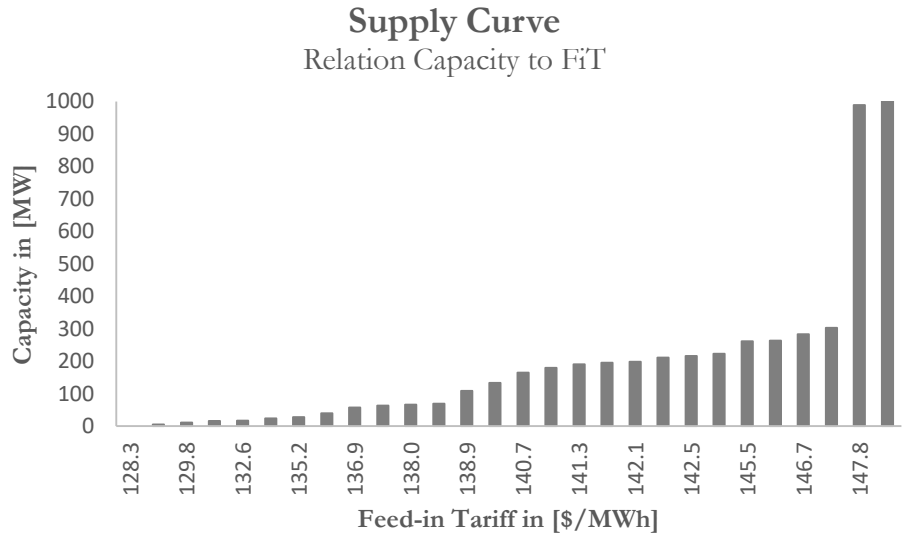

Figure 38: Supply curve energy and capacity pessimistic scenario - rooftop PV

5.3.6 Critical review of the rooftop PV results

The validity of the rooftop PV results is highly dependent on the quality of the LULC map that is used for the analysis and its corresponding resolution. The resolution of 300 x 300 is detailed, still, smaller villages are probably not captured by such a resolution, hence the potential for installing rooftop PV could even be higher. The accuracy of the classification process of the LULC data may also impact the result.

The critical assessment in section 5.2.6 concerning solar irradiation and investment costs are also valid in case of rooftop PV.

5.4 Result summary

In summary, the geographical analysis revealed that 300 727 km² are suitable for installing wind power plants, 128 011 km² are suitable for installing ground-mounted photovoltaics and 27 km² are suitable for installing rooftop photovoltaics.

The technical analysis yielded a technical potential of 2.13 TW of wind, 5.12 TW of ground-mounted photovoltaic and 1.11 GW of rooftop photovoltaic. In total Mongolia has a technical wind and solar potential of 7.25 TW, which could provide 12.17 PWh/year of electricity.

The techno-economic analysis included the current FiT support scheme and suggests a techno-economic wind potential of 1.15 GW (3.05 TWh), a techno-economic ground-mounted photovoltaic potential of 5 120.44 GW (9 567.95 TWh) and a techno-economic rooftop photovoltaic potential of 1.11 GW (1.92 TWh). The total combined techno-economic wind and photovoltaic potential is 5 123.70 GW (9 572.92 TWh). Without the current FiT support scheme, however, none of the three technologies would be economically feasible, due to the low regulated electricity rate.

In terms of Levelized Cost of Electricity, ground-mounted photovoltaic is the cheapest option among the three investigated technologies, with least cost locations offering electricity at a LCOE as low as 48.6 $/MWh or 127.89 MNT/kWh. In case of rooftop PV the least cost locations generate electricity starting at a LCOE of 69.8 $/MWh or 183.7 MNT/kWh. LCOE for onshore wind starts at 70.0 $/MWh or 185.5 MNT/kWh for the most economic locations.

In 2050, the LCOE of the most economic locations of ground-mounted PV will decrease to 27 $/MWh or 70.9 MNT/kWh, which is lower than the current electricity rate of 89.6 MNT/kWh paid by the ERC. The LCOE of rooftop PV will reduce to 49.7 $/MWh or 130.8 MNT/kWh. Onshore wind will experience a reduction in LCOE to 62.4 $/MWh or 164.2 $/MWh. In 2050, around 880 GW of ground-mounted PV

would be economically feasible without needing subsidies. These 880 GW could generate around 1 735 TWh per year.

Due to the generous renumeration for photovoltaics from the current Feed-in Tariff support scheme, a rate adjustment is proposed to lower the total annual cost of subsidy for the Mongolian state. Furthermore, the FiT for grid-connected PV should be split up into a separate tariff for ground-mounted PV and a separate tariff for rooftop PV, if the introduction of rooftop PV systems is a desired goal for the Mongolian Government.

The adequate FiT for ground-mounted photovoltaic to reach the required capacity for the national renewable energy target of 30% in 2030 should be selected between 58.4 $/MWh in the optimistic scenario and 85.0 $/MWh in the pessimistic scenario.

For a full switch from coal power to renewable energy sources, in particular ground-mounted PV, a FiT of between 58.9 $/MWh and 85.7 $/MWh is needed (based on generated electricity in 2018).

Using the adjusted rates proposed in this study, the Mongolia Government could save between 88.6 and 113.5 million dollars of tax money annually, when comparing to the current FiT rate of 180 $/MWh. This would translate into 65.2 to 83.5% relative cost reductions.

5.5 Discussion

The results show, that renewable energy sources would have a hard time competing in the current market environment, where the regulated electricity rate received by generating units is as low as 34 $/MWh. Removing the FiT would make all renewable energy projects economically unfeasible in 2020. Nevertheless, the doubt was formulated, that the regulated electricity rate in Mongolia does not reflect the true cost of electricity generation and hence is set at an unsustainably low level.

In fact, reports stated, that the current regulated electricity rate set by the ERC, also forced currently online coal power plants to operate at a financial loss. The CEE Bankwatch Network stated, that the entire energy sector has operated at a loss of 68 billion MNT or 30 million Euros in 2014 [42]. On top of that, coal is still subsidized by the Mongolian Government [6]. An interview with a coal-industry insider revealed, that in 2010 the Mongolian Government subsidized coal power plants with 15 billion MNT [120], creating further market distortions.

In addition to having to compete with a subsidized fuel, RES also have to compete with fully depreciated coal power plants [6]. This puts additional pressure on RES.

Another problem RES face in Mongolia are of technical nature, where the current infrastructure is not able to cope with a high penetration of intermittent electricity sources, resulting in some of the already granted licenses for renewable projects to be rejected after a thorough power flow analysis [6]. Additionally, experiences with the first wind farm in Mongolia showed curtailment rates of 8.8% in its first year of operation [6].

The issues mentioned so far have led to an increased risk perception of investors in renewable energy projects, which in turn leads to increased interest rates for loans [6]. Hence, it is very important to keep a parameter of certainty, which is the Feed-in Tariff. The Feed-in Tariff gives investors certainty of future cash flows for the first 10 years of the project lifetime, assuming the FiT paying institution is solvent. Predictable future cash flows mitigate at least parts of the risk.

Neglecting the mentioned challenges for a while, reveals that renewable energy sources, especially utility scale PV, are highly competitive, when comparing to the long-run operational costs of coal power plants globally. With a LCOE as low as 48.6 $/MWh, solar PV could already today provide a clean and cheap alternative to coal in Mongolia. Yet, the regulated electricity price alone cannot sustain a further growth of RES. It is understood, that the electricity prices are kept at a low level to assure affordability for Mongolian citizens. Still, it is believed, that affordability and sustainability are two goals that do not exclude each other, when it comes to ground-mounted PV.

With fair conditions for RES, Mongolia could tap its enormous renewable energy potential, redirecting its economy towards a more sustainable one. In addition to the domestic benefits of reduced local pollution and increased energy security, Mongolia could also become a major hub for exporting sustainable electricity. Exporting renewable electricity could also support neighboring countries with their decarbonization efforts, while at the same time allowing for the establishment of a domestic renewable energy industry large enough to leverage economy of scale effects, as has been observed in other Asian countries [115]. Therefore, Mongolia should further promote the Asian Super Grid Initiative, which looks into increased cooperation between north-east Asian countries in terms of electricity transmission, unlocking access to load centers found on the east coast of China [121].

Of course, this vision of Mongolia being a major renewable energy exporter will have to overcome additional challenges such as introducing renewable means to supply the required heat in winter times. Furthermore, a workforce has to be trained and proper supply chains have to be implemented to support this energy transition. Even so, it is believed that with increased support also from the international community, this transition is possible.

6 Conclusion

The last chapter concludes the degree project by summarizing the key findings and insights. Furthermore, recommendations for decision-makers regarding wind and solar power is provided. The chapter finishes with a statement on future work, complementing this study.

This study set out to estimate the techno-economic potential of onshore wind and solar photovoltaic in Mongolia, since most previous studies are either outdated or do not include economic considerations into their analysis.

Therefore, a GIS-based multiprocessing modelling approach for renewable energy site suitability is developed, allowing for estimation of the geographical potential. An energy system model named Enertile is then used to calculate the techno-economic potential, based on the LCOE method. Final economic interpretations are made in Excel and Python, using the NPV approach.

The results support statements by earlier studies, that Mongolia has vast domestic wind and solar resources. The total technical wind and solar potential is estimated at 7.25 TW capacity and 12.17 PWh/year of electricity. The study also reveals, that electricity from ground-mounted PV can generate electricity at a very competitive LCOE starting at 48.6 $/MWh.

This study estimates, that an area of 325 431 km² is suitable for installing wind power plants. A total technical wind potential of 2.13 TW can be installed on the suitable area, yielding 2.60 PWh/year of electricity. The economic potential, given the current FiT support scheme, is 1.15 GW capacity with an annual electricity output of 3.05 TWh. Wind power plants would generate at a LCOE starting from 70 $/MWh or 185.5 MNT/kWh. The wind power hot spots are found in the south of the country.

In terms of ground-mounted photovoltaic, 118 484 km² area is considered suitable. The estimated technical potential is 5.12 TW, which could generate 9.57 PWh electricity per year. The same capacity is also economically feasible, due to the generous FiT support scheme. Highest solar irradiation locations can generate electricity starting at a LCOE of 48.6 $/MWh or 127.9 MNT/kWh. Economically feasible locations are found throughout the country.

The rooftop photovoltaic calculation resulted in a suitable area of 27 km². The technical potential of 1.11 GW would yield an electricity output of 1.92 TWh/year. The economic analysis also shows, that the entire technical potential is economically feasible. Rooftop solar PV systems installed at locations with the best solar irradiation, generate electricity at a LCOE starting at 69.8 $/MWh, which expressed in Mongolian Tugrik is 183.7 MNT/kWh. The most feasible locations for rooftop PV systems are found in the western and central regions.

The ground-mounted and rooftop PV results indicate, that the FiT support scheme might be oversized. To support this statement, the average IRR in case of ground-mounted PV for all grid cells is calculated, resulting in an average IRR of 46.7%, which is significantly higher than the feasibility threshold of 9% selected in this study and even higher than the 15% found in Grassi et al. [7]. Hence, a revision of the Feed-in Tariff support scheme for solar photovoltaic systems is proposed, with the first proposition being a separation of the current grid-connected PV FiT, into a FiT for grid-connected ground-mounted PV and another FiT for rooftop PV.

A target-value calculation is performed to estimate a more appropriate FiT. Therefore, two scenarios are used, one in which the same parameters of this study are chosen (IRR = 9%) and another more conservative scenario, where a 12% IRR and 20% increased investment costs are used. In case of ground-mounted PV, a FiT adjustment between 58.4 $/MWh and 85 $/MWh should be made in order for Mongolia to reach its 2030 renewable targets. In case of a full decarbonization of the electricity system (based on 2018 values), a FiT adjustment between 58.9 $/MWh and 85.7 $/MWh is recommended.

Adjusting the FiT rate for ground-mounted PV to the recommended level for reaching the 2030 goal could potentially cut costs between 65.7% and 83.5%. Absolutely, this could mean savings of around 88.6 to 113.5 million dollars annually for the Mongolian Government, when comparing it with the current FiT rate.

In order to promote the installation of rooftop PV systems in the capital Ulaanbaatar, a FiT in the range of 108.1 to 147.8 $/MWh is sufficient.

The conclusion drawn from these statements is, that in the current market environment renewables are not yet competitive. Nevertheless, the study also concludes that the regulated electricity rate does not reflect the actual cost of generating electricity, being at an unprofitable level for both coal-fired and renewable energy sources. Acknowledging the fact that electricity rates are kept low to ensure low-cost access to electricity for all Mongolian citizens, results in the conclusion that the FiT support scheme for renewables should remain in place for the upcoming years, to promote further growth in the renewable sector. Yet, the FiT should be adjusted to the proposed level and periodically reevaluated, to avoid windfall profits for RES project developers.

Moreover, Mongolia should also focus on improving its current energy infrastructure, to allow for a higher penetration of RES. This can be achieved by improving the transmission grid and increasing flexibility of the current installed capacity.

Nevertheless, the challenge remains the same: To limit global average temperature to 1.5°C, immediate climate action is required. This in-turn is a globally shared responsibility. A responsibility also Mongolia has to acknowledge, even though its share in global GHG emissions is small and its GDP per capita is low. Its vast low-cost solar photovoltaic resources put Mongolia in a position, where inaction is not an option anymore. The Mongolian State should leverage its extensive renewable resources and recognize the co-benefits for the Mongolian society, ranging from reduced local air pollution to increased energy security.

Increased commitment by the international community is required to support Mongolia in its herculean task to decarbonize its economy. Strengthening economic ties between Mongolia and its neighboring countries can further create the opportunity for Mongolia to become a regional export powerhouse of renewable energy, supporting other countries in reducing their GHG emissions.

All in all, it must be stated that no country in this world is too small to have a positive impact on tackling climate change. As the Dalai Lama once said: "If you think you are too small to make a difference, try sleeping with a mosquito" [122].

6.1 Future work

Based on this study, future work includes a detailed power flow analysis in a high penetration of intermittent renewable energy sources scenario. A complementary study could also incorporate other RES such as biomass, geothermal, hydro and concentrated solar power. Concentrated solar power, geothermal and biomass could be of particular interest, due to their ability to also generate renewable heat, which is another key sector for decarbonization efforts to be successful and hence worth investigating.

7 Bibliography

[1] J. Rogelj *et al.*, 'Mitigation Pathways Compatible with 1.5°C in the Context of Sustainable Development', p. 82.

[2] IEA, 'Global Energy and CO2 Status Report 2018', *Energy Demand*, p. 29, 2018.

[3] O. Edenhofer, J. C. Steckel, M. Jakob, and C. Bertram, 'Reports of coal's terminal decline may be exaggerated', *Environ. Res. Lett.*, vol. 13, no. 2, p. 024019, Feb. 2018, doi: 10.1088/1748-9326/aaa3a2.

[4] World Bank, 'CO2 emissions | Data', 18-Aug-2019. [Online]. Available: https://data.worldbank.org/indicator/EN.ATM.CO2E.PC?end=2014&locations=AT-MN-CN-DK&start=1960&view=chart. [Accessed: 18-Aug-2019].

[5] IRENA, 'Renewable Readiness Assessment: Mongolia', International Renewable Energy Agency, Abu Dhabi, 2016.

[6] Government of Mongolia and SREP, 'Investment Plan for Mongolia', Dec. 2019.

[7] S. Grassi, N. Chokani, and R. S. Abhari, 'Large scale technical and economical assessment of wind energy potential with a GIS tool: Case study Iowa', *Energy Policy*, vol. 45, pp. 73–85, Jun. 2012, doi: 10.1016/j.enpol.2012.01.061.

[8] S. Rauner, M. Eichhorn, and D. Thrän, 'The spatial dimension of the power system: Investigating hot spots of Smart Renewable Power Provision', *Appl. Energy*, vol. 184, pp. 1038–1050, Dec. 2016, doi: 10.1016/j.apenergy.2016.07.031.

[9] D. Voivontas, D. Assimacopoulos, A. Mourelatos, and J. Corominas, 'Evaluation of Renewable Energy potential using a GIS decision support system', *Renew. Energy*, vol. 13, no. 3, pp. 333–344, Mar. 1998, doi: 10.1016/S0960-1481(98)00006-8.

[10] S. M. J. Baban and T. Parry, 'Developing and applying a GIS-assisted approach to locating wind farms in the UK', *Renew. Energy*, vol. 24, no. 1, pp. 59–71, Sep. 2001, doi: 10.1016/S0960-1481(00)00169-5.

[11] D. Voivontas, G. Tsiligiridis, and D. Assimacopoulos, 'Solar potential for water heating explored by GIS', *Sol. Energy*, vol. 62, no. 6, pp. 419–427, Jun. 1998, doi: 10.1016/S0038-092X(98)00027-9.

[12] D. Mentis, S. H. Siyal, A. Korkovelos, and M. Howells, 'A geospatial assessment of the techno-economic wind power potential in India using geographical restrictions', *Renew. Energy*, vol. 97, pp. 77–88, Nov. 2016, doi: 10.1016/j.renene.2016.05.057.

[13] V. Gass, J. Schmidt, F. Strauss, and E. Schmid, 'Assessing the economic wind power potential in Austria', *Energy Policy*, vol. 53, pp. 323–330, Feb. 2013, doi: 10.1016/j.enpol.2012.10.079.

[14] S. H. Siyal, U. Mörtberg, D. Mentis, M. Welsch, I. Babelon, and M. Howells, 'Wind energy assessment considering geographic and environmental restrictions in Sweden: A GIS-based approach', *Energy*, vol. 83, pp. 447–461, Apr. 2015, doi: 10.1016/j.energy.2015.02.044.

[15] D. Mentis *et al.*, 'A GIS-based approach for electrification planning—A case study on Nigeria', *Energy Sustain. Dev.*, vol. 29, pp. 142–150, Dec. 2015, doi: 10.1016/j.esd.2015.09.007.

[16] J. R. Janke, 'Multicriteria GIS modeling of wind and solar farms in Colorado', *Renew. Energy*, vol. 35, no. 10, pp. 2228–2234, Oct. 2010, doi: 10.1016/j.renene.2010.03.014.

[17] H. T. Nguyen and J. M. Pearce, 'Estimating potential photovoltaic yield with r.sun and the open source Geographical Resources Analysis Support System', *Sol. Energy*, vol. 84, no. 5, pp. 831–843, May 2010, doi: 10.1016/j.solener.2010.02.009.

[18] Y. Charabi and A. Gastli, 'PV site suitability analysis using GIS-based spatial fuzzy multi-criteria evaluation', *Renew. Energy*, vol. 36, no. 9, pp. 2554–2561, Sep. 2011, doi: 10.1016/j.renene.2010.10.037.

[19] A. Yushchenko, A. de Bono, B. Chatenoux, M. Kumar Patel, and N. Ray, 'GIS-based assessment of photovoltaic (PV) and concentrated solar power (CSP) generation potential in West Africa', *Renew. Sustain. Energy Rev.*, vol. 81, pp. 2088–2103, Jan. 2018, doi: 10.1016/j.rser.2017.06.021.

[20] J. Polo *et al.*, 'Solar resources and power potential mapping in Vietnam using satellite-derived and GIS-based information', *Energy Convers. Manag.*, vol. 98, pp. 348–358, Jul. 2015, doi: 10.1016/j.enconman.2015.04.016.

[21] R. Mahtta, P. K. Joshi, and A. K. Jindal, 'Solar power potential mapping in India using remote sensing inputs and environmental parameters', *Renew. Energy*, vol. 71, pp. 255–262, Nov. 2014, doi: 10.1016/j.renene.2014.05.037.

[22] I.-A. Yeo and J.-J. Yee, 'A proposal for a site location planning model of environmentally friendly urban energy supply plants using an environment and energy geographical information system (E-GIS) database (DB) and an artificial neural network (ANN)', *Appl. Energy*, vol. 119, pp. 99–117, Apr. 2014, doi: 10.1016/j.apenergy.2013.12.060.

[23] J. M. Sánchez-Lozano, C. Henggeler Antunes, M. S. García-Cascales, and L. C. Dias, 'GIS-based photovoltaic solar farms site selection using ELECTRE-TRI: Evaluating the case for Torre Pacheco, Murcia, Southeast of Spain', *Renew. Energy*, vol. 66, pp. 478–494, Jun. 2014, doi: 10.1016/j.renene.2013.12.038.
[24] D. Mentis, S. Hermann, M. Howells, M. Welsch, and S. H. Siyal, 'Assessing the technical wind energy potential in Africa a GIS-based approach', *Renew. Energy*, vol. 83, pp. 110–125, Nov. 2015, doi: 10.1016/j.renene.2015.03.072.
[25] C. Balmuş, 'Design and Implementation of a New GIS-based Modelling Approach for Renewable Energy Site Suitability and Potential Assessment in Europe and Northern Africa', Hochschule Karlsruhe Technik und Wirtschaft, Karlsruhe, 2015.
[26] D. Elliot, M. Schwartz, G. Scott, S. Haymes, D. Heimiller, and R. George, 'Wind Energy Resource Atlas of Mongolia', NREL, Aug. 2001.
[27] Fraunhofer IEE, 'Wind Monitor - Turbine size', *Wind Monitor*. [Online]. Available: http://windmonitor.iee.fraunhofer.de/windmonitor_en/3_Onshore/2_technik/4_anlagengroesse/. [Accessed: 24-Jun-2019].
[28] Earth Resources Observation And Science Center, 'Global Multi-resolution Terrain Elevation Data 2010 (GMTED2010)'. U.S. Geological Survey, 2017, doi: 10.5066/F7J38R2N.
[29] X. Sheng, P. Zeng, H. Xing, L. Philippe, and Q. Dai, 'A GIS+MCDA based assessment method of potential onshore wind power development sites in Mongolia', presented at the 2018 International Conference on Power System Technology, Guangzhou, China, 2018.
[30] The World Bank, IFC, ESMAP, and SOLARGIS, 'Global Solar Atlas', *Global Solar Atlas*. [Online]. Available: https://globalsolaratlas.info/?c=2.328918,-8.989485,2. [Accessed: 25-Jun-2019].
[31] IRENA, 'Global Atlas for Renewable Energy'. [Online]. Available: https://irena.masdar.ac.ae/gallery/#map/543. [Accessed: 25-Jun-2019].
[32] O. Bayasgalan, J. Hashimoto, K. Otani, T. S. Ustun, S. N. Hameed, and A. Adiyabat, 'Estimation of Solar Energy Potential Over Mongolia Based on Satellite Data', *Gd. Renew. Energy Proc.*, vol. 1, p. 70, 2018, doi: 10.24752/gre.1.0_70.
[33] IEA, 'Mongolia'. [Online]. Available: https://www.iea.org/countries/Mongolia/. [Accessed: 21-Oct-2019].
[34] Green Climate Fund, 'Country Programme: Mongolia', Green Climate Fund.
[35] K. Levin, 'New Global CO2 Emissions Numbers Are In. They're Not Good.', *World Resources Institute*, 05-Dec-2018. [Online]. Available: https://www.wri.org/blog/2018/12/new-global-co2-emissions-numbers-are-they-re-not-good. [Accessed: 27-Oct-2019].
[36] World Bank, 'China'. [Online]. Available: https://data.worldbank.org/country/china. [Accessed: 27-Oct-2019].
[37] Mongolian Energy Economics Institute, 'Current Status and Progress in Mongolia for Power Interconnnection', presented at the North-East Asian Regional Power Interconnection and Cooperation Forum 2018, Ulaanaatar, 1028.
[38] Energy Regulatory Commission, 'Electricity Price Structure in WRIPG'. [Online]. Available: http://erc.gov.mn/web/en/wripg. [Accessed: 27-Oct-2019].
[39] Energy Regulatory Commission, 'Statistics on Energy Performance'. [Online]. Available: http://erc.gov.mn/web/en/contents/19. [Accessed: 26-Oct-2019].
[40] Energy Charter Secretariat, 'In-depth review of the investment climate and market structure in the energy sector of Mongolia', Brussels, 2013.
[41] L. S. Beliâ̂ev, *Electricity market reforms: economics and policy challenges*. New York: Springer, 2011.
[42] A.-M. Seman, 'Mongolia's Energy Sector', CEE Bankwatch Network, Apr. 2017.
[43] IRENA, 'Mongolia', *Tableau Software*. [Online]. Available: https://public.tableau.com/views/IRENAREsourceRenewableEnergyCapacity_CountryProfile/Charts?:embed=y&:showVizHome=no&:size=443,1&:embed=y&:showVizHome=n&:bootstrapWhenNotified=y&:tabs=n&:toolbar=n&allowtransparency=true&Country=Mongolia&:apiID=host0#navType=2&navSrc=Parse. [Accessed: 04-Nov-2019].
[44] Asian Development Bank, 'Updating the Energy Sector Development Plan - Energy Sector Policy Review'.
[45] SE4ALL, 'Rapid Assessment and Gap Analysis - Mongolia'.
[46] World Energy Council, *New renewable energy resources. A guide to the future*. London: Kogan Page Limited, 1994.

[47] M. Hoogwijk, 'On the global and regional potential of renewable energy sources', Universiteit Utrecht, Faculteit Scheikunde, Utrecht, 2004.
[48] E. Doris, A. Lopez, and D. Beckley, 'Geospatial Analysis of Renewable Energy Technical Potential on Tribal Lands', DOE/IE-0013, 1067906, Feb. 2013.
[49] Y. Sun, A. Hof, R. Wang, J. Liu, Y. Lin, and D. Yang, 'GIS-based approach for potential analysis of solar PV generation at the regional scale: A case study of Fujian Province', *Energy Policy*, vol. 58, pp. 248–259, Jul. 2013, doi: 10.1016/j.enpol.2013.03.002.
[50] ESRI, 'What is GIS?' [Online]. Available: https://www.esri.com/en-us/what-is-gis/overview. [Accessed: 27-Oct-2019].
[51] ESRI, 'About ArcGIS'. [Online]. Available: https://www.esri.com/en-us/arcgis/about-arcgis/overview. [Accessed: 18-Feb-2019].
[52] Fraunhofer ISI, 'Energy system models - Fraunhofer ISI', *Fraunhofer Institute for Systems and Innovation Research ISI*. [Online]. Available: https://www.isi.fraunhofer.de/en/competence-center/energiepolitik-energiemaerkte/modelle.html. [Accessed: 05-Jun-2019].
[53] ESRI, 'What is ArcPy?—Help | ArcGIS for Desktop'. [Online]. Available: http://desktop.arcgis.com/en/arcmap/10.3/analyze/arcpy/what-is-arcpy-.htm. [Accessed: 06-Jul-2019].
[54] Eurostat and GISCO, 'Administrative Units / Statistical Units - Eurostat'. [Online]. Available: https://ec.europa.eu/eurostat/web/gisco/geodata/reference-data/administrative-units-statistical-units. [Accessed: 05-Sep-2019].
[55] Flanders Marine Institute (VLIZ), Belgium, 'Maritime Boundaries Geodatabase'. VLIZ, 2018, doi: 10.14284/319.
[56] O. Arino, S. Bontemps, P. Defourny, E. Van Bogaert, V. Kalogirou, and J. R. Perez, 'GlobCover 2009 - Products Description and Validation Report', Feb. 2011.
[57] Stanford.edu, 'RMS Error'. [Online]. Available: http://statweb.stanford.edu/~susan/courses/s60/split/node60.html. [Accessed: 10-Nov-2019].
[58] J. J. Danielson and D. B. Gesch, 'Global Multi-resolution Terrain Elevation Data 2010 (GMTED2010)', p. 34, Nov. 2019.
[59] BODC, 'Gridded bathymetry data (General Bathymetric Chart of the Oceans).', *GEBCO*. [Online]. Available: https://www.gebco.net/data_and_products/gridded_bathymetry_data/. [Accessed: 11-Jun-2019].
[60] D. Megginson, 'Map of airports in the World'. [Online]. Available: http://ourairports.com/world.html. [Accessed: 05-Sep-2019].
[61] UNEP-WCMC, 'User Manual for the World Database on Protected Areas and world database on other effective area- based conservation measures: 1.6', p. 79.
[62] GeoCommons, 'Global Shipping Lane Network'. [Online]. Available: http://geocommons.com/datasets?id=25. [Accessed: 05-Sep-2019].
[63] CIESIN and ITOS, 'Global Roads Open Access Data Set, Version 1 (gROADSv1)'. Palisades, NY: NASA Socioeconomic Data and Applications Center (SEDAC), 2013, doi: 10.7927/H4VD6WCT.
[64] gis-lab.info, 'VMap0 data'. [Online]. Available: https://money.yandex.ru/quickpay/shop-widget. [Accessed: 05-Sep-2019].
[65] ECMWF, 'ERA5 data documentation'. [Online]. Available: https://confluence.ecmwf.int/display/CKB/ERA5+data+documentation. [Accessed: 25-Oct-2019].
[66] N. Y. Aydin, E. Kentel, and H. Sebnem Duzgun, 'GIS-based site selection methodology for hybrid renewable energy systems: A case study from western Turkey', *Energy Convers. Manag.*, vol. 70, pp. 90–106, Jun. 2013, doi: 10.1016/j.enconman.2013.02.004.
[67] R. Cowell, 'Wind power, landscape and strategic, spatial planning—The construction of "acceptable locations" in Wales', *Land Use Policy*, vol. 27, no. 2, pp. 222–232, Apr. 2010, doi: 10.1016/j.landusepol.2009.01.006.
[68] P. Enevoldsen *et al.*, 'How much wind power potential does europe have? Examining european wind power potential with an enhanced socio-technical atlas', *Energy Policy*, vol. 132, pp. 1092–1100, Sep. 2019, doi: 10.1016/j.enpol.2019.06.064.
[69] A. D. Mekonnen and P. V. Gorsevski, 'A web-based participatory GIS (PGIS) for offshore wind farm suitability within Lake Erie, Ohio', *Renew. Sustain. Energy Rev.*, vol. 41, pp. 162–177, Jan. 2015, doi: 10.1016/j.rser.2014.08.030.

[70] J. L. Beacham, J. R. Jensen, and Z. Wang, 'A Feasibility Analysis of South Carolina Wind Resources for Electric Power Generation', p. 24.
[71] B. Pfluger *et al.*, 'Langfristszenarien für die Transformation des Energiesystems in Deutschland - Modul 2: Modelle und Modellverbund'.
[72] G. Dufficy *et al.*, 'Best Practices for Siting Solar Photovoltaics on Municipal Solid Waste Landfills', NREL, Golden, Technical Report, Feb. 2013.
[73] L.-I. Tegou, H. Polatidis, and D. A. Haralambopoulos, 'Environmental management framework for wind farm siting: Methodology and case study', *J. Environ. Manage.*, vol. 91, no. 11, pp. 2134–2147, Nov. 2010, doi: 10.1016/j.jenvman.2010.05.010.
[74] Y. Zhou, W.X.Wu, and G. X. Liu, 'Assessment of Onshore Wind Energy Resource and Wind-Generated Electricity Potential in Jiangsu, China', *Energy Procedia*, vol. 5, pp. 418–422, 2011, doi: 10.1016/j.egypro.2011.03.072.
[75] T. Huang, S. Wang, Q. Yang, and J. Li, 'A GIS-based assessment of large-scale PV potential in China', *Energy Procedia*, vol. 152, pp. 1079–1084, Oct. 2018, doi: 10.1016/j.egypro.2018.09.126.
[76] G. Hellman, 'Über die Bewegung der Luft in den untersten Schichten der Atmosphäre', 1916.
[77] F. Sensfuss *et al.*, *Enertile*. Karlsruhe: Fraunhofer ISI.
[78] G. Gualtieri and S. Secci, 'Methods to extrapolate wind resource to the turbine hub height based on power law: A 1-h wind speed vs. Weibull distribution extrapolation comparison', *Renew. Energy*, vol. 43, pp. 183–200, Jul. 2012, doi: 10.1016/j.renene.2011.12.022.
[79] LM Wind Power, 'What is a wind class?' [Online]. Available: https://www.lmwindpower.com/en/stories-and-press/stories/learn-about-wind/what-is-a-wind-class. [Accessed: 10-Nov-2019].
[80] Enercon, 'ENERCON product overview'. .
[81] IE Leipzig, 'Vorbereitung und Begleitung der Erstellung des Erfahrungsberichts 2014 gemäß § 65 EEG - Vorhaben IIe Stromerzeugung aus Windenergie', Leipzig, Germany, Jul. 2014.
[82] IRENA, 'Renewable Energy Technologies: Cost Analysis Series', vol. 1, no. 5, Jun. 2012.
[83] Agora Energiewende, 'Kostenoptimaler Ausbau der Erneuerbaren Energien in Deutschland - Ein Vergleich möglicher Strategien für den Ausbau von Wind- und Solarenergie in Deutschland bis 2033', Berlin, Study, May 2013.
[84] G. Schubert, 'Modeling hourly electricity generation from PV and wind plants in Europe', in *2012 9th International Conference on the European Energy Market*, Florence, Italy, 2012, pp. 1–7, doi: 10.1109/EEM.2012.6254782.
[85] V. Quaschning, *Simulation der Abschattungsverluste bei solarelektrischen Systemen*, 1. Aufl. Berlin: Köster, 1996.
[86] J. A. Duffie and W. A. Beckman, *Solar engineering of thermal processes: John A. Duffie, William A. Beckman*. New York: Wiley, 1980.
[87] D. T. Reindl, W. A. Beckman, and J. A. Duffie, 'Diffuse fraction correlations', *Sol. Energy*, vol. 45, no. 1, pp. 1–7, 1990, doi: 10.1016/0038-092X(90)90060-P.
[88] R. Perez and R. Stewart, 'Solar irradiance conversion models', *Sol. Cells*, vol. 18, no. 3–4, pp. 213–222, Sep. 1986, doi: 10.1016/0379-6787(86)90120-1.
[89] T. Huld, R. Gottschalg, H. G. Beyer, and M. Topič, 'Mapping the performance of PV modules, effects of module type and data averaging', *Sol. Energy*, vol. 84, no. 2, pp. 324–338, Feb. 2010, doi: 10.1016/j.solener.2009.12.002.
[90] W. N. Macêdo and R. Zilles, 'Operational results of grid-connected photovoltaic system with different inverter's sizing factors (ISF)', *Prog. Photovolt. Res. Appl.*, vol. 15, no. 4, pp. 337–352, Jun. 2007, doi: 10.1002/pip.740.
[91] ZSW, 'Vorbereitung und Begleitung der Erstellung des Erfahrungsberichts 2014 gemäß § 65 EEG - Vorhaben IIc Solare Strahlungsenergie', Zentrum für Sonnenenergie und Wasserstoffforschung BW, Stuttgart, Germany, Jul. 2014.
[92] M. B. McElroy, X. Lu, C. P. Nielsen, and Y. Wang, 'Potential for Wind-Generated Electricity in China', *Science*, vol. 325, no. 5946, pp. 1378–1380, Sep. 2009, doi: 10.1126/science.1175706.
[93] Asian Development Bank, 'Updating the Energy Sector Development Plan - Electricity Expansion Plan', vol. Part C, no. Volume VI, p. 91.
[94] IRENA, 'Renewable Power Generation Costs in 2017', International Renewable Energy Agency, Abu Dhabi, 2018.

[95] Chifeng Xinsheng Wind Power Co., 'CDM Project 1487: Inner Mongolia Wudaogou 50.25MW Wind Power Project'. [Online]. Available: https://cdm.unfccc.int/Projects/DB/DNV-CUK1198674466.99/view. [Accessed: 30-Dec-2019].
[96] Inner Mongolia Datang International New Energy Co., 'CDM Project 9955: Inner Mongolia Chayouhouqi Hongmu Phase I 20MWp Solar Power Project'. [Online]. Available: https://cdm.unfccc.int/Projects/DB/CTI1399882315.23/view. [Accessed: 30-Dec-2019].
[97] Inner Mongolia Zhuozi Wind Power Co., 'CDM Project 1327: Inner Mongolia Zhuozi 40MW Wind Power Project'. [Online]. Available: https://cdm.unfccc.int/Projects/DB/TUEV-SUED1188906688.93/view. [Accessed: 30-Dec-2019].
[98] Government of Mongolia, *Law of Mongolia on Renewable Energy*. 2007.
[99] Energy Regulatory Commission, 'Electricity Price Structure in CRIPG'. [Online]. Available: http://erc.gov.mn/web/en/cripg. [Accessed: 24-Oct-2019].
[100] OFX, 'Yearly Average Rates & Forex History Data'. [Online]. Available: https://www.ofx.com/en-au/forex-news/historical-exchange-rates/yearly-average-rates/. [Accessed: 24-Oct-2019].
[101] xe.com, 'XE: Convert MNT/EUR. Mongolia Tughrik to Euro Member Countries'. [Online]. Available: https://www.xe.com/currencyconverter/convert/?Amount=1&From=MNT&To=EUR. [Accessed: 24-Oct-2019].
[102] xe.com, 'XE: Convert MNT/USD. Mongolia Tughrik to United States Dollar'. [Online]. Available: https://www.xe.com/currencyconverter/convert/?Amount=1&From=MNT&To=USD. [Accessed: 24-Oct-2019].
[103] 'ESA Data User Element'. [Online]. Available: http://due.esrin.esa.int/page_globcover.php. [Accessed: 08-Jun-2019].
[104] J. Chepkemoi, 'Which Are The Island Countries Of The World?', 25-Apr-2017. [Online]. Available: https://web.archive.org/web/20171207094959/http://www.worldatlas.com/articles/which-are-the-island-countries-of-the-world.html. [Accessed: 21-Oct-2019].
[105] Kartverket, 'Arealstatistikk for Norge'. [Online]. Available: https://www.kartverket.no/Kunnskap/Fakta-om-Norge/Arealstatistikk/Arealstatistikk-Norge/. [Accessed: 21-Oct-2019].
[106] CIA, 'Italy - Factbook', 15-Oct-2019. [Online]. Available: https://www.cia.gov/library/publications/the-world-factbook/geos/it.html. [Accessed: 21-Oct-2019].
[107] IEA, 'China'. [Online]. Available: https://www.iea.org/countries/China/. [Accessed: 22-Oct-2019].
[108] geology.com, 'Largest Desert in the World'. [Online]. Available: https://geology.com/records/largest-desert.shtml. [Accessed: 21-Oct-2019].
[109] IEA, 'France'. [Online]. Available: https://www.iea.org/countries/France/. [Accessed: 26-Oct-2019].
[110] World Bank, ESMAP, Technical University of Denmark, and Vortex, 'Global Wind Atlas', *Global Wind Atlas*. [Online]. Available: https://globalwindatlas.info. [Accessed: 02-Nov-2019].
[111] Vortex, 'Global Wind Atlas meets a unique global 3km ERA5-driven dataset designed by Vortex', *VORTEX*, 22-Oct-2019. [Online]. Available: https://vortexfdc.com/global-wind-atlas-meets-a-unique-global-3km-era5-driven-dataset-designed-by-vortex/. [Accessed: 02-Nov-2019].
[112] G. Feller, 'Investors Keen to Support Mongolia's Renewable Energy Goals', *Renewable Energy World*, 29-Dec-2017. [Online]. Available: https://www.renewableenergyworld.com/2017/12/29/investors-keen-to-support-mongolia-s-renewable-energy-goals/. [Accessed: 01-Nov-2019].
[113] worldpopulationreview.com, 'Poland Population 2019'. [Online]. Available: http://worldpopulationreview.com/countries/poland-population/. [Accessed: 30-Oct-2019].
[114] CIA, 'Togo - Factbook'. [Online]. Available: https://www.cia.gov/library/publications/the-world-factbook/geos/to.html. [Accessed: 30-Oct-2019].
[115] IRENA, 'Renewable Power Generation Costs in 2018', International Renewable Energy Agency, Abu Dhabi.
[116] M. Gray, S. Ljungwaldh, L. Watson, and I. Kok, 'Powering down coal - Navigating the economic and financial risks in the last years of coal power', Carbon Tracker, London, Nov. 2018.

[117] A. Pyrgou, A. Kylili, and P. A. Fokaides, 'The future of the Feed-in Tariff (FiT) scheme in Europe: The case of photovoltaics', *Energy Policy*, vol. 95, pp. 94–102, Aug. 2016, doi: 10.1016/j.enpol.2016.04.048.
[118] D. R. Biggar and M. Hesamzadeh, *The economics of electricity markets*. Chichester, West Sussex, United Kingdom: Wiley, 2014.
[119] MIT, 'Principles of Welfare Economics | Unit 4: Welfare Economics'. [Online]. Available: https://ocw.mit.edu/courses/economics/14-01sc-principles-of-microeconomics-fall-2011/unit-4-welfare-economics/principles-of-welfare-economics/. [Accessed: 04-Nov-2019].
[120] Mongolian Economy, 'Т.Цэрэнпүрэв: Эрчим хүчний салбар татаасаар амь зогоодог биш, улсын төсвийн орлого бүрдүүлэгч салбар болно', *Mongolian Economy*. [Online]. Available: http://mongolianeconomy.mn/post/1058/. [Accessed: 04-Nov-2019].
[121] J. Zhao, J. Wang, and Z. Su, 'Power generation and renewable potential in China', *Renew. Sustain. Energy Rev.*, vol. 40, pp. 727–740, Dec. 2014, doi: 10.1016/j.rser.2014.07.211.
[122] Dalai Lama, 'Quote'.

Appendix

Onshore wind power – Capacity Factor

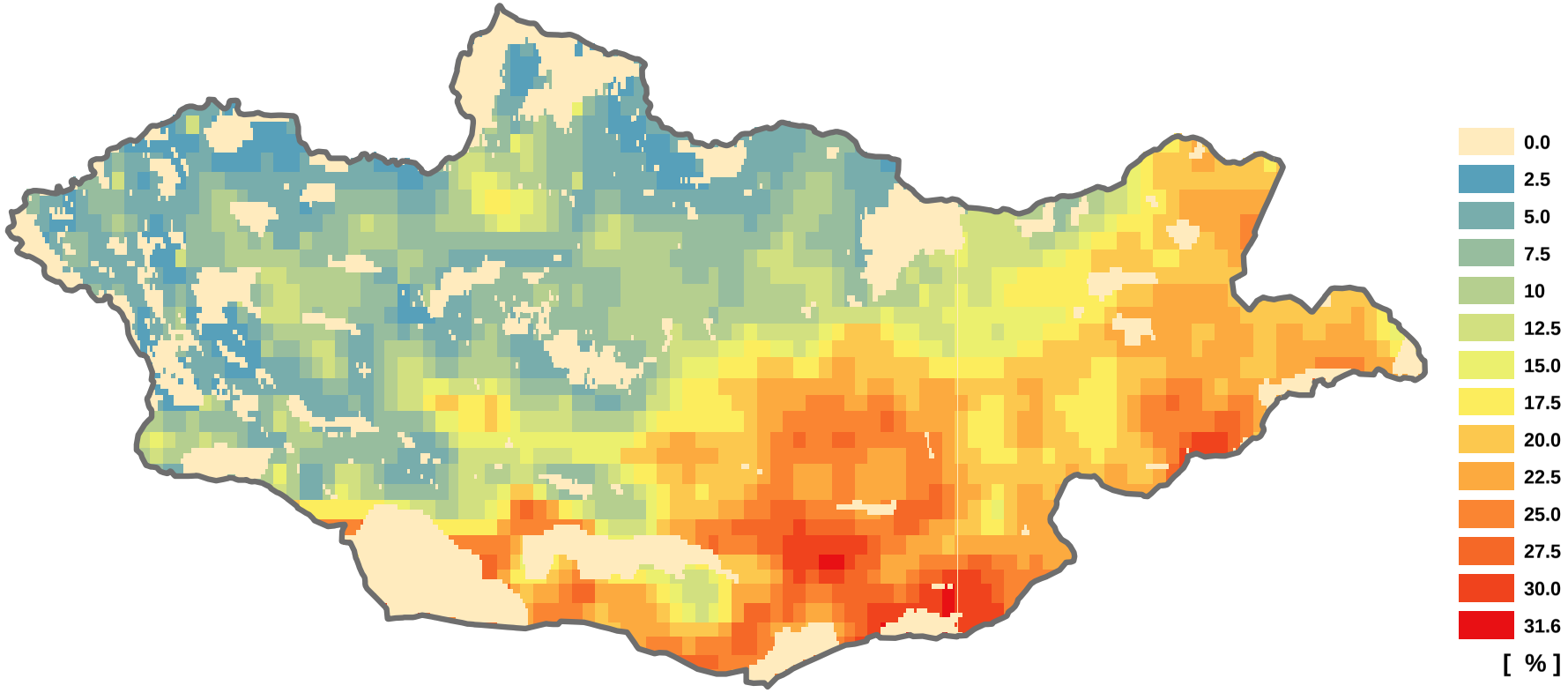

Onshore wind power - LCOE

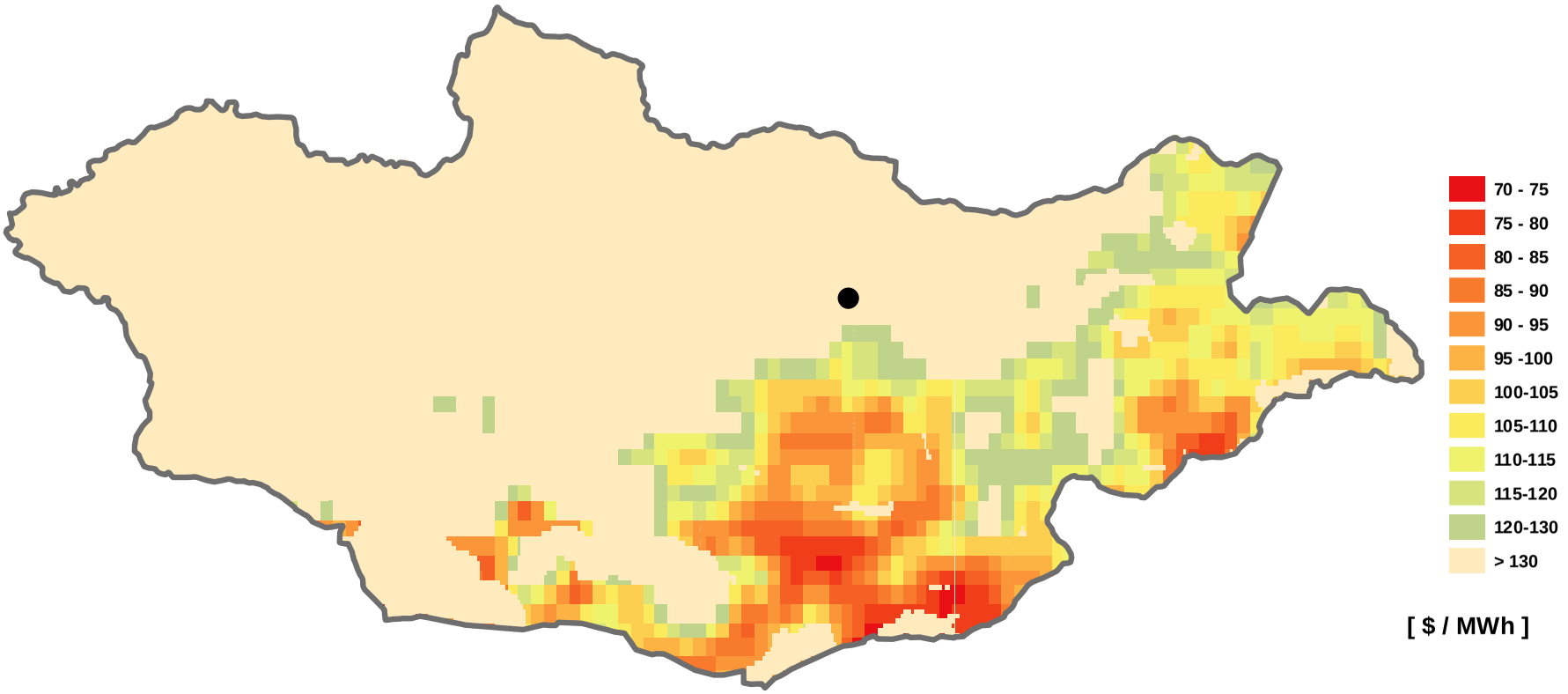

Ground-mounted photovoltaics – Capacity factor

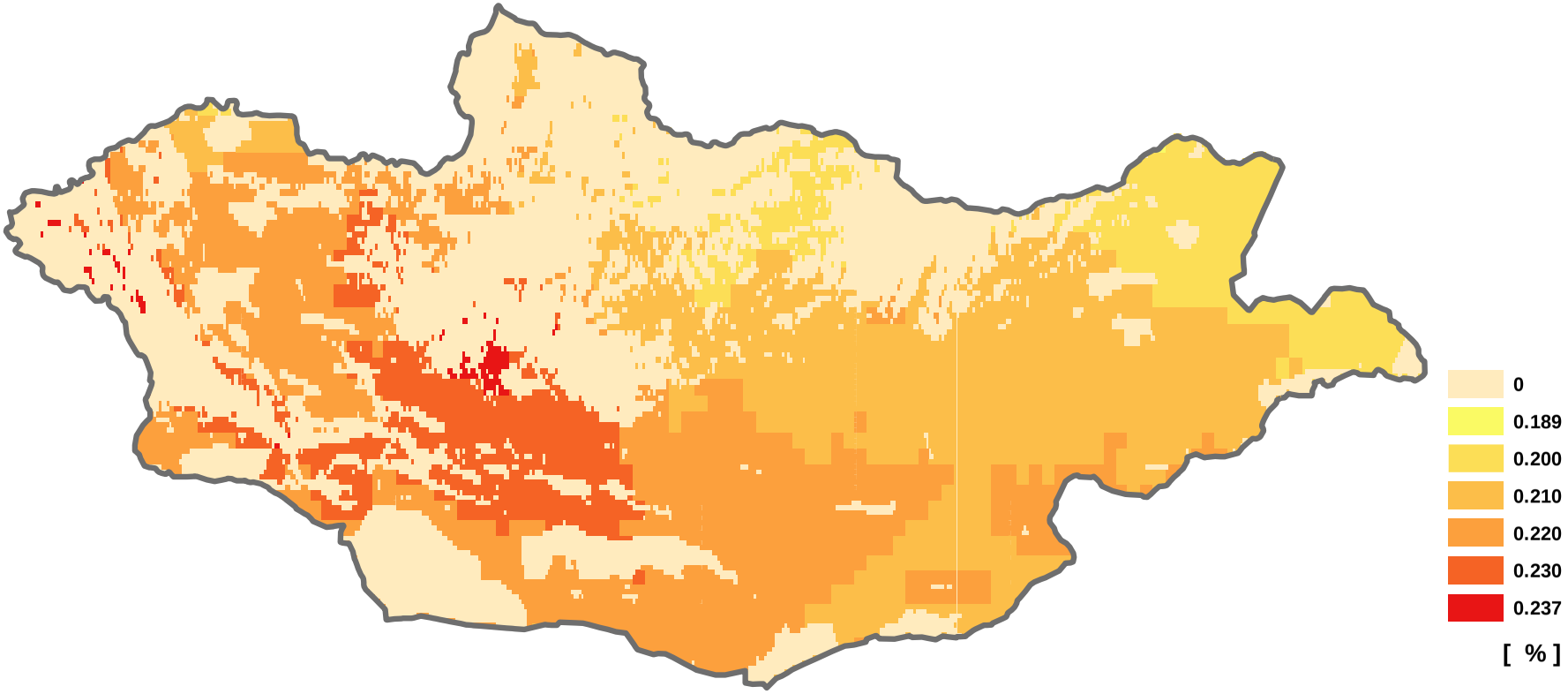

Ground-mounted photovoltaics – LCOE

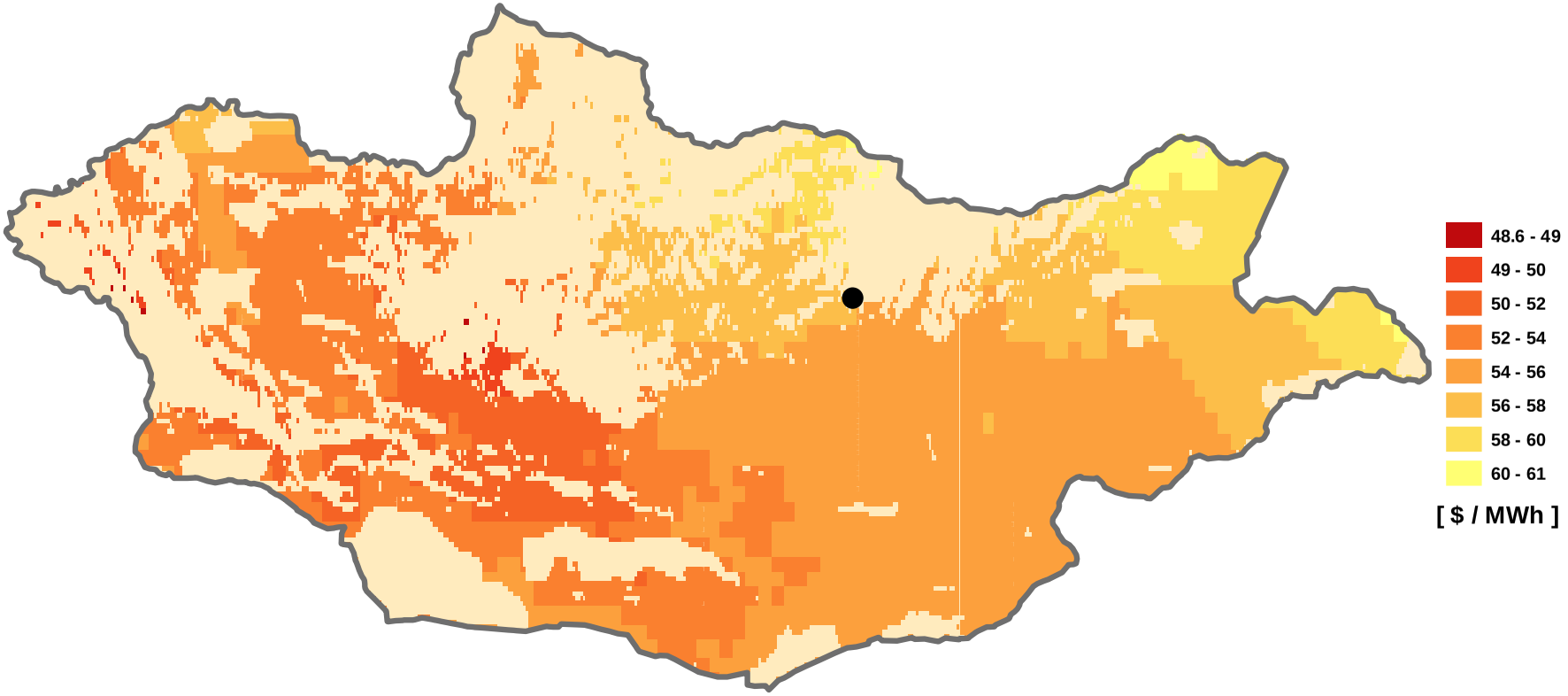

Rooftop photovoltaics – LCOE

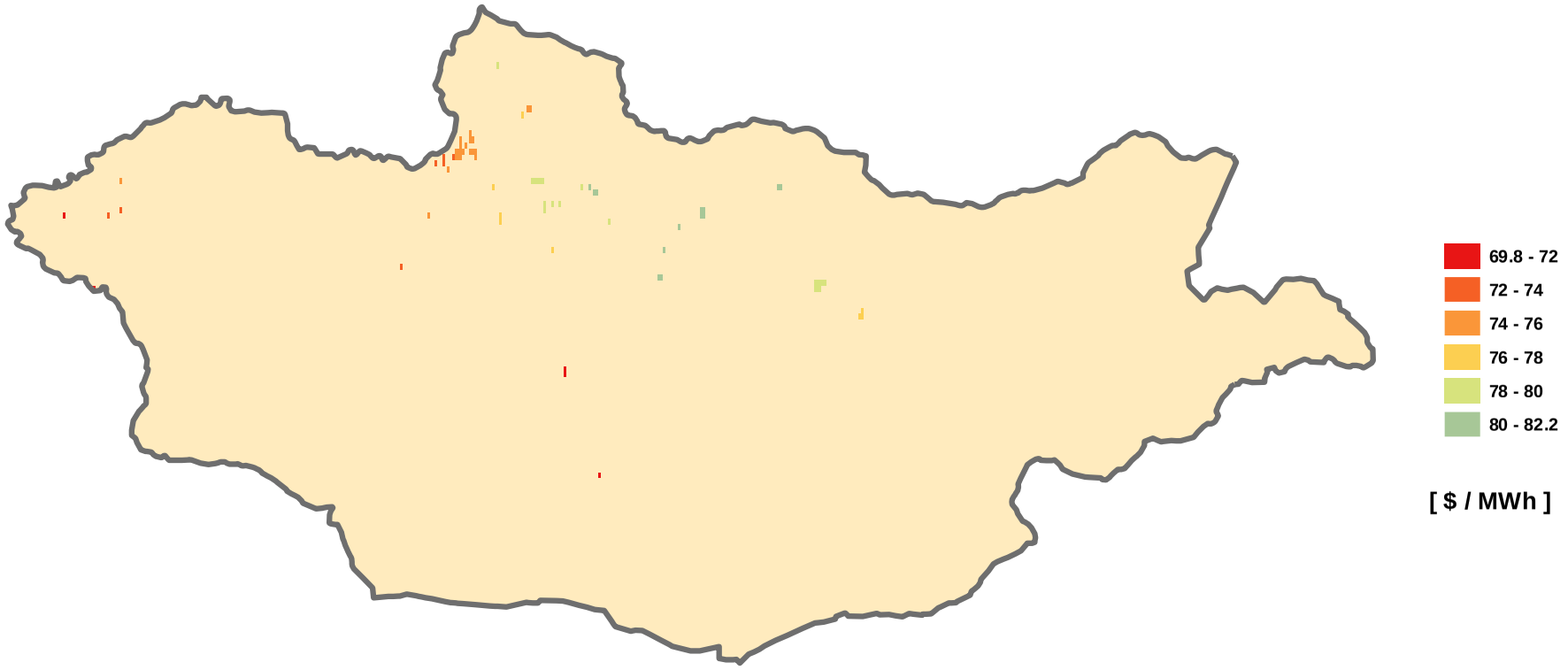

Ground-mounted photovoltaics – Supply curves (IRR 9%)

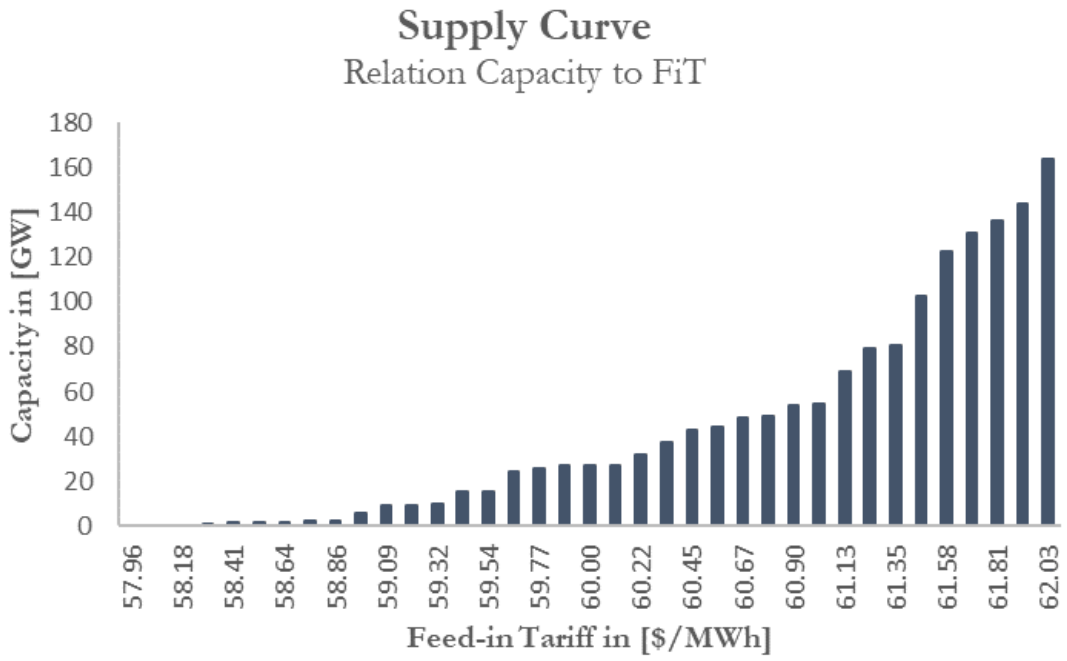

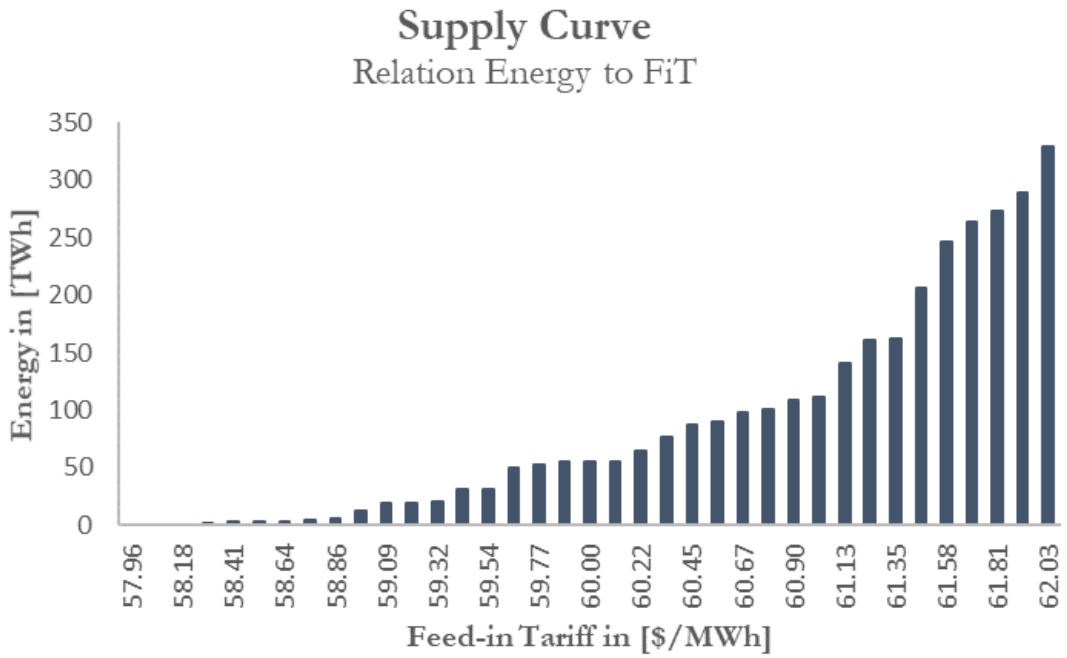

Ground-mounted photovoltaics – Supply curve data (IRR 9%)

IRR = 9%		
FiT Rate	Capacity GW	Electricity TWh
[$/MWh]	[GW]	[TWh]
57.96	0.00	0.00
58.07	0.00	0.00
58.18	0.00	0.00
58.30	0.32	0.66
58.41	1.23	2.54
58.52	1.23	2.54
58.64	1.76	3.64
58.75	2.16	4.47
58.86	2.50	5.17
58.98	5.75	11.87
59.09	9.04	18.61
59.20	9.04	18.61
59.32	9.94	20.45
59.43	15.01	30.81
59.54	15.01	30.81
59.66	24.22	49.60
59.77	25.39	51.98
59.88	27.05	55.37
60.00	27.15	55.56
60.11	27.15	55.56
60.22	31.64	64.66
60.34	37.28	76.08
60.45	42.91	87.44
60.56	44.39	90.43
60.67	48.37	98.43
60.79	49.23	100.18
60.90	53.64	109.02
61.01	54.64	111.03
61.13	69.18	140.16
61.24	79.13	160.08
61.35	80.34	162.49
61.47	102.51	206.69
61.58	122.50	246.51
61.69	130.87	263.17
61.81	136.05	273.46
61.92	143.88	288.99
62.03	163.86	328.57
62.15	191.01	382.28
62.26	208.95	417.70
62.37	230.67	460.55
62.49	248.11	494.88
62.60	287.08	571.55
62.71	327.43	650.83
62.83	357.49	709.81
62.94	400.91	794.89
63.05	439.24	869.89
63.17	484.36	958.07
63.28	550.24	1086.60
63.39	602.15	1187.77
63.50	631.44	1244.80
63.62	662.90	1305.94
63.73	713.46	1404.05
63.84	783.43	1539.70
63.96	813.33	1597.57
64.07	843.38	1655.67
64.18	866.65	1700.60
64.30	918.42	1800.41
64.41	966.74	1893.44
64.52	1050.54	2054.57

Ground-mounted photovoltaics – Supply curves (IRR 12%)

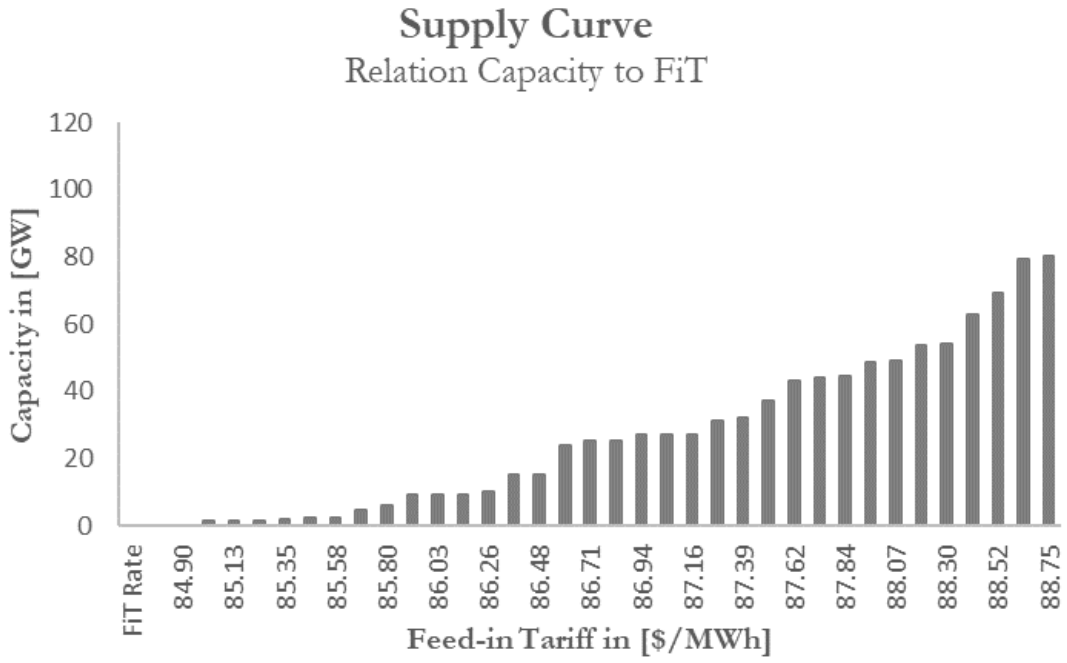

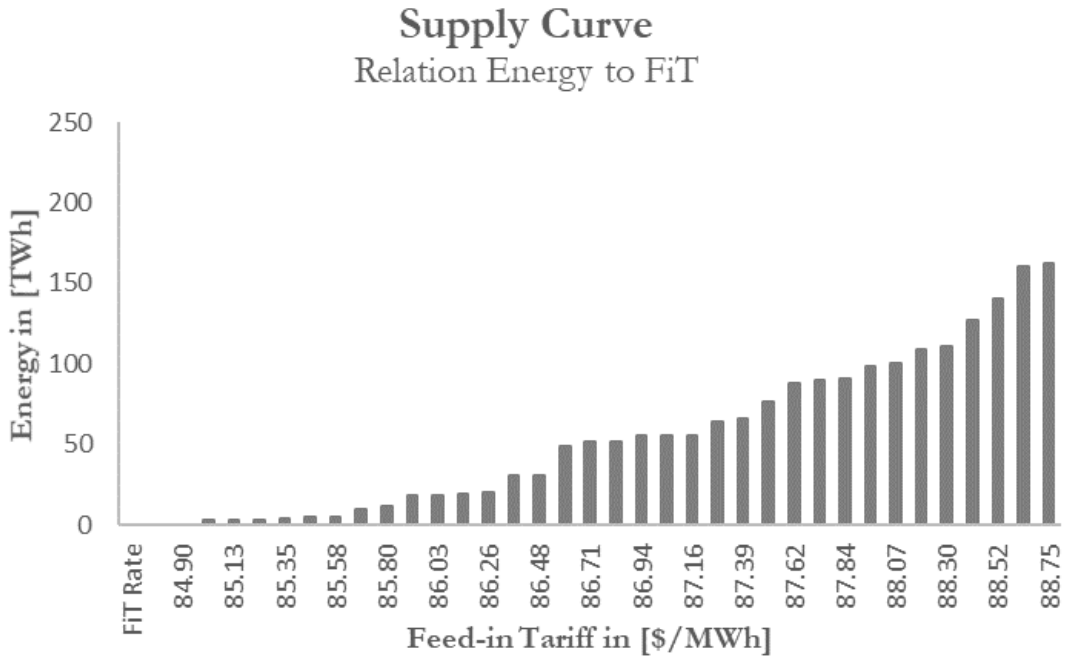

Ground-mounted photovoltaics – Supply curve data (IRR 12%)

IRR = 12%		
FiT Rate	Capacity	Electricity
[$/MWh]	[GW]	[TWh]
84.90	0	0.00
85.01	1.23	2.54
85.13	1.23	2.54
85.24	1.23	2.54
85.35	1.76	3.64
85.47	2.16	4.47
85.58	2.50	5.17
85.69	4.45	9.18
85.80	5.75	11.87
85.92	9.04	18.61
86.03	9.04	18.61
86.14	9.07	18.67
86.26	9.94	20.45
86.37	15.01	30.81
86.48	15.01	30.81
86.60	23.91	48.97
86.71	25.06	51.31
86.82	25.39	51.98
86.94	27.05	55.37
87.05	27.15	55.56
87.16	27.15	55.56
87.28	31.37	64.11
87.39	32.15	65.70
87.50	37.28	76.08
87.62	42.91	87.44
87.73	44.07	89.79
87.84	44.46	90.58
87.96	48.37	98.43
88.07	49.23	100.18
88.18	53.64	109.02
88.30	54.31	110.38
88.41	62.73	127.24
88.52	69.18	140.16
88.63	79.13	160.08
88.75	80.34	162.49
88.86	85.56	172.89
88.97	112.16	225.93
89.09	122.50	246.51
89.20	130.87	263.17
89.31	131.00	263.43
89.43	139.74	280.78
89.54	150.13	301.38
89.65	163.86	328.57
89.77	181.47	363.41
89.88	195.84	391.82
89.99	212.37	424.44
90.11	230.67	460.55
90.22	241.69	482.24
90.33	274.60	547.02
90.45	314.65	625.73
90.56	339.02	673.58
90.67	361.73	718.12
90.79	400.91	794.89
90.90	429.07	850.01
91.01	464.23	918.74
91.13	484.70	958.73
91.24	550.24	1086.60
91.35	589.40	1162.93
91.46	627.21	1236.57
91.58	636.12	1253.89
91.69	673.70	1326.90
91.80	706.75	1391.06

Rooftop photovoltaics – Supply curves (IRR 9%)

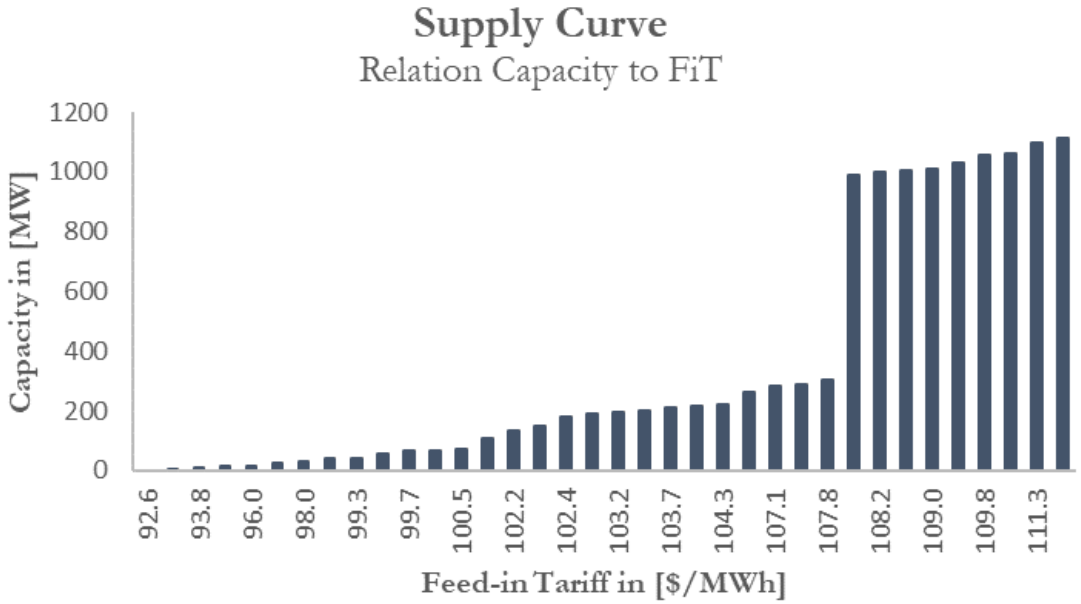

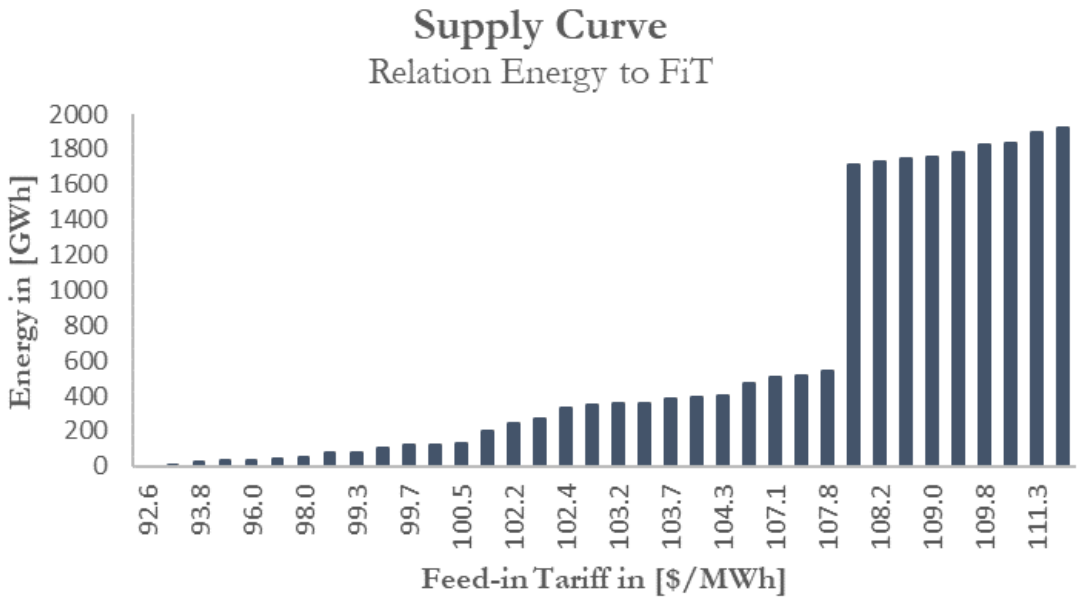

Rooftop photovoltaics – Supply curve data (IRR 9%)

IRR = 9%		
FiT Rate	Capacity GW	Electricity TWh
[$/MWh]	[GW]	[TWh]
92.60	0.00	0.00
92.71	4.87	9.45
93.84	10.28	19.84
94.63	15.14	29.13
95.99	16.76	32.19
96.67	23.25	44.36
98.03	27.58	52.38
99.16	38.94	73.24
99.28	38.94	73.24
99.39	56.78	105.95
99.73	63.27	117.81
100.29	65.98	122.73
100.52	69.22	128.62
100.97	108.70	200.04
102.22	133.04	243.61
102.33	146.02	266.82
102.45	179.00	325.78
102.90	190.36	346.01
103.24	194.69	353.69
103.46	197.93	359.45
103.69	210.91	382.41
103.80	215.78	391.01
104.26	222.27	402.44
106.18	260.67	469.06
107.09	282.84	507.24
107.54	287.71	515.59
107.77	302.31	540.61
108.11	989.12	1714.38
108.22	998.32	1730.08
108.90	1005.89	1742.93
109.01	1011.30	1752.10
109.58	1030.22	1784.07
109.80	1057.26	1829.65
110.82	1060.51	1835.08
111.27	1096.20	1894.58
112.63	1110.80	1918.68

Rooftop photovoltaics – Supply curves (IRR 12%)

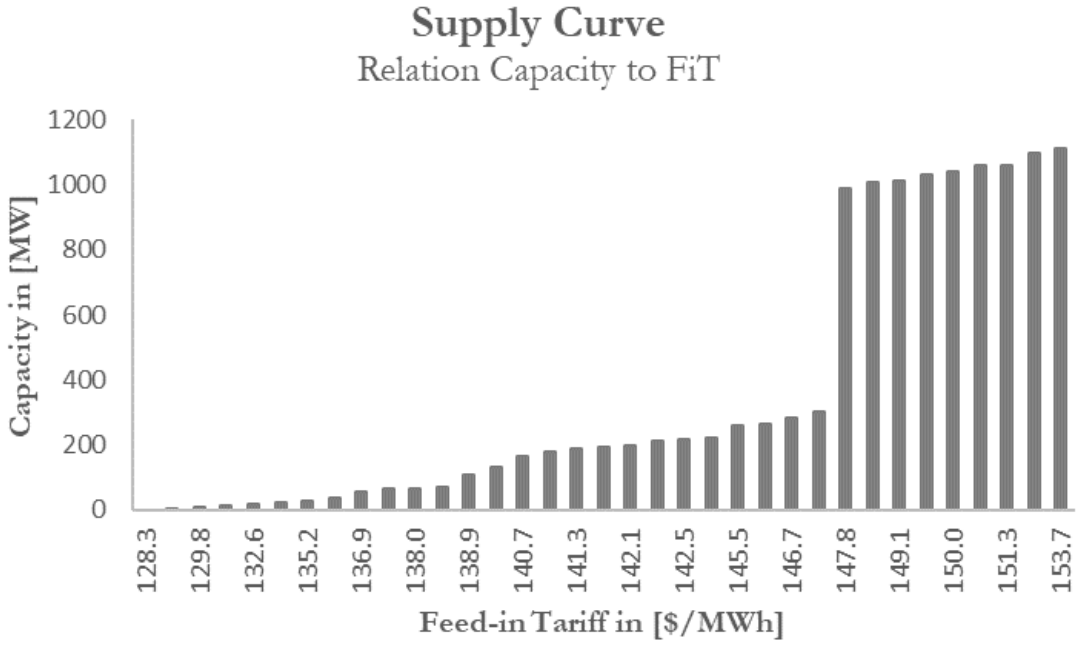

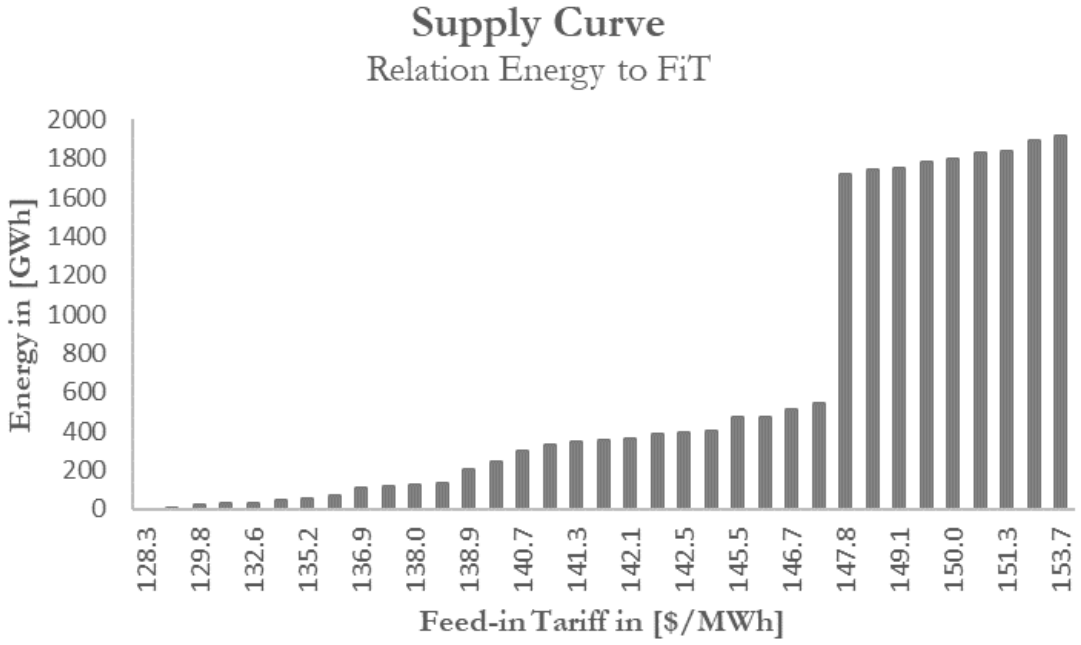

Rooftop photovoltaics – Supply curve data (IRR 12%)

IRR = 12%		
FiT Rate	Capacity	Electricity
[$/MWh]	[GW]	[TWh]
128.25	0.00	0.00
128.37	4.87	9.45
129.84	10.28	19.84
130.86	15.14	29.13
132.56	16.76	32.19
133.35	23.25	44.36
135.16	27.58	52.38
136.52	38.94	73.24
136.86	56.78	105.95
137.42	63.27	117.81
137.99	65.98	122.73
138.33	69.22	128.62
138.90	108.70	200.04
140.48	133.04	243.61
140.71	164.94	300.66
140.82	179.00	325.78
141.27	190.36	346.01
141.73	194.69	353.69
142.06	197.93	359.45
142.29	210.91	382.41
142.52	215.78	391.01
142.97	222.27	402.44
145.46	260.67	469.06
146.59	263.37	473.71
146.71	282.84	507.24
147.39	302.31	540.61
147.84	989.12	1714.38
148.97	1005.89	1742.93
149.08	1011.30	1752.10
149.88	1030.22	1784.07
149.99	1038.88	1798.66
150.10	1057.26	1829.65
151.35	1060.51	1835.08
152.03	1096.20	1894.58
153.72	1110.80	1918.68

WiSo-GERI – Main script

```
'''                                                    WiSoGERI
'''
# Author: Alexander HARRUCKSTEINER
# Main script of the Wind and Solar Global Energy Resources Identification model

# import relevant python modules
import arcpy
import time
import sys
from functools import partial
import tqdm
import os
from multiprocessing import Process, Queue, Pool, cpu_count, Manager, Lock
from WiSoGERI_Intro import intro_general, intro_lulc, intro_slope
from WiSoGERI_Check import cntry_check, eez_check, prj_check, iso_transform
from WiSoGERI_Worker import execute_LULCanalysis, execute_SLOPEanalysis,
execute_DEPTHanalysis

if __name__ == '__main__':

    ''' USER INPUT '''
    # Enter Country of Interest (Be aware of correct spelling!)
    country_name = 'St. Helena'
    # Enter True if selected Country has EEZ. Enter False if selected Country has
no EEZ
    # Enter Name of the EEZ name
    EEZ_existing = True
    eez_name = 'Saint Helena'

    # take time
    t_start = time.time()
    # make a date stamp and define a headline for the .txt file
    datestamp = time.strftime('%Y%m%d')

    # show introduction text to WiSo-GERI model and LULC script
    # functions defined in WiSoGERI_Intro.py
    intro_general()

    # set workspace
    gdb_path = r'K:\X\User\harrucksteiner\ArcGIS\WiSoGERI\WiSoGERI_GDB.gdb'
    arcpy.env.workspace = gdb_path
    arcpy.env.overwriteOutput = True

    # define general input data sources
    Fishnet_Grid = 'FishnetG_World'
    AdmBorders_World = 'AdmBorders_World'
    EEZ_World = 'EEZ_World'
    # transform full country name into three letter code/iso alpha label
    isoAlpha_name = iso_transform(AdmBorders_World, country_name)

    # define LULC specific input data sources
    LULC_World = 'LULC12_World'
    ProtectedAreas_Buffer = 'ProtectedAreas_World_Buffer'
    Rail_Buffer = 'Railroad_World_Buffer'
    Road_Buffer = 'gRoads_World_Buffer'
    Airport_Buffer = 'Airport2019_Buffer'
    Settlement_Buffer = 'Settlements_World_Buffer'
    Shoreline_Buffer = 'ShorelineAdm_World_Buffer'
    Waterways_Buffer = 'Waterways_World_Buffer'

    # define SLOPE specific input data sources
    Slope_World = 'Slope_World'

    # define DEPTH specific input data sources
    WaterDepth_World = 'WaterDepth_China_WGS'
```

```
    # define lists for multiple inputs to worker functions
    general_list = [Fishnet_Grid, AdmBorders_World, EEZ_World]
    supplement_data = [isoAlpha_name, datestamp, EEZ_existing, gdb_path]

    # run projection check on all input data. Add new data source if necessary
    # function defined in WiSoGERI_Check.py
    prj_list = [Fishnet_Grid, AdmBorders_World, EEZ_World, LULC_World,
ProtectedAreas_Buffer,
                Rail_Buffer, Road_Buffer, Airport_Buffer, Settlement_Buffer,
Slope_World]
    for i in prj_list:
        prj_check(i)
    print('\n')

    # screens whether or not the entered country is available in the
AdmBorders_World map
    # function defined in WiSoGERI_Check.py
    cntry_check(AdmBorders_World, country_name)
    if EEZ_existing == True:
        eez_check(EEZ_World, eez_name)

    # Make Feature layer to allow SelectByAttribute operation
    ''' Change SelectByLocation to SelectByAttribute after successfully joining
Fishnet '''
    AdmBorders_lyr = arcpy.MakeFeatureLayer_management(AdmBorders_World,
'border_lyr')
    Fishnet_lyr = arcpy.MakeFeatureLayer_management(Fishnet_Grid, 'fishnetG_lyr')

    # isolate fishnet grid cells belonging to the mainland of chosen country, by
copying features
    print('Creating Feature Layers..')
    tempCntryShape = arcpy.SelectLayerByAttribute_management(AdmBorders_lyr,
'NEW_SELECTION',
                                                             """ "FIRST_NAME" =
'{}' """.format(country_name))
    tempCntry = arcpy.SelectLayerByAttribute_management(Fishnet_lyr,
'NEW_SELECTION',
                                                        """ "FIRST_NAME" = '{}'
""".format(country_name))

    print('Initializing Mainland isolation..')
    MainlandShape = arcpy.FeatureClassToFeatureClass_conversion(tempCntryShape,

'K:\X\User\harrucksteiner\ArcGIS\WiSoGERI\TempGDB.gdb',

'AdmB_Shape_{}'.format(isoAlpha_name))
    MainlandCntry = arcpy.FeatureClassToFeatureClass_conversion(tempCntry,

'K:\X\User\harrucksteiner\ArcGIS\WiSoGERI\TempGDB.gdb',

'FishnetG_AdmB_{}'.format(isoAlpha_name))

    # Code will only be executed if the selected country has an EEZ
    if EEZ_existing == True:
        # isolate fishnet grid cells belonging to both the Mainland and EEZ of the
chosen country, by copying features
        tempCombi = arcpy.SelectLayerByAttribute_management(Fishnet_lyr,
'ADD_TO_SELECTION',
                                                            """ "Territory1" = '{}'
""".format(eez_name))

        print('Initializing total Territory (Mainland + EEZ) isolation..')
        CombiCntry = arcpy.FeatureClassToFeatureClass_conversion(tempCombi,

'K:\X\User\harrucksteiner\ArcGIS\WiSoGERI\TempGDB.gdb',

'FishnetG_Combi_{}'.format(isoAlpha_name))
```

```
        tempEEZ = arcpy.SelectLayerByAttribute_management(Fishnet_lyr,
'NEW_SELECTION',
                                                          """ "Territory1" = '{}'
""".format(eez_name))

        print('Initializing EEZ isolation..')
        EEZCntry = arcpy.FeatureClassToFeatureClass_conversion(tempEEZ,

'K:\X\User\harrucksteiner\ArcGIS\WiSoGERI\TempGDB.gdb',

'FishnetG_EEZ_{}'.format(isoAlpha_name))

    else:
        # set isolated mainland fishnet grid cells to variable CombiCntry
        CombiCntry = MainlandCntry

    t1 = time.time()
    t_isolation = str((t1 - t_start)/60)
    print('{} successfully isolated!'.format(country_name))
    print('Time required: {} mins\n'.format(t_isolation))

###                                                     LULC
###
    intro_lulc()

    headerLULC = (['AREA_ID', 'LULC1', 'LULC2', 'LULC3', 'LULC4', 'LULC5', 'LULC6',
'LULC7',
                   'LULC8', 'LULC9', 'LULC10', 'LULC11', 'LULC12'])

    os.chdir('../results')
    if not os.path.exists(country_name):
        os.makedirs(country_name)
    os.chdir('./{}'.format(country_name))

    # write headline into .txt file
    with open('{}_InputEnertile_LULC_{}.txt'.format(datestamp, isoAlpha_name), 'a')
as headerwriter:
        for i in headerLULC:
            headerwriter.write(str(i) + ';')
        headerwriter.write('\n')

    # Read in fishnet Area_IDs and Extents (X Y coordinates)
    print('Scanning Fishnet Features..')
    # define a dictionary and an increment counter variable
    extDict = {}
    counter = 1
    for row in arcpy.da.SearchCursor(CombiCntry, ['Area_ID', 'SHAPE@']):
        # define a list for every Area_ID
        # append Area_ID as first element in list. Append extent of fishnet grid
cell to list
        ext_list = []
        ext_list.append(row[0])
        extent_curr = row[1].extent
        ext_list.append(extent_curr.XMin)
        ext_list.append(extent_curr.YMin)
        ext_list.append(extent_curr.XMax)
        ext_list.append(extent_curr.YMax)
        # set counter variable as dictionary key. Define ext_list as dictionary
values
        # increment counter variable for next fishnet grid cell
        extDict[counter] = ext_list
        counter += 1

    if EEZ_existing == True:
        buffer_list = [ProtectedAreas_Buffer, Rail_Buffer, Road_Buffer,
Airport_Buffer, Settlement_Buffer,
                       Shoreline_Buffer, Waterways_Buffer
```

```
                        ]
    else:
        buffer_list = [ProtectedAreas_Buffer, Rail_Buffer, Road_Buffer,
Airport_Buffer, Settlement_Buffer]

    print('Area_IDs and Extents have been successfully scanned!')
    # cpu_count() returns number of CPU cores as an Integer
    Cores = cpu_count()
    print('{} CPU cores ready for utilization detected!'.format(Cores))
    print('Initializing multicore LULC Analysis..\n')

    # define how many processes are executed at the same time. Should not exceed
number of cores
    # define a lock for .txt file
    # partial() allows multiple inputs to the worker function
(execute_LULCanalysis)
    pool = Pool(processes=Cores)
    m = Manager()
    lock = m.Lock()
    lulc_func = partial(execute_LULCanalysis, lock, supplement_data, LULC_World,
buffer_list)

    # distribute worker function to different CPU cores and start process
    # tqdm() is used for displaying the progress bar
    # execute_LULCanalysis function is defined in WiSoGERI_WorkerForLoop.py
    for _ in tqdm.tqdm(pool.imap_unordered(lulc_func, extDict.items()),
total=len(extDict.items()), desc='Progress', unit='Grid Cells'):
        pass


    t2 = time.time()
    t_lulc = str((t2 - t1) / 60)
    print('LULC Analysis finished!')
    print('Time required: {} mins\n'.format(t_lulc))


###                                                    SLOPE
###
    intro_slope()
    print('Initializing multicore SLOPE Analysis..\n')
    # header show upper limit of Slope categories.
    # Unit of Slope is percent degree, meaning 90 degrees equals 100 percent
    headerSLOPE = (['AREA_ID', 'SLOPE5', 'SLOPE10', 'SLOPE15', 'SLOPE20',
'SLOPE30', 'SLOPE100'])

    with open('{}_InputEnertile_SLOPE_{}.txt'.format(datestamp, isoAlpha_name),
'a') as headerwriter:
        for i in headerSLOPE:
            headerwriter.write(str(i) + ';')
        headerwriter.write('\n')

    extDict = {}
    counter = 1
    for row in arcpy.da.SearchCursor(MainlandCntry, ['Area_ID', 'SHAPE@']):
        # define a list for every Area_ID
        # append Area_ID as first element in list. Append extent of fishnet grid
cell to list
        ext_list = []
        ext_list.append(row[0])
        extent_curr = row[1].extent
        ext_list.append(extent_curr.XMin)
        ext_list.append(extent_curr.YMin)
        ext_list.append(extent_curr.XMax)
        ext_list.append(extent_curr.YMax)
        # set counter variable as dictionary key. Define ext_list as dictionary
values
        # increment counter variable for next fishnet grid cell
        extDict[counter] = ext_list
```

```
        counter += 1

    slope_list = [Slope_World]

    slope_func = partial(execute_SLOPEanalysis, lock, supplement_data, slope_list)

    # distribute worker function to different CPU cores and start process
    # tqdm() is used for displaying the progress bar
    # execute_SLOPEanalysis function is defined in WiSoGERI_WorkerForLoop.py
    for _ in tqdm.tqdm(pool.imap_unordered(slope_func, extDict.items()),
total=len(extDict.items()), desc='Progress', unit='Grid Cells'):
        pass

    t3 = time.time()
    t_slope = str((t3 - t2) / 60)
    print('SLOPE Analysis finished!')
    print('Time required: {} mins\n'.format(t_slope))


###                                                    DEPTH
###
    if EEZ_existing == True:

        # headerDEPTH = (['AREA_ID', 'DEPTH25', 'DEPTH50', 'DEPTH75', 'DEPTH100',
'DEPTH500', 'DEPTH12000', 'DISTANCE_SHORE')

        headerDEPTH = (['AREA_ID', 'DISTANCE_SHORELINE', 'AVERAGE_DEPTH'])

        with open('{}_InputEnertile_DEPTH_{}.txt'.format(datestamp, isoAlpha_name),
'a') as headerwriter:
            for i in headerDEPTH:
                headerwriter.write(str(i) + ';')
            headerwriter.write('\n')

        # read in global extent for Near_analysis in execute_DEPTHanalysis
        # create a list with four emtpy entries
        globExt_list = []
        for i in range(4):
            globExt_list.append(0)
        # read in global extent and write them into list
        globExt = arcpy.Describe(AdmBorders_World).extent
        globExt_list[0] = globExt.XMin
        globExt_list[1] = globExt.YMin
        globExt_list[2] = globExt.XMax
        globExt_list[3] = globExt.YMax

        extDict3 = {}
        counter = 1
        for row in arcpy.da.SearchCursor(EEZCntry, ['Area_ID', 'SHAPE@']):
            # define a list for every Area_ID
            # append Area_ID as first element in list. Append extent of fishnet
grid cell to list
            ext_list = []
            ext_list.append(row[0])
            extent_curr = row[1].extent
            ext_list.append(extent_curr.XMin)
            ext_list.append(extent_curr.YMin)
            ext_list.append(extent_curr.XMax)
            ext_list.append(extent_curr.YMax)
            # set counter variable as dictionary key. Define ext_list as dictionary
values
            # increment counter variable for next fishnet grid cell
            extDict3[counter] = ext_list
            counter += 1

        print('Initializing multicore DEPTH Analysis..\n')

        depth_list = [EEZCntry, WaterDepth_World, MainlandShape]
```

```
        depth_func = partial(execute_DEPTHanalysis, lock, supplement_data,
depth_list, globExt_list)
        pool3 = Pool(processes=Cores)
        # distribute worker function to different CPU cores and start process
        # tqdm() is used for displaying the progress bar
        # execute_LULCanalysis function is defined in WiSoGERI_WorkerForLoop.py
        for _ in tqdm.tqdm(pool3.imap(depth_func, extDict3.items()),
total=len(extDict3.items()), desc='Progress',
                           unit='Grid Cells'):
            pass


        t4 = time.time()
        t_depth = str((t4 - t3) / 60)
        print('DEPTH Analysis finished!')
        print('Time required: {} mins\n'.format(t_depth))

    pool.close()
    pool.join()
    t_final = time.time()
    t_total = str((t_final - t_start) / 60)
    print('WiSo-GERI has finished the entire analysis for
{}!'.format(country_name))
    print('Total time required: {} mins'.format(t_total))
```

WiSo-GERI – Worker script

```
# Author: Alexander HARRUCKSTEINER
# contains worker functions for multiprocessing
# functions are called in WiSoGERI_MAIN.py

# import relevant python modules
import arcpy
import time
import sys
from functools import partial
from multiprocessing import Process, Queue, Pool, cpu_count, Manager, Lock

def calc_percentage(share, total):
    return share / total * 100


def execute_LULCanalysis(file_lock, sup_data, lulc_map, in_bufferList, in_extDict):
    excluded = 12
    # unpack dictionary items
    countkey = in_extDict[0]
    items = in_extDict[1]
    # unpack list containing the Area_ID of the current fishnet grid cell and its
Extent
    areaid = items[0]
    XMin = items[1]
    YMin = items[2]
    XMax = items[3]
    YMax = items[4]
    # Set working environment to one fishnet grid cell extent and perform Raster To
Point operation
    arcpy.env.extent = arcpy.Extent(XMin, YMin, XMax, YMax)

    # unpack supplementary data
    iso_name = sup_data[0]
    date = sup_data[1]
    EEZ_existing = sup_data[2]
    gdb_path = sup_data[3]

    arcpy.env.workspace = gdb_path

    # unpack LULC file and excluded files from in_fileList
    # newly addded buffer layers have to be unpacked here
    LULC_World = lulc_map
    ProtectedAreas_Buffer = in_bufferList[0]
    Rail_Buffer = in_bufferList[1]
    Road_Buffer = in_bufferList[2]
    Airport_Buffer = in_bufferList[3]
    Settlement_Buffer = in_bufferList[4]

    if EEZ_existing == True:
        Shoreline_Buffer = in_bufferList[5]
        Waterways_Buffer = in_bufferList[6]

    # Raster cell is converted to point containing LULC value
    tempPnt = arcpy.RasterToPoint_conversion(LULC_World,

r'in_memory\tempOutput{}'.format(countkey))
                                            # if you want to display inbetween
steps, uncomment the following:
                                            # r'C:\KTH_Stockholm\Master
Thesis\Fraunhofer\ArcGIS_Files\NorthKoreaPnt\Fishnet_{}'.format(areaid))

    tempPnt_lyr = arcpy.MakeFeatureLayer_management(tempPnt, 'tempPnt_lyr')
    tempPA = arcpy.MakeFeatureLayer_management(ProtectedAreas_Buffer, 'PAexcl_lyr')
    tempRail = arcpy.MakeFeatureLayer_management(Rail_Buffer, 'RailExcl_lyr')
    tempRoad = arcpy.MakeFeatureLayer_management(Road_Buffer, 'RoadExcl_lyr')
    tempAir = arcpy.MakeFeatureLayer_management(Airport_Buffer, 'AirExcl_lyr')
```

```
    tempSettle = arcpy.MakeFeatureLayer_management(Settlement_Buffer,
'SettleExcl_lyr')

    if EEZ_existing == True:
        tempShore = arcpy.MakeFeatureLayer_management(Shoreline_Buffer,
'ShoreExcl_lyr')
        tempWaterways = arcpy.MakeFeatureLayer_management(Waterways_Buffer,
'WaterwaysExcl_lyr')

    # All points intersecting with an excluded zone will be selected
    arcpy.SelectLayerByLocation_management(tempPnt_lyr, 'INTERSECT', tempPA, '',
'NEW_SELECTION')
    arcpy.SelectLayerByLocation_management(tempPnt_lyr, 'INTERSECT', tempRail, '',
'ADD_TO_SELECTION')
    arcpy.SelectLayerByLocation_management(tempPnt_lyr, 'INTERSECT', tempRoad, '',
'ADD_TO_SELECTION')
    arcpy.SelectLayerByLocation_management(tempPnt_lyr, 'INTERSECT', tempSettle,
'', 'ADD_TO_SELECTION')
    temp_Sel = arcpy.SelectLayerByLocation_management(tempPnt_lyr, 'INTERSECT',
tempAir, '', 'ADD_TO_SELECTION')

    if EEZ_existing == True:
        arcpy.SelectLayerByLocation_management(tempPnt_lyr, 'INTERSECT', tempShore,
'', 'ADD_TO_SELECTION')
        temp_Sel = arcpy.SelectLayerByLocation_management(tempPnt_lyr, 'INTERSECT',
tempWaterways, '', 'ADD_TO_SELECTION')

    # UpdateCursor which changes value of selected points to the excluded value 12
    with arcpy.da.UpdateCursor(temp_Sel, 'grid_code') as update_cursor:
        for row in update_cursor:
            row[0] = excluded
            update_cursor.updateRow(row)

    # calculates the total amount of points existing inside a fishnet grid cell
    with arcpy.da.SearchCursor(tempPnt, ['grid_code']) as total_cursor:
        total = 0
        for row in total_cursor:
            total += 1

    # calculates the occurrence of each LULC class inside one fishnet grid cell
    # defines an array, where the occurrence number of each LULC class is written
into
    with arcpy.da.SearchCursor(tempPnt, ['grid_code']) as lulc_cursor:
        resultList = []

        lulc_array = []
        for i in range(12):
            lulc_array.append(float(0))

        for row in lulc_cursor:
            if row[0] == 1:
                lulc_array[0] += 1
            elif row[0] == 2:
                lulc_array[1] += 1
            elif row[0] == 3:
                lulc_array[2] += 1
            elif row[0] == 4:
                lulc_array[3] += 1
            elif row[0] == 5:
                lulc_array[4] += 1
            elif row[0] == 6:
                lulc_array[5] += 1
            elif row[0] == 7:
                lulc_array[6] += 1
            elif row[0] == 8:
                lulc_array[7] += 1
            elif row[0] == 9:
                lulc_array[8] += 1
```

```
            elif row[0] == 10:
                lulc_array[9] += 1
            elif row[0] == 11:
                lulc_array[10] += 1
            elif row[0] == 12:
                lulc_array[11] += 1

    # First the Area_ID of the current fishnet grid cell is appended to the
resultList
    # and then the occurrence values (in percent) are appended as well
    # the calc_percentage function converts shares into percentage values
    for i in range(len(lulc_array)):
        lulc_array[i] = calc_percentage(lulc_array[i], total)

    resultList.append(areaid)
    resultList.extend(lulc_array)

    # all temporary files are deleted to allow the next process to proceed
    del_list = [tempPnt, tempPnt_lyr, tempPA, tempRail, tempAir, tempRoad,
tempSettle, temp_Sel]

    if EEZ_existing == True:
        del_list.append(tempShore)
        del_list.append(tempWaterways)

    for i in del_list:
        arcpy.Delete_management(i)

    # the .txt file is temporarily locked, in order to avoid interference from
processes on other CPU cores
    file_lock.acquire()
    # results are written from the resultList to the .txt file
    with open('{}_InputEnertile_LULC_{}.txt'.format(date, iso_name), 'a') as txt:
        for i in resultList:
            txt.write(str(i) + ';')
        txt.write('\n')
    # the lock on the .txt file is released to allow the other CPU cores to write
into the file
    file_lock.release()


def execute_SLOPEanalysis(file_lock, sup_data, in_fileList, in_extDict):
    # unpack dictionary items
    countkey = in_extDict[0]
    items = in_extDict[1]
    # unpack list containing the Area_ID of the current fishnet grid cell and its
extent
    areaid = items[0]
    XMin = items[1]
    YMin = items[2]
    XMax = items[3]
    YMax = items[4]
    # Set working/spatial environment to one fishnet grid cell extent and perform
Raster To Point operation
    arcpy.env.extent = arcpy.Extent(XMin, YMin, XMax, YMax)

    # unpack supplementary data
    iso_name = sup_data[0]
    date = sup_data[1]
    gdb_path = sup_data[2]
    arcpy.env.workspace = gdb_path

    # unpack SLOPE file
    Slope_World = in_fileList[0]

    # Raster cell is converted to point containing SLOPE value
    tempPnt = arcpy.RasterToPoint_conversion(Slope_World,
```

```
#r'K:\X\User\harrucksteiner\ArcGIS\WiSoGERI\TempGDB.gdb\tempOutput{}'.format(countk
ey))

r'in_memory\tempOutput{}'.format(countkey))

    # calculates the total amount of points existing inside a fishnet grid cell
    with arcpy.da.SearchCursor(tempPnt, ['grid_code']) as total_cursor:
        total = float(0)
        for row in total_cursor:
            total += 1

    with arcpy.da.SearchCursor(tempPnt, ['grid_code']) as slope_cursor:
        total_slope = float(0)
        for row in slope_cursor:
            total_slope += row[0]

    average_slope = total_slope/total
    resultList= []

    # calculates the occurrence of each SLOPE class inside one fishnet grid cell
    # defines an array, where the occurrence number of each SLOPE class is written
into
    resultList.append(areaid)
    resultList.append(average_slope)

    file_lock.acquire()
    # results are written from the resultList to the .txt file
    with open('{}_InputEnertile_SLOPE_{}.txt'.format(date, iso_name), 'a') as txt:
        for i in resultList:
            txt.write(str(i) + ';')
        txt.write('\n')
    # the lock on the .txt file is released to allow the other CPU cores to write
into the file
    file_lock.release()

    arcpy.Delete_management(tempPnt)


def execute_DEPTHanalysis(file_lock, sup_data, in_fileList, globe_ext, in_extDict):
    # unpack gobal extent list
    glob_xmin = globe_ext[0]
    glob_ymin = globe_ext[1]
    glob_xmax = globe_ext[2]
    glob_ymax = globe_ext[3]

    # reset working extent to global in order to allow Near_analysis to not be
limited to the fishnet grid cell extent
    # and allow it to find the nearest Shoreline of the selected country
    arcpy.env.extent = arcpy.Extent(glob_xmin, glob_ymin, glob_xmax, glob_ymax)

    # unpack supplementary data
    iso_name = sup_data[0]
    date = sup_data[1]
    gdb_path = sup_data[2]
    arcpy.env.workspace = gdb_path

    # unpack in_extDict containing the counter variable and a list, which is
further unpacked
    countkey = in_extDict[0]
    items = in_extDict[1]
    # unpack list containing the Area_ID of the current fishnet grid cell and its
extent
    areaid = items[0]
    fish_xmin = items[1]
    fish_ymin = items[2]
    fish_xmax = items[3]
    fish_ymax = items[4]
```

```
    # unpack necessary files found in in_fileList
    FishnetG_EEZ = in_fileList[0]
    Depth_World = in_fileList[1]
    Shoreline_Cntry = in_fileList[2]


    tempGrid_lyr = arcpy.MakeFeatureLayer_management(FishnetG_EEZ,
'fishnet_eez_lyr')

    tempSelect = arcpy.SelectLayerByAttribute_management(tempGrid_lyr,
'NEW_SELECTION',
                                                         """ "Area_ID" = {0}
""".format(areaid))

    # Creates a feature point in the center of the fishnet grid cell
    tempLabel = arcpy.FeatureToPoint_management(tempSelect,

r'in_memory\tempPoint{}'.format(countkey), 'INSIDE')

    # Near_analysis measures closest distance from center point of fishnet grid
cell to the country shoreline
    # Unit of measurement is meters [m]
    arcpy.Near_analysis(tempLabel, Shoreline_Cntry, '400 Kilometers', '', '',
'GEODESIC')

    # the distance value is extracted from the feature point and stored in a
variable
    # the column NEAR_DIST in the attribute table contains the distance value
    distance = float(0)
    with arcpy.da.SearchCursor(tempLabel, ['NEAR_DIST']) as dist_cursor:
        for row in dist_cursor:
            distance = row[0]

    # Set extent to single fishnet grid cell in order to limit RasterToPoint
operation to single fishnet grid cell
    arcpy.env.extent = arcpy.Extent(fish_xmin, fish_ymin, fish_xmax, fish_ymax)

    tempPnt = arcpy.RasterToPoint_conversion(Depth_World,

r'in_memory\tempOutput{}'.format(countkey))

    # calculate sum of all points found inside the fishnet grid cell
    with arcpy.da.SearchCursor(tempPnt, ['grid_code']) as total_cursor:
        total = float(0)
        for row in total_cursor:
            total += 1

    with arcpy.da.SearchCursor(tempPnt, ['grid_code']) as depth_cursor:
        total_seadepth = float(0)
        for row in depth_cursor:
            total_seadepth += row[0]

    average_seadepth = total_seadepth/total

    resultList = []

    # Area_ID, average sea depth and the distance to shoreline are written to the
resultList
    resultList.append(areaid)
    resultList.append(distance/1000)
    resultList.append(average_seadepth)

    file_lock.acquire()
    # results are written from the resultList to the .txt file
    with open('{}_InputEnertile_DEPTH_{}.txt'.format(date, iso_name), 'a') as txt:
        for i in resultList:
            txt.write(str(i) + ';')
        txt.write('\n')
```

```
    # the lock on the .txt file is released to allow the other CPU cores to write
into the file
    file_lock.release()


    arcpy.Delete_management(tempGrid_lyr)
    arcpy.Delete_management(tempPnt)
    arcpy.Delete_management(tempLabel)
```

WiSo-GERI – Intro script

```
# Author: Alexander HARRUCKSTEINER
# contains functions for printing introduction text when running WiSo-GERI
# functions are called in WiSoGERI_MAIN.py

# import relevant python modules
import time

# function printing general information on WiSo-GERI model
def intro_general():
    model_name_long = 'Wind and Solar - Geospatial Energy Resource Identification'
    model_name_short = 'WiSo - GERI'

    print
    print(model_name_long.center(70, ' '))
    print(model_name_short.center(70, ' '))
    print
    print('Author: {}'.format('Alexander Harrucksteiner'))
    print('A collaborative product by Royal Institute of Technology KTH and
Fraunhofer ISI')
    print('Created on 10.08.2019\n')
    print
    time.sleep(3)
    return

# function printing specific information on the LULC analysis
def intro_lulc():
    script_name = 'LULC and EXCLUDED script'

    print(script_name.center(70, ' '))
    print('Description: ')
    print('Isolates the fishnet grid cells of the selected Country + EEZ')
    print('Incorporates the excluded zones into the LULC map')
    print('Performs an occurrence statistic of every land-use class found inside a
fishnet grid cell\n')
    print
    return

# function printing specific information on the SLOPE analysis
def intro_slope():
    script_name = 'SLOPE script'

    print(script_name.center(70, ' '))
    print('Description: ')
    print('Calculates the average slope of a fishnet grid cell\n')
    print
    return


# function printing specific information on the DEPTH analysis Part 1
def intro_depthp1():
    script_name = 'DEPTH script Part 1'

    print(script_name.center(70, ' '))
    print('Description: ')
    print('Preparatory script for the spatial analysis of DEPTH')
    print('Isolates data from the country of interest\n')
    print
    return


# function printing specific information on the DEPTH analysis Part 2
def intro_depthp2():
    script_name = 'DEPTH script Part 2'

    print(script_name.center(70, ' '))
```

```
print('Description: ')
print('Uses the isolated data and the global data to perform spatial analysis')
print('Calculates distance to shoreline and average sea depth\n')
print
return
```

WiSo-GERI – Check script

```
# Author: Alexander HARRUCKSTEINER
# contains functions for checking input files
# functions are called in WiSoGERI_MAIN.py

# import relevant python modules
import arcpy
import sys

# function checking spelling of country name input
def cntry_check(cntry_file, cntry):
    country_list = []

    with arcpy.da.SearchCursor(cntry_file, ['FIRST_NAME']) as check_cursor:
        for row in check_cursor:
            country_list.append(row[0])

    if cntry in country_list:
        print('Selected Country is valid!')
    else:
        sys.exit('Invalid Country! Please check spelling..')

    return

# function checking spelling of EEZ name input
def eez_check(eez_file, eez):
    eez_list = []

    with arcpy.da.SearchCursor(eez_file, ['Territory1']) as check_cursor:
        for row in check_cursor:
            eez_list.append(row[0])

    if eez in eez_list:
        print('Selected EEZ is valid!')
    else:
        sys.exit('Invalid EEZ! Please check spelling..')

    return

# function checking projection of all input data
def prj_check(in_map):
    # enter new spatial reference name here, if necessary
    spatial_ref = 'World_Cylindrical_Equal_Area'

    file_name = arcpy.Describe(in_map).name
    SF_code = arcpy.Describe(in_map).SpatialReference
    input_SR = SF_code.Name

    if input_SR == spatial_ref:
        print('{} has correct projection!'.format(file_name))
    else:
        sys.exit('File {} has invalid projection: {}'.format(file_name, input_SR))
    return

# function transforms country name into iso_alpha3 style of input country
def iso_transform(cntry_file, cntry):
    global iso
    country_dic = {}

    with arcpy.da.SearchCursor(cntry_file, ['FIRST_NAME', 'iso_alpha3']) as
iso_cursor:
        for row in iso_cursor:
            country_dic[row[0]] = row[1]

    iso = country_dic[cntry]

    return iso
```